



Charge-Coupled Devices

Steve Holland / Lawrence Berkeley National Laboratory
November 18th, 2024





Physical Cosmology Roadmap

CCD-based detectors

— The Dark Energy Survey

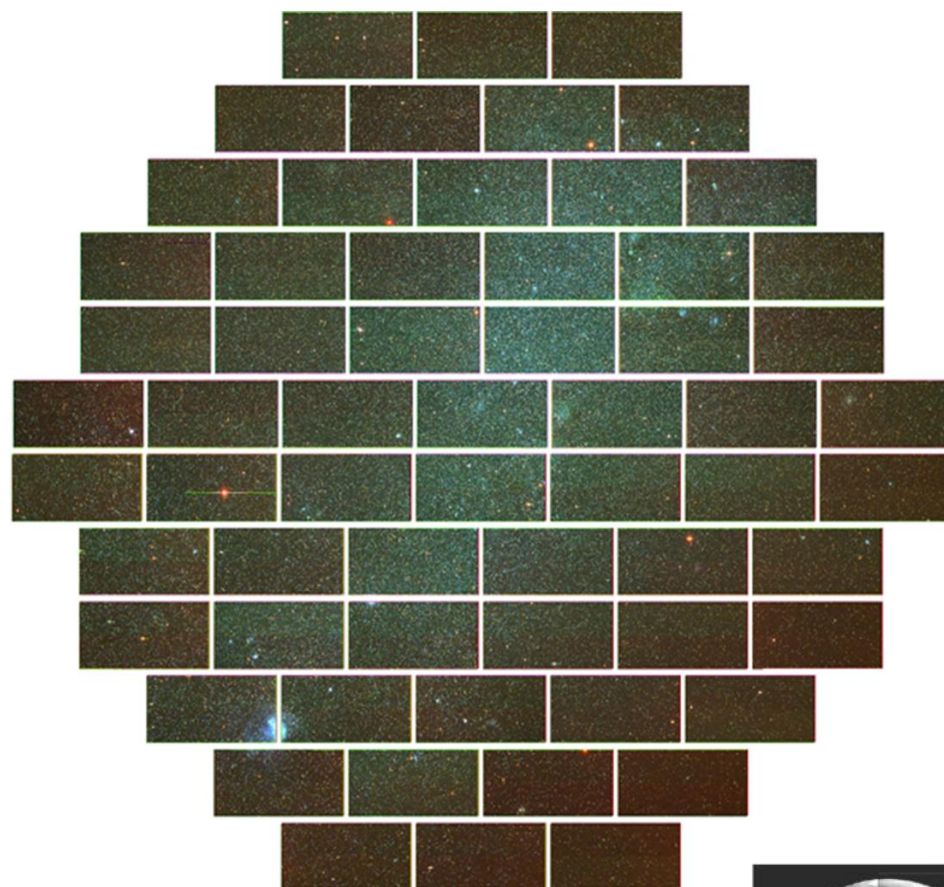
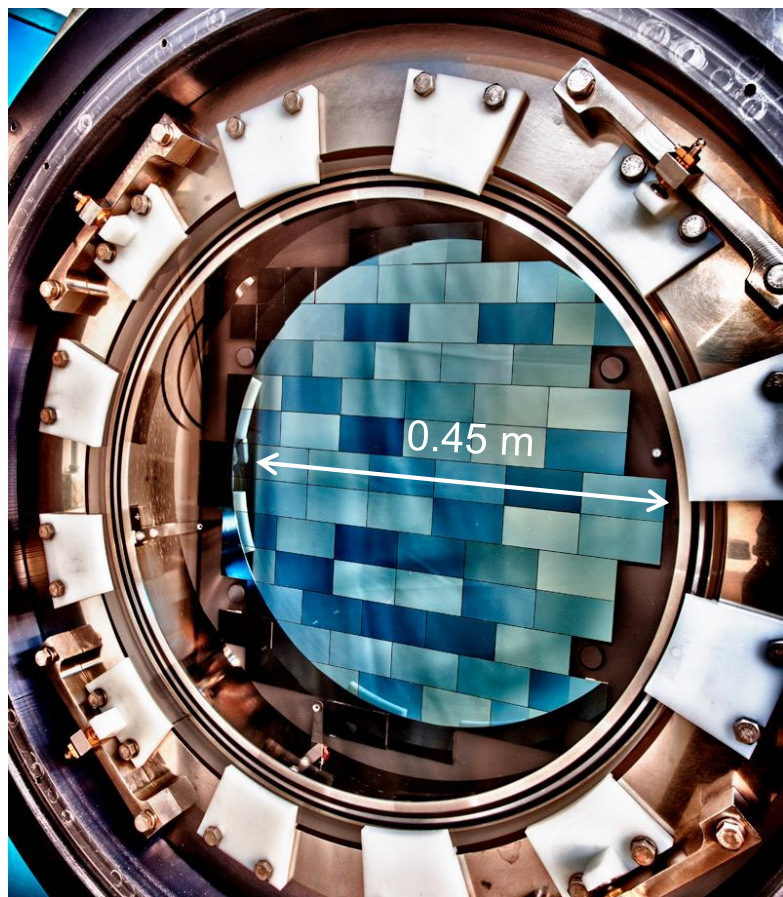
- Observations with the Dark Energy Camera (2013 – 2019)
- DECam operation continues with 1+ million images to date

— The Dark Energy Spectroscopic Instrument (2019 – present)

— Rubin LSST Camera (1st light 2025)

The vast majority of the CCDs in the above instruments are “Fully depleted”, with the exception being the “blue-sensitive” CCDs in DESI

Dark Energy Camera CCDs and Image

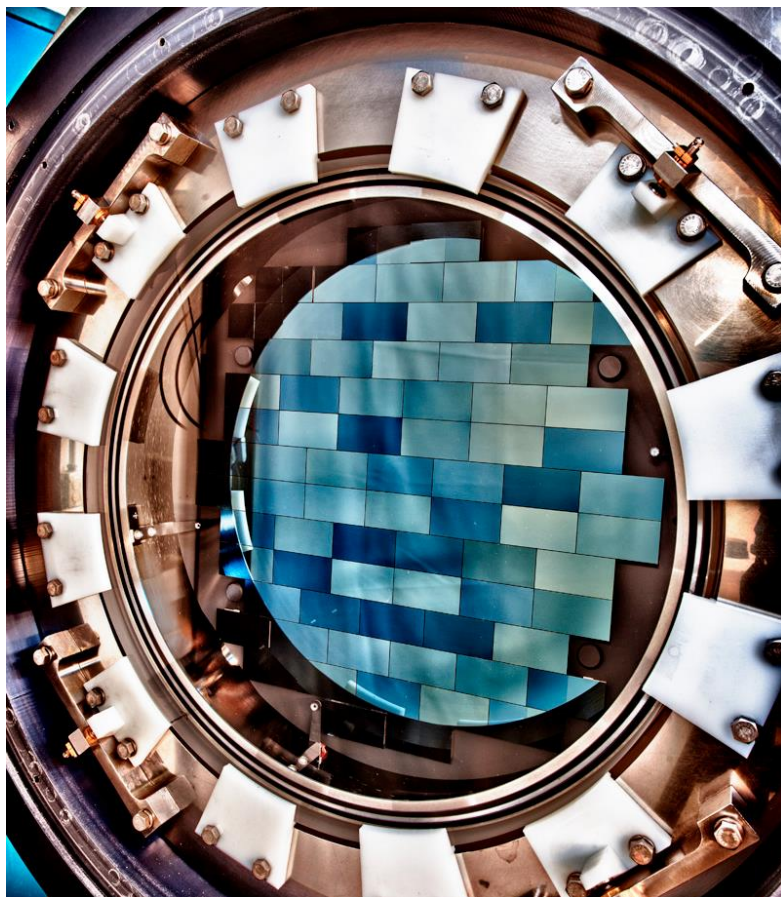


Cerro Tololo Inter-American Observatory 4-m Blanco Telescope
1st light Sept 2012 / Lead Laboratory: FermiLab
520 Mpixel Camera (64 x 2k x 4k, 15 um pixels)
CCDs from Teledyne DALSA Semiconductor and LBNL



Full moon for scale

Dark Energy Camera (DECam)

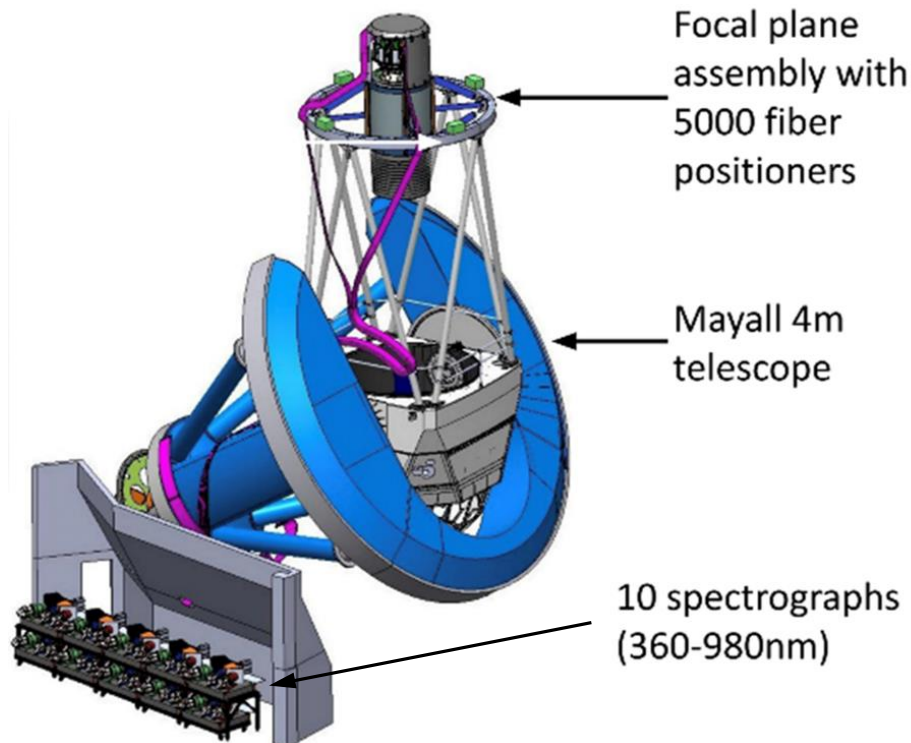
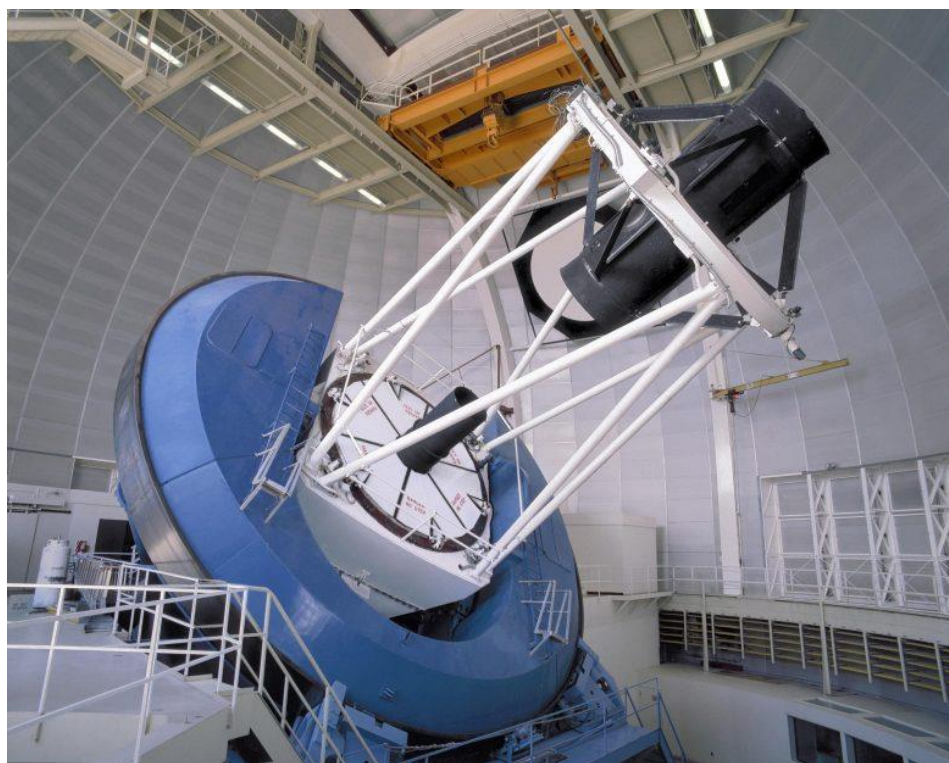


Brenna Flaugher
Distinguished Scientist (FermiLab)
Led the development of DECam

Dark Energy Camera (DECam)

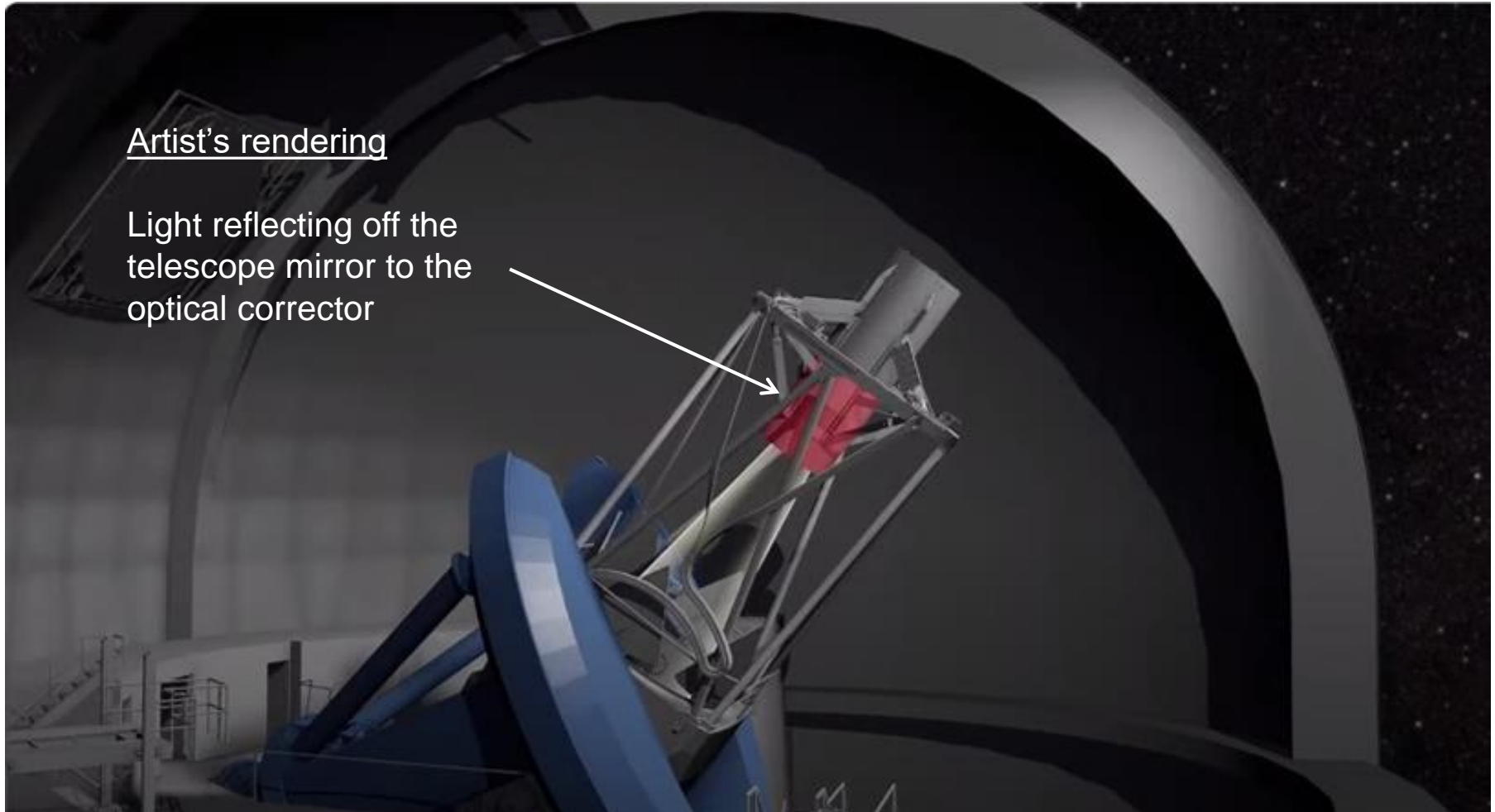
CCDs from Teledyne DALSA Semiconductor and LBNL
250 um thick, fully depleted

The Dark Energy Spectroscopic Instrument



Massively multiplexed, multi-object fiber-fed spectrograph
NOIRLab Kitt Peak Mayall 4-m Telescope
1st light October 2019
Lead Laboratory: Lawrence Berkeley National Laboratory

The Dark Energy Spectroscopic Instrument

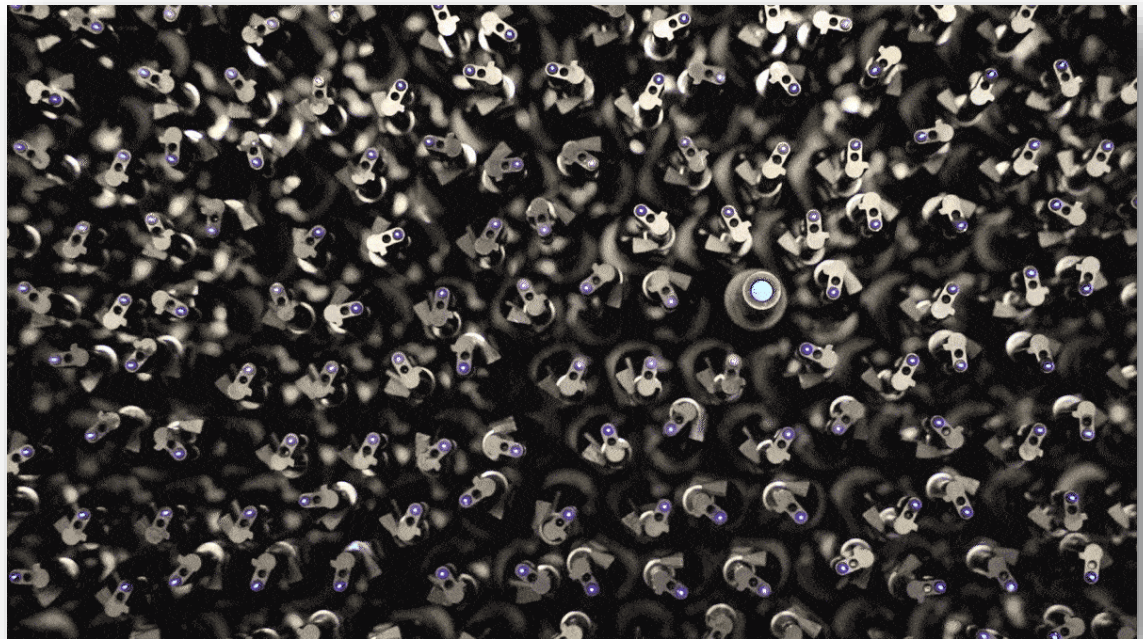


Credit: Dongjae "Krystofer" Kim/Kryated.com, DESI collaboration,
U.S. DOE Office of Science, Lawrence Berkeley National Lab

The Dark Energy Spectroscopic Instrument



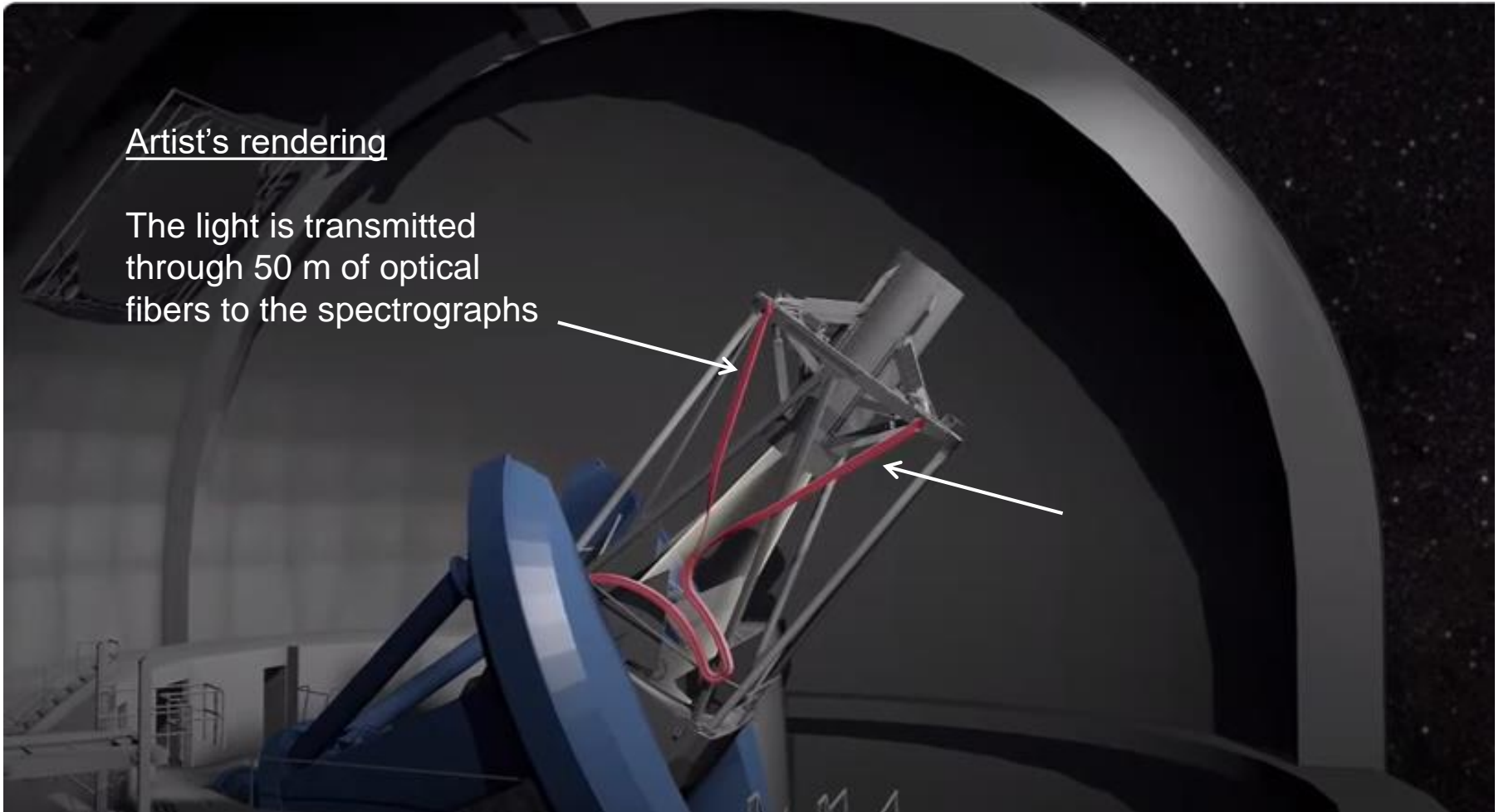
5000 fiber
positioners



The Dark Energy Spectroscopic Instrument

Artist's rendering

The light is transmitted through 50 m of optical fibers to the spectrographs



Credit: Dongjae "Krystofer" Kim/Kryated.com, DESI collaboration, U.S. DOE Office of Science, Lawrence Berkeley National Lab

The Dark Energy Spectroscopic Instrument

Artist's rendering



10 Spectrographs

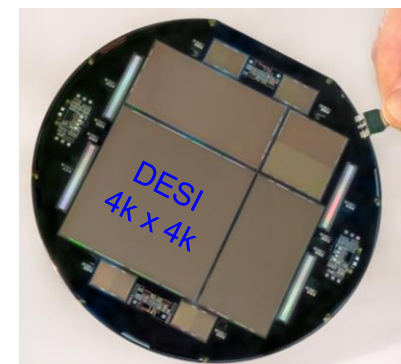
480 Mpixels: 30 x 4k x 4k (15 um pixel) CCDs

Semiconductor Technology Associates (STA) / DALSA
U of Arizona Imaging Technology Lab (blue)

DALSA/LBNL (red / near infrared)



Artist's rendering



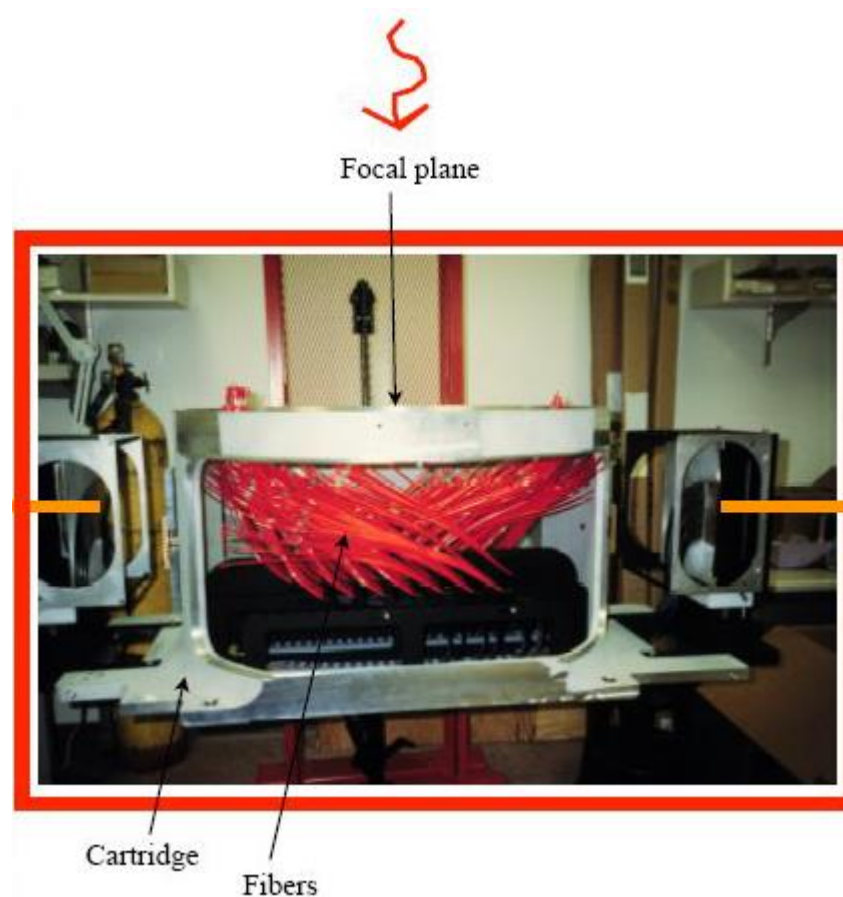
150-mm wafer
DALSA/LBNL

Credit: Dongjae "Krystofer" Kim/Kryated.com, DESI collaboration,
U.S. DOE Office of Science, Lawrence Berkeley National Lab

March 10, 2022 | Elaina Hancock - UConn Communications

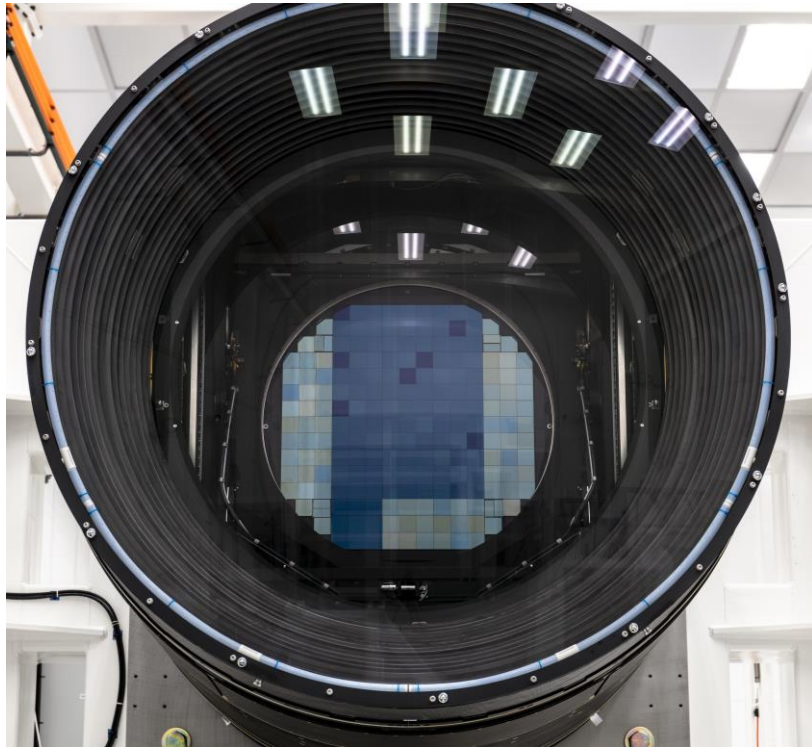
Plates that Helped Map the Universe, Now at UConn

Distant galaxies, black holes, and more secrets of the universe via tiny holes in aluminum



Aluminum plates with 1000 precisely placed holes for manual connection to the optical fibers
1.5M spectra taken Fall 2009 – Spring 2014
DESI: ~ 1 million spectra / month

The world's highest resolution digital camera Vera C. Rubin LSST Camera



Vera C. Rubin LSST Camera
Installation in 2025 at the Vera C. Rubin LSST Observatory (8-m telescope)
Lead Laboratory: SLAC National Accelerator Laboratory
3 Gpixel camera (189 x 4k x 4k, 10 um pixels)



CCDs from e2V and
Semiconductor Technology Associates / DALSA /
University of Arizona Imaging Technology Laboratory



Remainder of the talk

- Invention of the CCD
- Brief history of scientific CCD development
- Fully depleted CCDs
 - Light absorption / charge generation
 - High red-shift Quasar & SuperNovae detection
- CCDs for Dark Matter



Bell Telephone Laboratories 1969

- The head of the Semiconductor Division Williard Boyle[†] was tasked to develop a semiconductor memory device to compete with magnetic bubble memories (also Bell Labs)
 - Magnetic domains propagate due to magnetic field gradients
 - Essentially a magnetic serial shift register
- Group leader George E. Smith met with Boyle on 17Oct1969
 - “In a discussion lasting not much more than an hour, the basic structure of the CCD was sketched out on the blackboard, the principles of operation defined, and some preliminary ideas concerning applications were developed.”

JOURNAL OF APPLIED PHYSICS **109**, 102421 (2011)

The invention and early history of the CCD

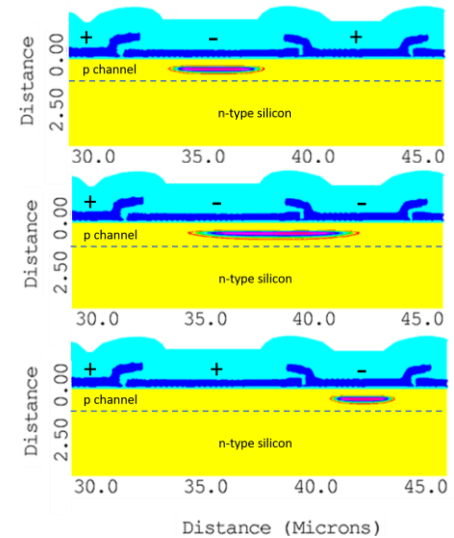
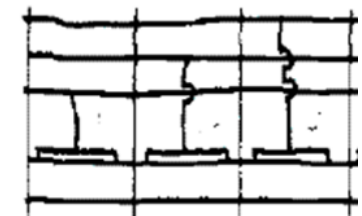
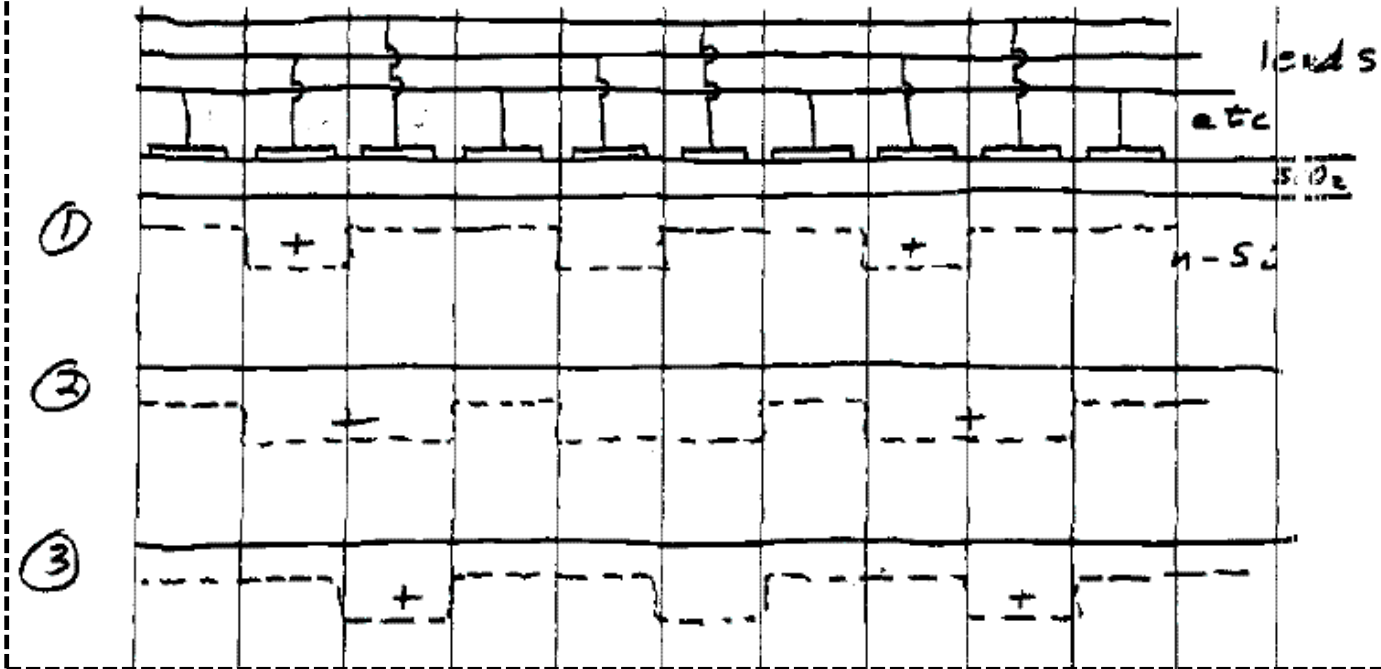
George E. Smith^{a)}

AT&T Bell Labs (Retired), 221 Teaneck Rd., P.O. Box 787, Barnegat, New Jersey 08005, USA

<http://aip.scitation.org/doi/full/10.1063/1.3578638>

Boyle and Smith lab notebook drawing Sept. 1969

Time

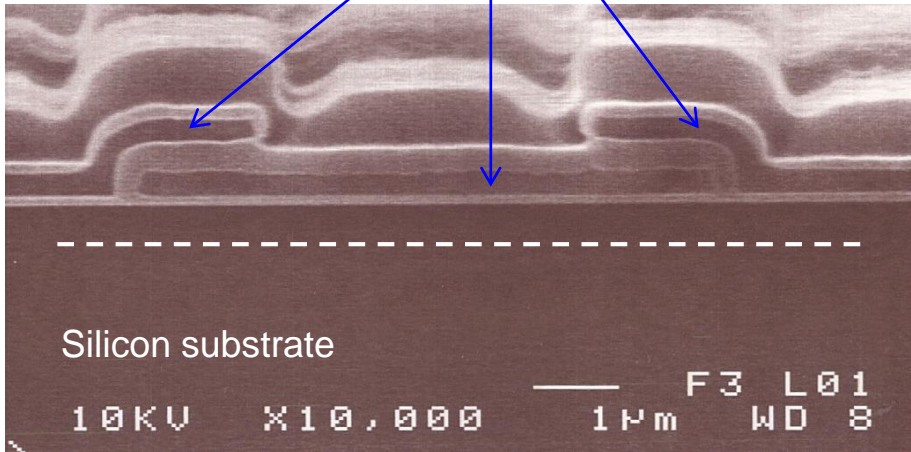


CCD simulation cross section

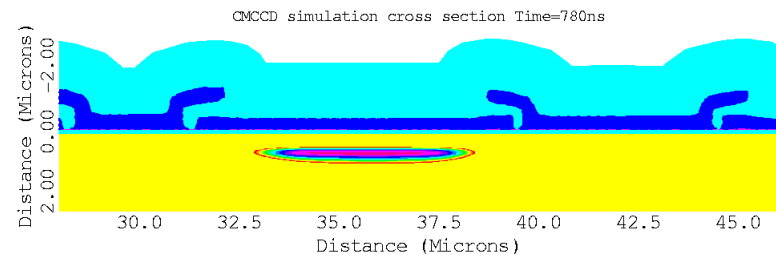
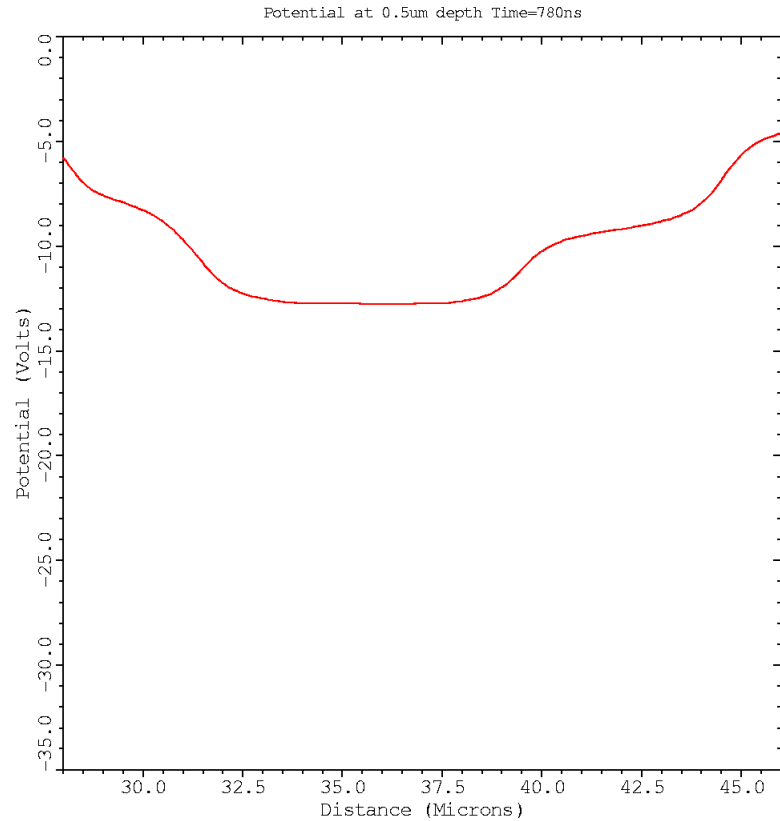
- Confine electrons or holes in potential wells
 - Metal Oxide Semiconductor capacitors
 - Dashed line is the depletion edge
- Shift the charge via clocking of closely spaced electrodes
 - “Charge coupling”

Charge-coupling simulation

Polycrystalline silicon electrodes (leads)



Electrostatic potential vs lateral distance
Simulated potential along dashed line above



The Nobel Prize in Physics 2009

The Nobel Prize in Physics 2009

Charles K. Kao
Willard S. Boyle
George E. Smith

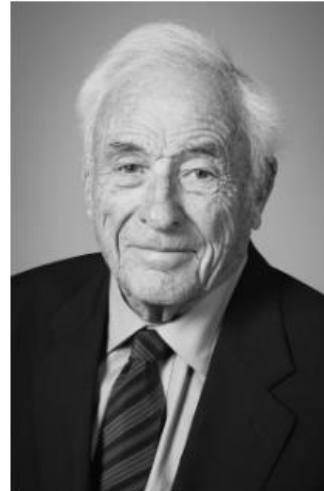
Share this



© The Nobel Foundation. Photo:
U. Montan

Charles Kuen Kao

Prize share: 1/2



© The Nobel Foundation. Photo:
U. Montan

Willard S. Boyle

Prize share: 1/4



© The Nobel Foundation. Photo:
U. Montan

George E. Smith

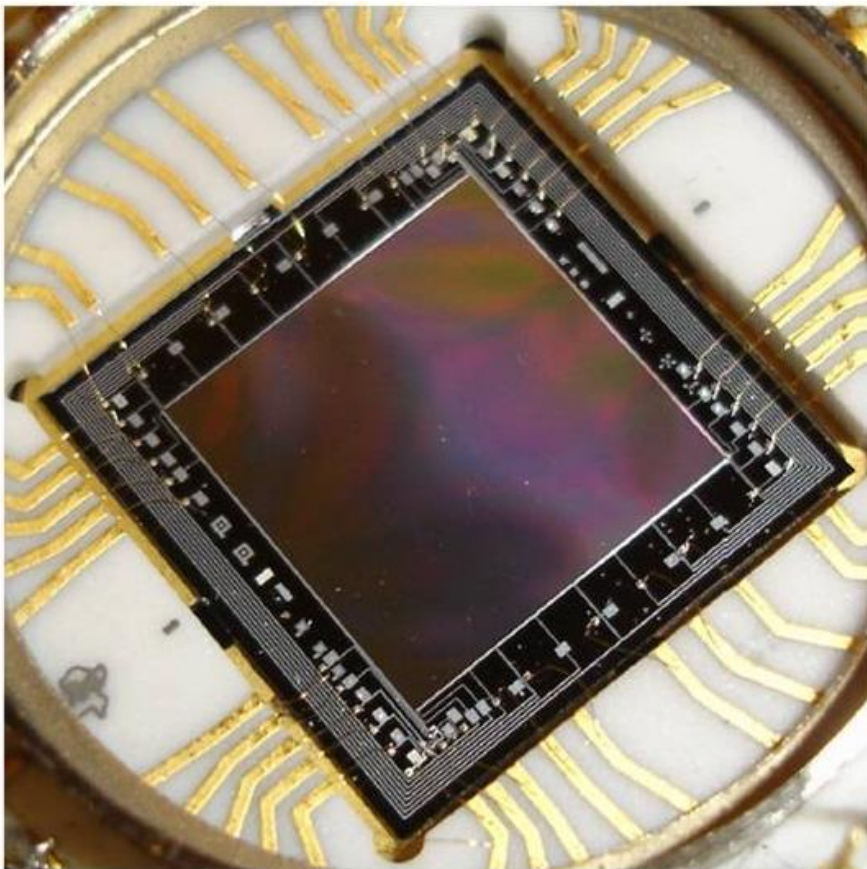
Prize share: 1/4

The Nobel Prize in Physics 2009 was divided, one half awarded to Charles Kuen Kao "for groundbreaking achievements concerning the transmission of light in fibers for optical communication", the other half jointly to Willard S. Boyle and George E. Smith "for the invention of an imaging semiconductor circuit - the CCD sensor"

Texas Instruments 800 x 800 CCD Developed for Hubble Space Telescope

**HUBBLE WF/PC I - 800 x 800 x 15 um
pixel backside illuminated (BSI) CCD
shown inside its package.**

Credit: Jim Janesick and
<http://www.digicamhistory.com/>



- 10 um thick membrane
- Back illuminated

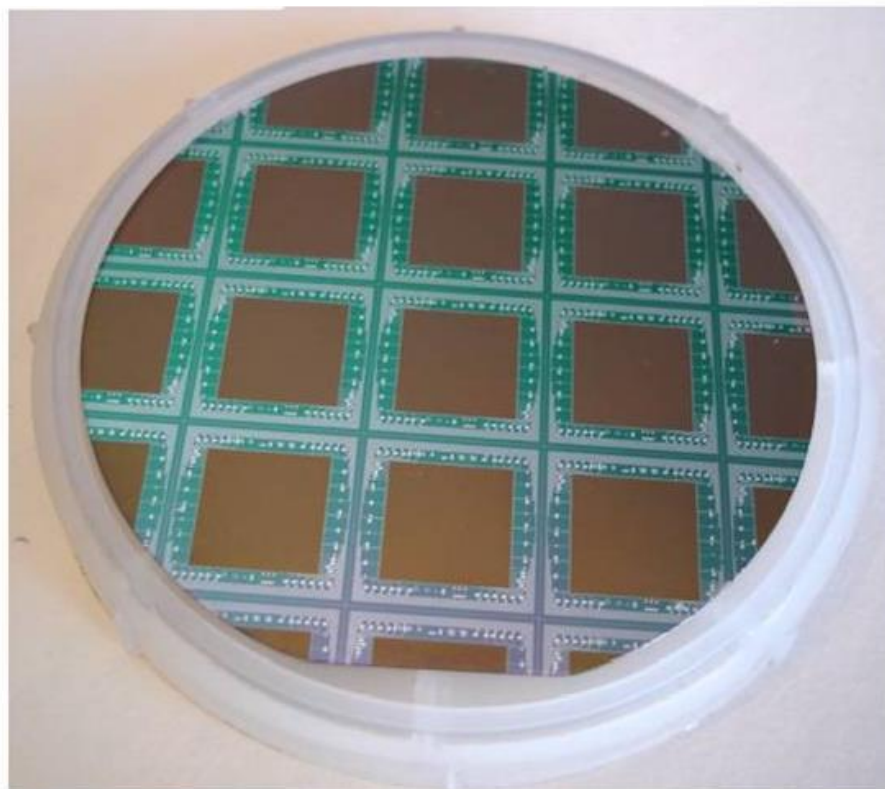
Image from 1978
Int. Solid State Circuits Conf.
paper ([Link](#))



SESSION II: ADVANCES IN CHARGE-COUPLED IMAGERS

WAM 2.5: Three-Phase, Backside Illuminated 500x500 CCD Imager*

*M. M. Blouke, J. F. Breitzmann and J. E. Hall
Texas Instruments, Inc.
Dallas, TX*



**Wide Field Planetary Camera (WF/PC I)
Hubble Space Telescope 800 x 800 x 15 um
pixel CCD fabricated on a 3-inch silicon
wafer.**

The Palomar Observatory Four-shooter camera

- A camera with 4 TI 800 x 800 CCDs was developed to gain experience prior to the Hubble launch (PI James Gunn)

Four-shooter: a large format charge-coupled-device camera for the Hale telescope

James E. Gunn
Princeton University
Astrophysical Sciences
Princeton, New Jersey 08544
and
Palomar Observatory
California Institute of Technology
Palomar Mountain, California 92060

Michael Carr
G. Edward Danielson
Ernest O. Lorenz
Richard Lucinio
Victor E. Neno
J. Devere Smith
James A. Westphal
California Institute of Technology
Geological and Planetary Sciences
Pasadena, California 91125

Donald P. Schneider
Institute for Advanced Study
Princeton, New Jersey 08540

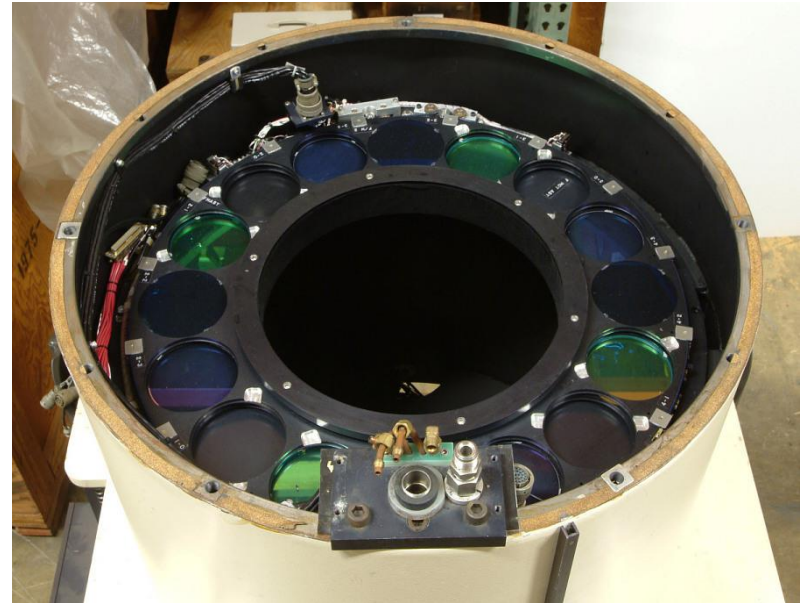
Barbara A. Zimmerman
Jet Propulsion Laboratory
California Institute of Technology
4800 Oak Grove Drive
Pasadena, California 91109

Abstract. We describe an astronomical camera for the 200-in. Hale telescope using four 800×800 Texas Instruments CCDs in an optical arrangement that allows imaging of a contiguous 1600-pixel-square region of sky. The system employs reimaging optics to yield a scale of 0.33 arcsec per pixel, a good match to the best seeing conditions at Palomar Observatory. Modern high-efficiency coatings are used in the complex optical system to yield a throughput at peak efficiency of nearly 50% (including the losses in the telescope), corresponding to a quantum efficiency on the sky of about 30%. The system uses a fifth CCD in a spectroscopic channel, and it is possible to obtain simultaneous imaging and spectroscopic observations with the system. The camera may also be used in a scanning mode, in which the telescope tracking rate is offset, and the charge is clocked in the chips in such a manner as to keep the charge image aligned with the optical image. In this way, a survey for high-redshift quasars has been carried out over a large area of sky. The instrument has produced images for the most distant clusters of galaxies yet discovered as well as spectra of the most distant galaxies yet observed.

Subject terms: charge-coupled device imager; astronomical instrumentation; low-light-level imaging.

Optical Engineering 26(8), 779-787 (August 1987).

1987 publication



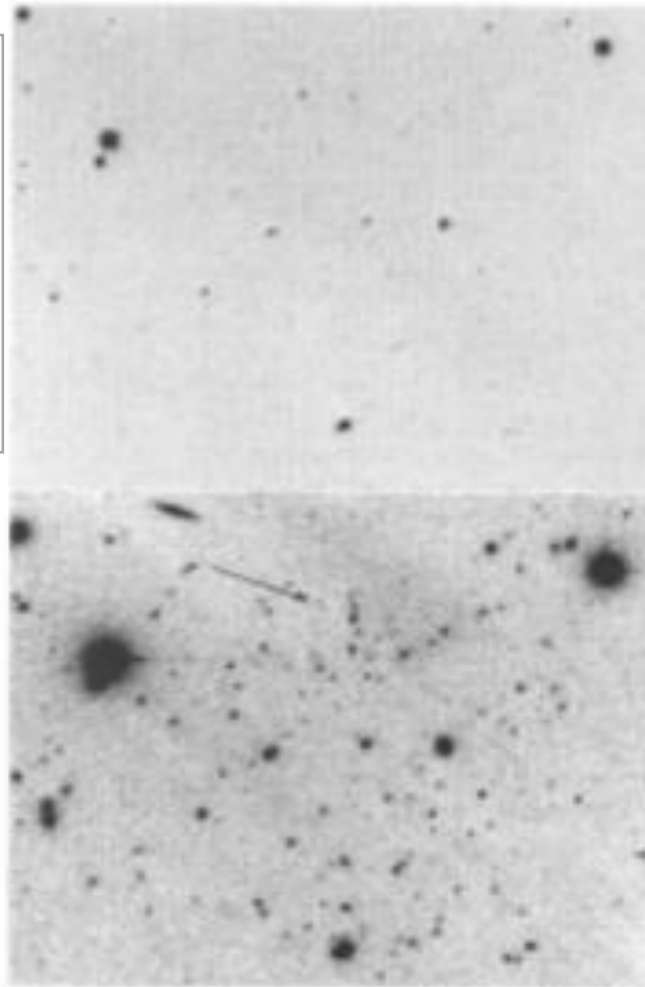
“... a survey for high-redshift quasars has been carried out ... The instrument has produced images for the most distant clusters of galaxies yet discovered as well as spectra of the most distant galaxies yet observed.”

The Palomar Observatory Four-shooter camera

90 min exposure with film

Quantum efficiency $\sim 1\%$

4-m Mayall Telescope



5 minute exposure

Four-Shooter camera

200" (5.08 m) Palomar telescope

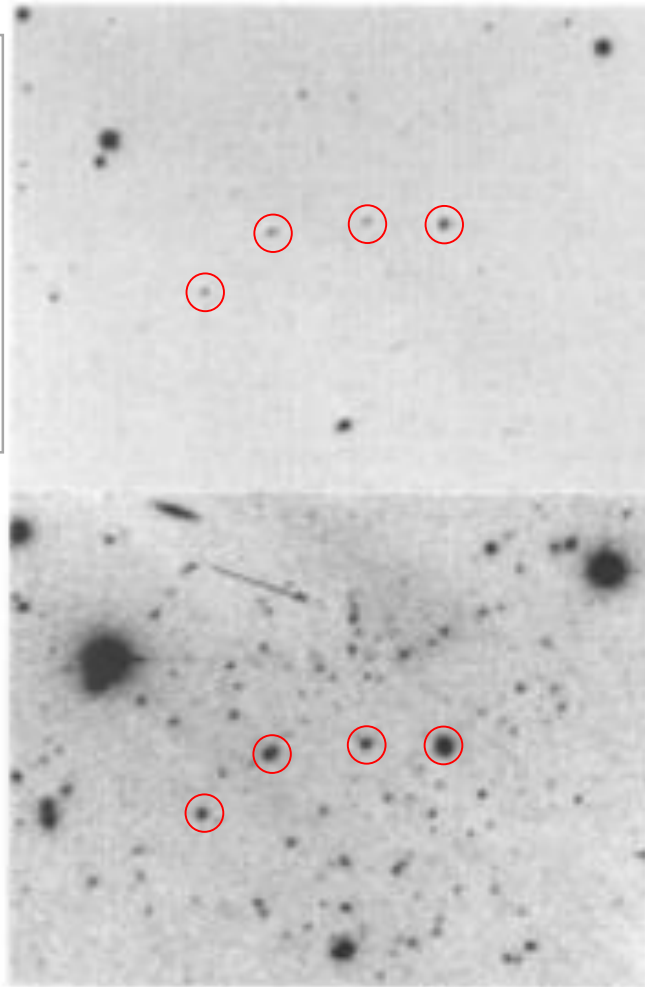
Fig. 11. Two images of the same region of the sky showing a cluster of galaxies at a redshift of 0.921. The upper image is a limiting photograph, 90-min exposure on a hypersensitized Kodak Spectroscopic Plate, type IIIa-F, obtained with the 4-m Mayall telescope on Kitt Peak. The lower image is the region as recorded with a 5-min four-shooter exposure; the arrow points to the cluster.

The Palomar Observatory Four-shooter camera

90 min exposure with film

Quantum efficiency ~ 1%

4-m Mayall Telescope

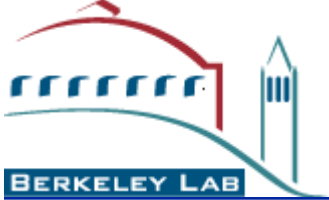


5 minute exposure

Four-Shooter camera

200" (5.08 m) Palomar telescope

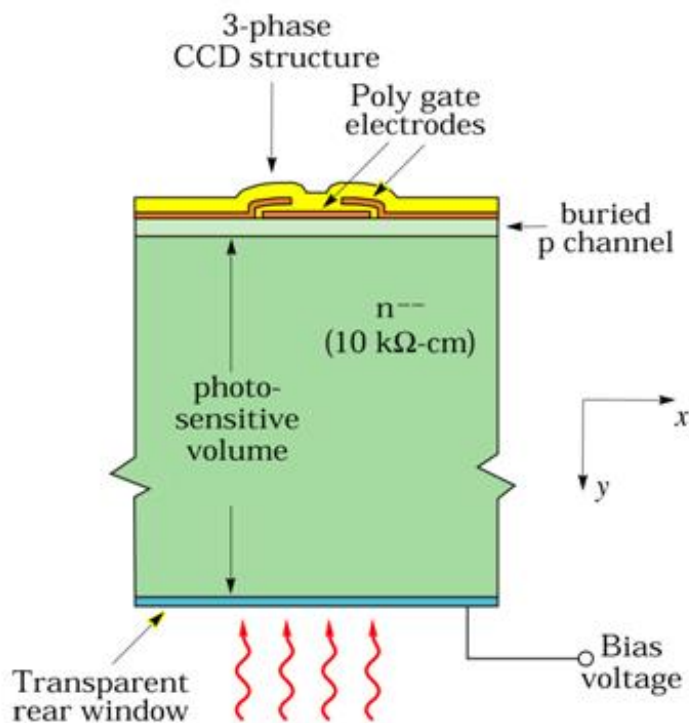
Fig. 11. Two images of the same region of the sky showing a cluster of galaxies at a redshift of 0.921. The upper image is a limiting photograph, 90-min exposure on a hypersensitized Kodak Spectroscopic Plate, type IIIa-F, obtained with the 4-m Mayall telescope on Kitt Peak. The lower image is the region as recorded with a 5-min four-shooter exposure; the arrow points to the cluster.



Remainder of the talk

- Invention of the CCD
- Brief history of scientific CCD development
- **Fully depleted CCDs**
 - Light absorption / charge generation
 - High red-shift Quasar & SuperNovae detection
- CCDs for Dark Matter

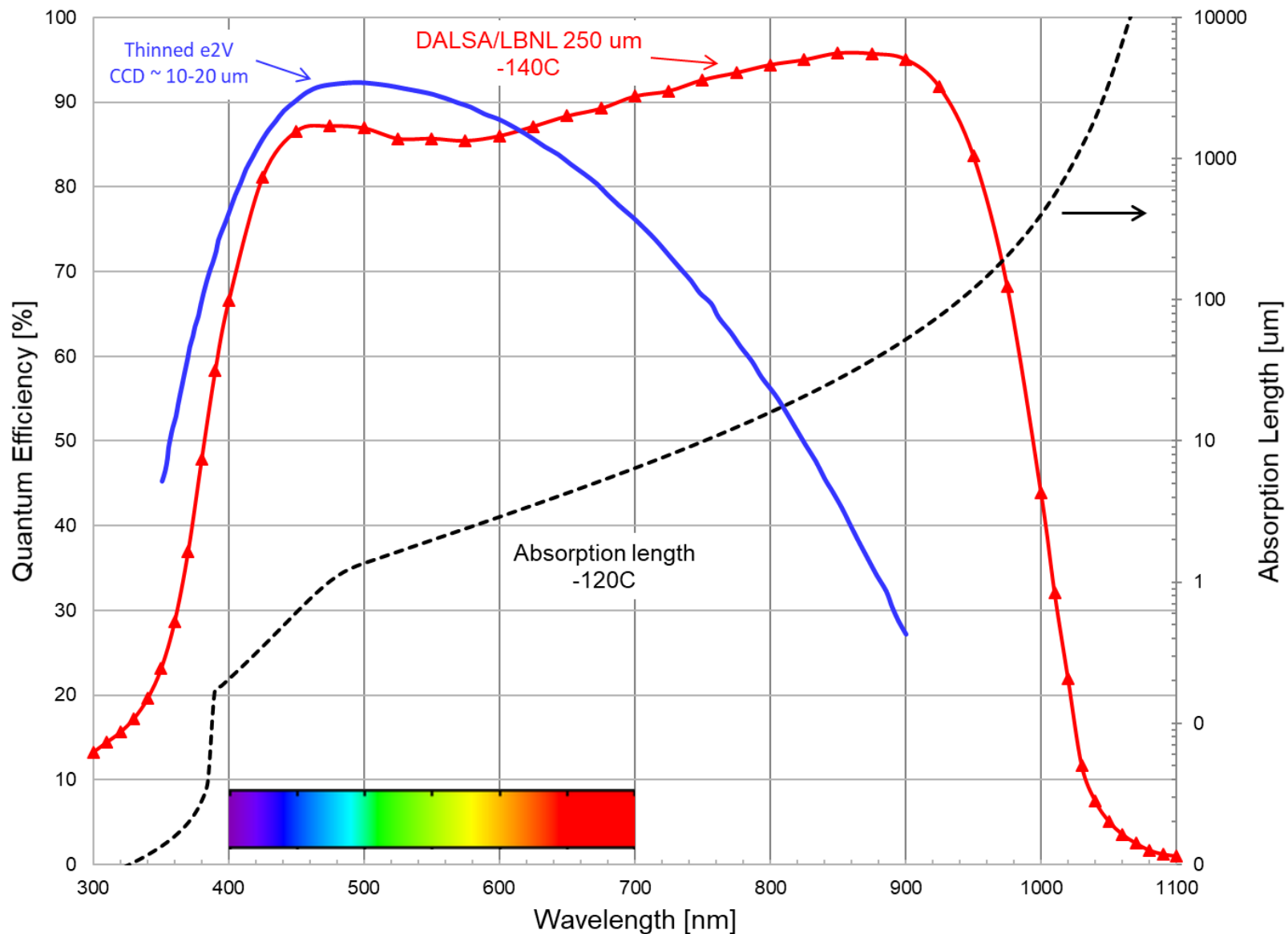
Fully depleted CCDs 101



Not to scale

CCD fabricated on a high-resistivity silicon substrate that is fully depleted by the application of a substrate bias

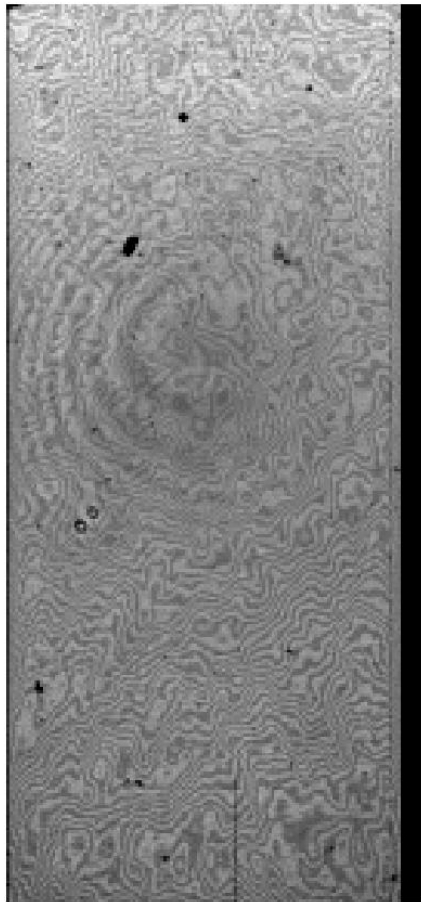
- Merging of CCD / p-i-n detector
HEP spinoff
- Typical thickness for astronomy
200 – 250 μm
- Thick device results in
High near-infrared response
- Main advantage for astronomy
Reduced “fringing”
Detect high redshift objects



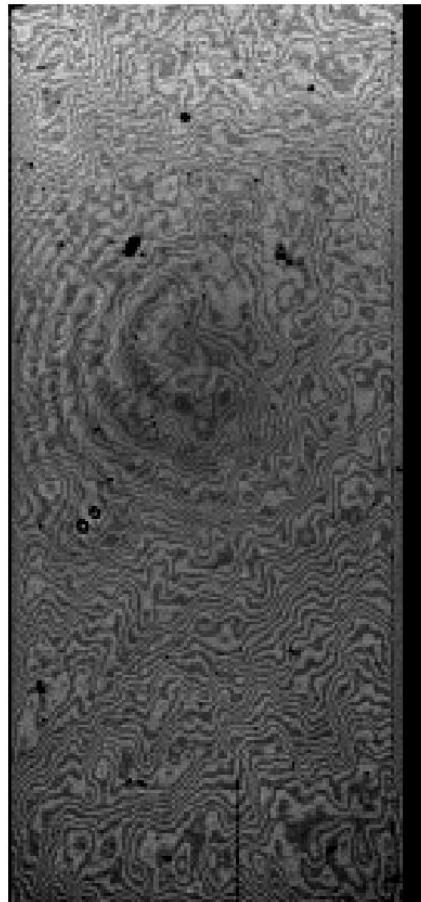
10 – 20 um thick, partially depleted CCD

250 um thick, fully depleted CCD (DECam, DESI red/near-IR)

Fringing in thinned CCDs



$\lambda = 8000\text{\AA}$



9000 \AA



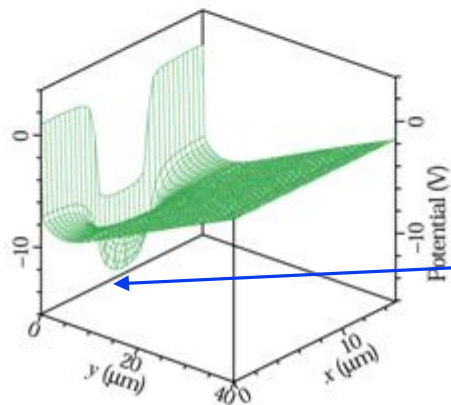
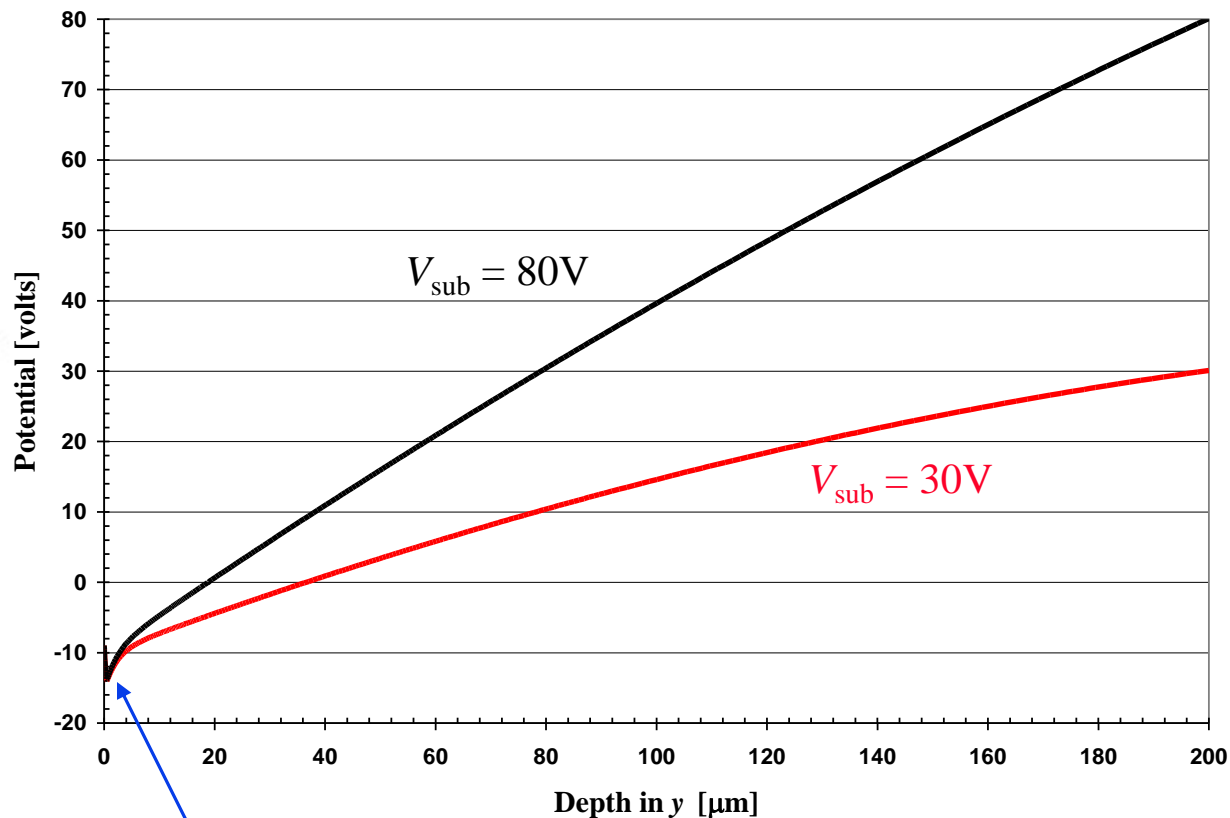
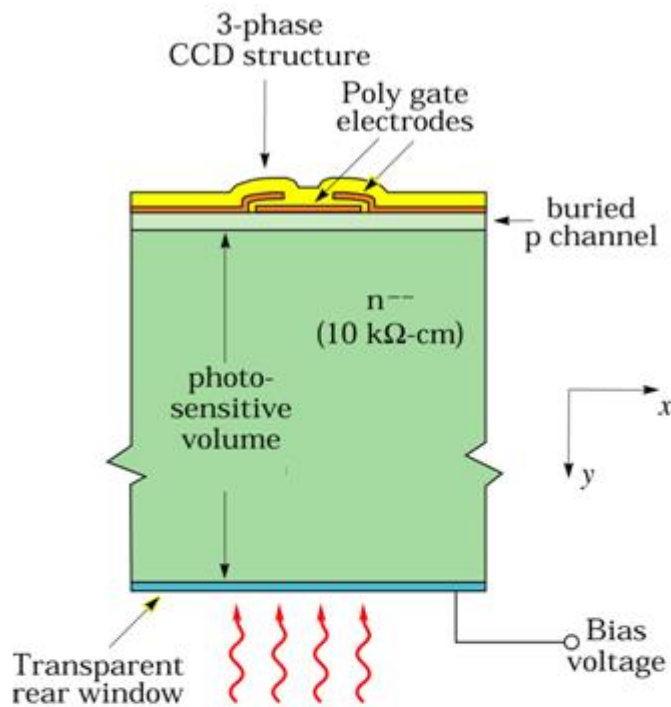
10,000 \AA

$\sim \pm 40\%$
(Laboratory)

For 250 μm thick
DECam CCDs, the
fringing is negligible

Fringing – Multiply reflected light in 10 – 20 μm thick CCDs
Uniform illumination (R. Stover / M. Wei Lick Observatory)

Fully depleted CCDs / 2D simulations

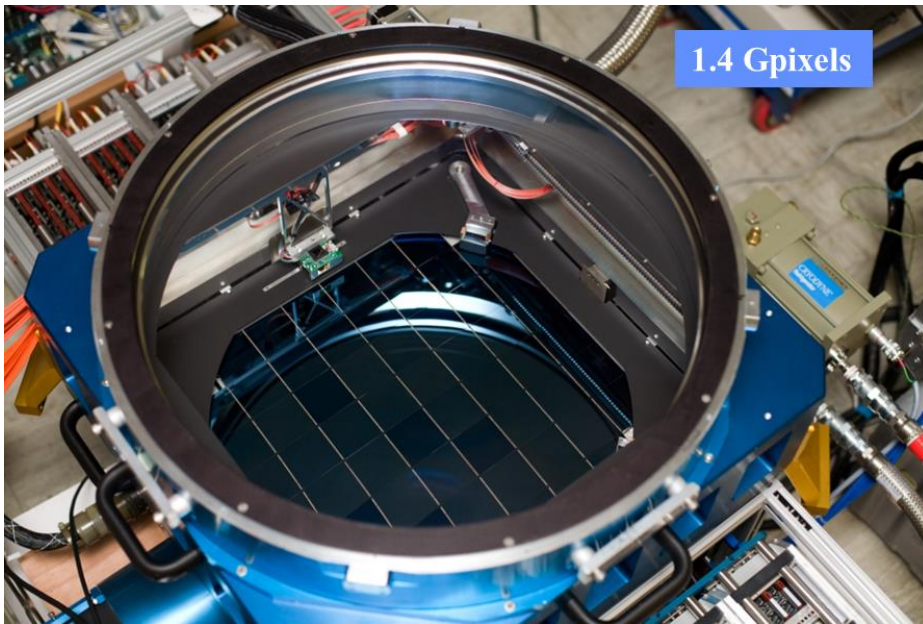


MEDICI 2-D simulation

MEDICI simulations
 Potential minimum (collecting phase)

Parallel to the DECam Development

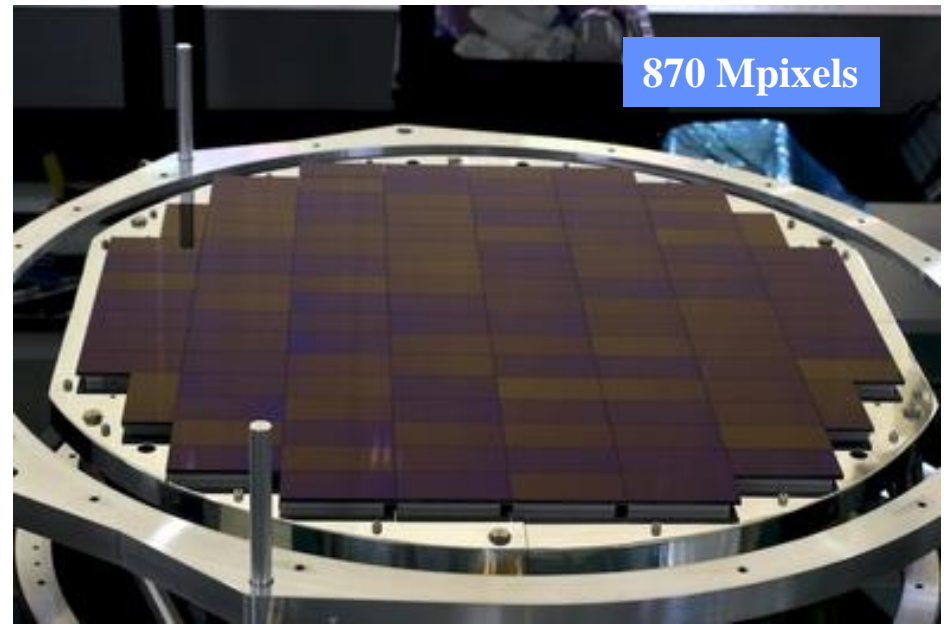
The Pan-STARRS and HyperSuprimeCam CCD cameras



PS1 camera – 60 5k x 5k, $(10 \mu\text{m})^2$ -pixels
Fabrication at MIT Lincoln Laboratory
(John Tonry, Barry Burke[†] et al)

75 μm thick, fully depleted CCDs

Pan-STARRS telescope (2010)







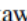







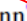


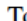



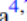

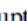
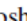
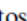

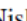
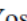
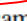
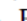



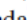
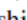
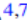

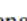
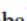
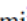
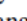
HyperSuprimeCam – 116 2k x 4k, $(15 \mu\text{m})^2$ -pixels
Fabrication at Hamamatsu Corporation
Satoshi Miyazaki, Yukiko Kamata et al

200 μm thick, fully depleted CCDs

Subaru 8-m Telescope (Fall 2012)

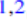


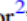
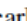


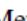
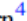






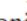









Subaru High- z Exploration of Low-luminosity Quasars (SHELLQs). XVI. 69 New Quasars at $5.8 < z < 7.0$

Yoshiki Matsuoka¹ , Kazushi Iwasawa² , Masafusa Onoue³ , Takuma Izumi⁴ , Nobunari Kashikawa⁵ , Michael A. Strauss⁶ , Masatoshi Imanishi^{4,7} , Tohru Nagao¹ , Masayuki Akiyama⁸ , John D. Silverman⁹ , Naoko Asami¹⁰, James Bosch⁶ , Hisanori Furusawa⁴ , Tomotsugu Goto¹¹, James E. Gunn¹ , Yuichi Harikane¹² , Hiroyuki Ikeda¹³ , Rikako Ishimoto⁵ , Toshihiro Kawaguchi¹⁴ , Nanako Kato¹⁵, Satoshi Kikuta¹⁶ , Kotaro Kohno^{17,18} , Yutaka Komiyama^{4,7} , Chien-Hsiu Lee¹⁹ , Robert H. Lupton⁶ , Takeo Minezaki¹⁷ , Satoshi Miyazaki^{4,7} , Hitoshi Murayama⁹ , Atsushi J. Nishizawa²⁰ , Masamune Oguri^{9,18,21} , Yoshiaki Ono¹² , Masami Ouchi^{9,12} , Paul A. Price⁶ , Hiroaki Sameshima¹⁷ , Naoshi Sugiyama^{9,22} , Philip J. Tait²³, Masahiro Takada⁹ , Ayumi Takahashi¹⁵ , Tadafumi Takata^{4,7} , Masayuki Tanaka^{4,7} , Yoshiki Toba²⁴ , Yousuke Utsumi²⁵ , Shiang-Yu Wang²⁶ , and Takuji Yamashita⁴ 








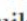

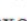













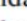



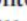


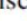
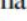





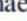

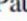



The Pan-STARRS1 $z > 5.6$ Quasar Survey. II. Discovery of 55 Quasars at $5.6 < z < 6.5$

Eduardo Bañados^{1,2} , Jan-Torge Schindler^{1,3} , Bram P. Venemans³ , Thomas Connor^{2,4,5} , Roberto Decarli⁶ , Emanuele Paolo Farina⁷ , Chiara Mazzucchelli⁸ , Romain A. Meyer¹ , Daniel Stern⁴ , Fabian Walter¹ , Xiaohui Fan⁹ , Joseph F. Hennawi^{3,10} , Yana Khusanova¹ , Nidia Morrell¹¹ , Riccardo Nanni³ , Gaël Noirot^{4,12} , Antonio Pensabene¹³ , Hans-Walter Rix¹ , Joseph Simon^{4,14} , Gijs A. Verdoes Kleijn¹⁵ , Zhang-Liang Xie (谢彰亮)¹ , Da-Ming Yang (羊达明)³ , and Andrew Connor¹⁶ 



DESI $z \gtrsim 5$ Quasar Survey. I. A First Sample of 400 New Quasars at $z \sim 4.7-6.6$

Jinyi Yang^{1,34} , Xiaohui Fan¹ , Ansh Gupta¹ , Adam D. Myers², Nathalie Palanque-Delabrouille^{3,4} , Feige Wang^{1,35} , Christophe Yèche⁴ , Jessica Nicole Aguilar³ , Steven Ahlen⁵ , David M. Alexander⁶ , David Brooks⁷ , Kyle Dawson⁸ , Axel de la Macorra⁹ , Arjun Dey¹⁰ , Govinda Dhungana¹¹ , Kevin Fanning^{12,13,14} , Andreu Font-Ribera¹⁵ , Satya Gontcho³ , Julien Guy³ , Klaus Honscheid^{13,16,17} , Stephanie Juneau¹⁰ , Theodore Kisner³ , Anthony Kremin³ , Laurent Le Guillou¹⁸ , Michael Levi³ , Christophe Magneville⁴ , Paul Martini^{13,16,19} , Aaron Meisner²⁰ , Ramon Miquel^{15,21} , John Moustakas²² , Jundan Nie²³ , Will Percival^{24,25,26} , Claire Poppett^{3,27,28} , Francisco Prada²⁹ , Edward Schlafly³⁰ , Gregory Tarle¹⁴ , Mariana Vargas Magana⁹ , Benjamin Alan Weaver²⁰ , Risa Wechsler^{31,32,33} , Rongpu Zhou³ , Zhimin Zhou²³ , and Hu Zou²³ 



red·shift

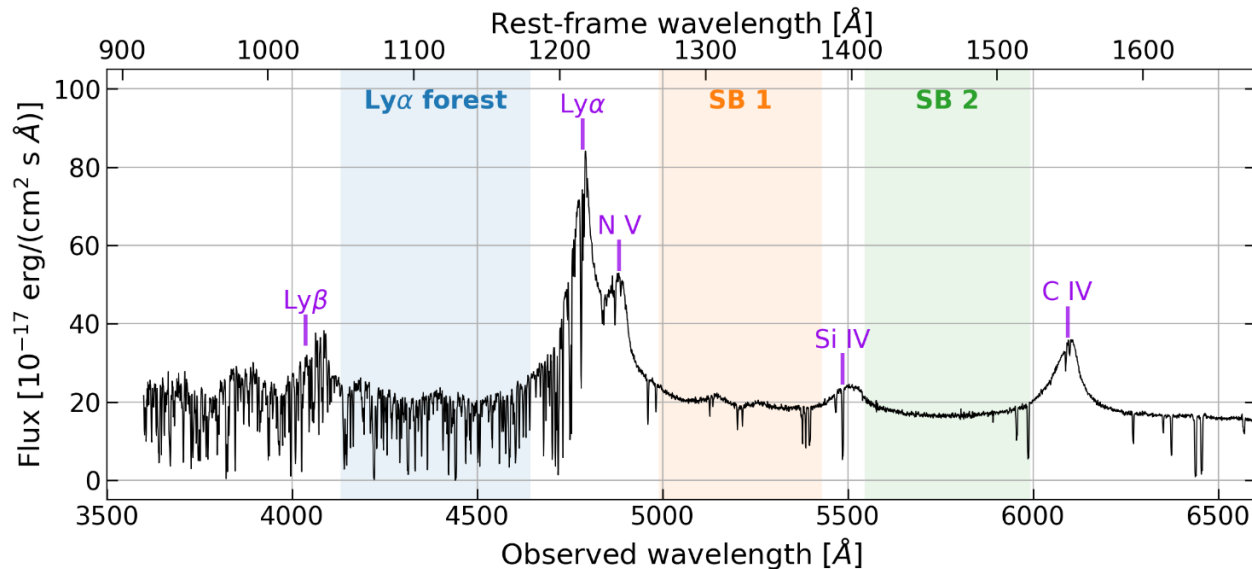
/ˈredˈʃɪft/

noun **ASTRONOMY**

noun: **red shift**; plural noun: **red shifts**; noun: **redshift**; plural noun: **redshifts**

the displacement of spectral lines toward longer wavelengths (the red end of the spectrum) in radiation from distant galaxies and celestial objects. This is interpreted as a Doppler shift that is proportional to the velocity of recession and thus to distance.

$$\text{Cosmological Redshift: } z + 1 = \frac{\lambda_{obs}}{\lambda_{rest}}$$



Quasar Redshift

Dark Energy Spectroscopic Instrument



DESI $z \gtrsim 5$ Quasar Survey. I. A First Sample of 400 New Quasars at $z \sim 4.7\text{--}6.6$

Yinyi Yang^{1,34}, Xiaohui Fan¹, Ansh Gupta¹, Adam D. Myers², Nathalie Palanque-Delabrouille^{3,4}, Feige Wang^{1,35},
Christophe Yèche⁴, Jessica Nicole Aguilar³, Steven Ahlen⁵, David M. Alexander⁶, David Brooks⁷, Kyle Dawson⁸,
Axel de la Macorra⁹, Arjun Dey¹⁰, Govinda Dhungana¹¹, Kevin Fanning^{12,13,14}, Andreu Font-Ribera¹⁵, Satya Gontcho³,
Julien Guy³, Klaus Honscheid^{13,16,17}, Stephanie Juneau¹⁰, Theodore Kisner³, Anthony Kremin^{3,15}, Laurent Le Guillou¹⁸,
Michael Levi³, Christophe Magneville⁴, Paul Martini^{13,16,19}, Aaron Meisner²⁰, Ramon Miquel^{15,21}, John Moustakas²²,
Jundan Nie²³, Will Percival^{24,25,26}, Claire Poppett^{3,27,28}, Francisco Prada²⁹, Edward Schlafly³⁰, Gregory Tarlé¹⁴,
Mariana Vargas Magana⁹, Benjamin Alan Weaver²⁰, Risa Wechsler^{31,32,33}, Rongpu Zhou³, Zhimin Zhou²³, and Hu Zou²³

Yang et al.

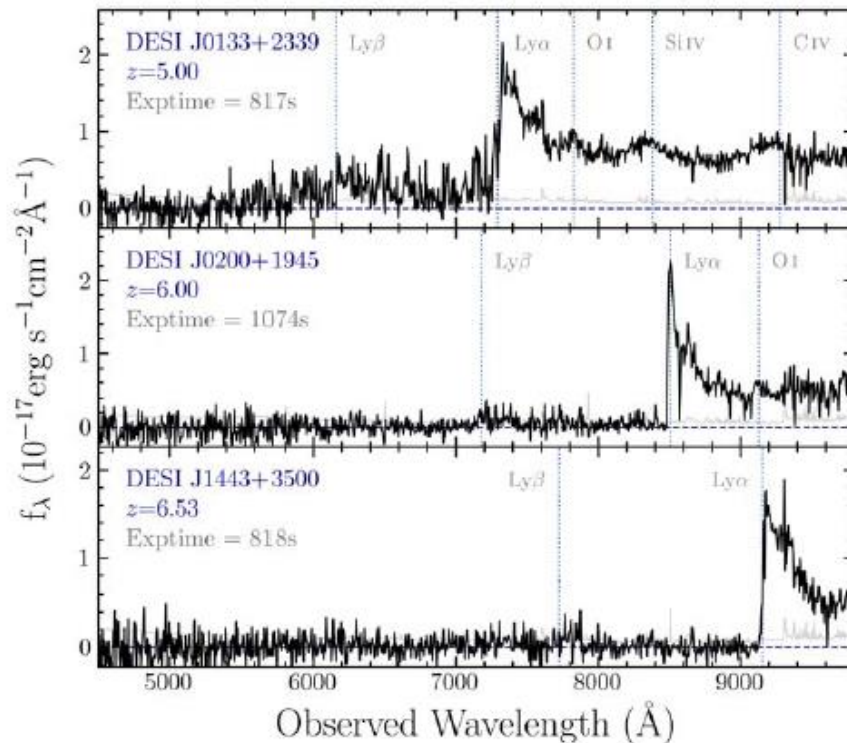


Figure 4. Examples of the DESI spectra for quasars at $z = 5, 6,$ and $6.5,$ binned with 7 pixels. The three spectra are from observations with $\sim 800\text{--}1000$ s actual exposure time. These three quasars are 20.55, 20.72, and 21.20 mag in the Legacy Survey z band. The quasar broad emission lines (i.e., $\text{Ly}\beta$, $\text{Ly}\alpha$, O I, Si IV, and C IV) used for redshift measurements are marked with blue dotted lines. The spectra of all 412 new quasars are shown in Figure 7.

H $\text{Ly}\alpha$ emission $\lambda_{\text{rest}} = 1216\text{\AA}$:
Quasars (Active Galactic Nuclei) &
 $\text{Ly}\alpha$ Galaxies

Thick CCDs can detect $\text{Ly}\alpha$
emission to $z \sim 7$

High near-IR QE
Negligible fringing

DECam detection of $Z \sim 7$ galaxies

THE ASTROPHYSICAL JOURNAL, 934:167 (7pp), 2022 August 1

<https://doi.org/10.3847/1538-4357/ac7cfl>





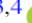











© 2022. The Author(s). Published by the American Astronomical Society.

OPEN ACCESS



CrossMark

New Spectroscopic Confirmations of $\text{Ly}\alpha$ Emitters at $Z \sim 7$ from the LAGER Survey

Santosh Harish¹ , Isak G. B. Wold² , Sangeeta Malhotra² , James E. Rhoads² , Weida Hu^{3,4} , Junxian Wang^{3,4} ,
Zhen-ya Zheng⁵ , L. Felipe Barrientos⁶ , Jorge González-López^{6,7} , Lucia A. Perez¹ , Ali Ahmad Khostovan²,
Leopoldo Infante⁸ , Chunyan Jiang⁵ , Cristóbal Moya-Sierralta⁶ , John Pharo¹ , Francisco Valdes⁹ , and Huan Yang⁸ 

¹School of Earth and Space Exploration, Arizona State University, Tempe, AZ 85287, USA; santosh.harish@asu.edu

²Astrophysics Science Division, NASA Goddard Space Flight Center, 8800 Greenbelt Road, Greenbelt, Maryland, 20771, USA

³CAS Key Laboratory for Research in Galaxies and Cosmology, Department of Astronomy, University of Science and Technology of China, Hefei, Anhui 230026, People's Republic of China

⁴School of Astronomy and Space Science, University of Science and Technology of China, Hefei 230026, People's Republic of China

⁵CAS Key Laboratory for Research in Galaxies and Cosmology, Shanghai Astronomical Observatory, Shanghai 200030, People's Republic of China

⁶Instituto de Astrofísica, Facultad de Física, Pontificia Universidad Católica de Chile, Santiago, Chile

⁷Núcleo de Astronomía de la Facultad de Ingeniería y Ciencias, Universidad Diego Portales, Av. Ejército Libertador 441, Santiago, Chile

⁸Las Campanas Observatory, Carnegie Institution of Washington, Casilla 601, La Serena, Chile

⁹National Optical Astronomy Observatory, 950 N. Cherry Avenue, Tucson, AZ 85719, USA

Received 2021 October 28; revised 2022 June 13; accepted 2022 June 29; published 2022 August 4

$\text{Ly}\alpha$ Galaxies in the Epoch of Reionization (LAGER)

Spectroscopic confirmation of 15 $Z \sim 7$ $\text{Ly}\alpha$ galaxies

Narrow band filter tuned to $\text{Ly}\alpha$ at $Z \sim 7$ (DECam)

Follow up spectroscopy at Keck/LRIS

500 um thick, fully depleted CCDs (DALSA/LBNL)

DECam detection of $Z \sim 7$ galaxies

THE ASTROPHYSICAL JOURNAL, 934:167 (7pp), 2022 August 1

<https://doi.org/10.3847/1538-4357/ac7cfl>

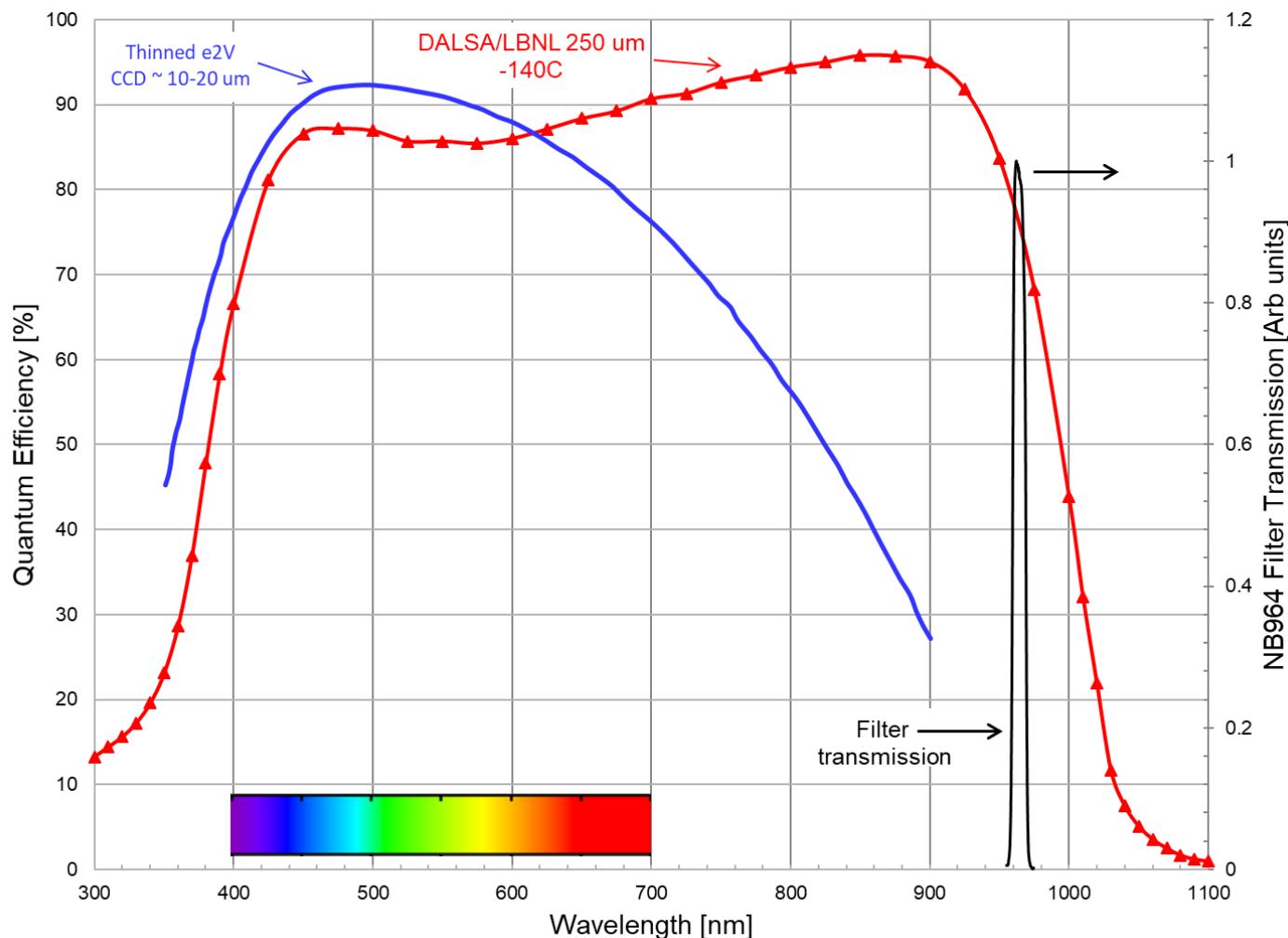
© 2022. The Author(s). Published by the American Astronomical Society.



OPEN ACCESS



CrossMark

New Spectroscopic Confirmations of $\text{Ly}\alpha$ Emitters at $Z \sim 7$ from the LAGER Survey



inxian Wang^{3,4} ,
ad Khostovan²,
, and Huan Yang⁸ 
i.edu
771, USA
hina, Hefei, Anhui 230026,
iblic of China
's Republic of China
Santiago, Chile



The Nobel Prize in Physics 2011

The Nobel Prize in Physics 2011

Saul Perlmutter
Brian P. Schmidt
Adam G. Riess

Share this



© The Nobel Foundation. Photo:
U. Montan

Saul Perlmutter

Prize share: 1/2



© The Nobel Foundation. Photo:
U. Montan

Brian P. Schmidt

Prize share: 1/4



© The Nobel Foundation. Photo:
U. Montan

Adam G. Riess

Prize share: 1/4

The Nobel Prize in Physics 2011 was divided, one half awarded to Saul Perlmutter, the other half jointly to Brian P. Schmidt and Adam G. Riess "for the discovery of the accelerating expansion of the Universe through observations of distant supernovae"

The discovery of "Dark Energy"

Supernova Cosmology from the Dark Energy Survey

*Cosmology Results With ~1500 New High-redshift Type Ia Supernovae
Using The Full 5-year Dataset*

<https://arxiv.org/abs/2401.02929>

Phil Wiseman (he/his) on behalf of the
DES Supernova Working Group

<https://arxiv.org/abs/2401.02945>



Maria Vincenzi, Dillon Brout
Cosmology Analysis Leads



U.S. DEPARTMENT OF
ENERGY

Office of
Science¹

- DES Supernova talk from the 2024 AAS Meeting
- ~ 1500 Type 1a Supernovae spectroscopically confirmed
 - Compare to 42 for the original Berkeley group report
 - Supernova Cosmology Project (SCP)

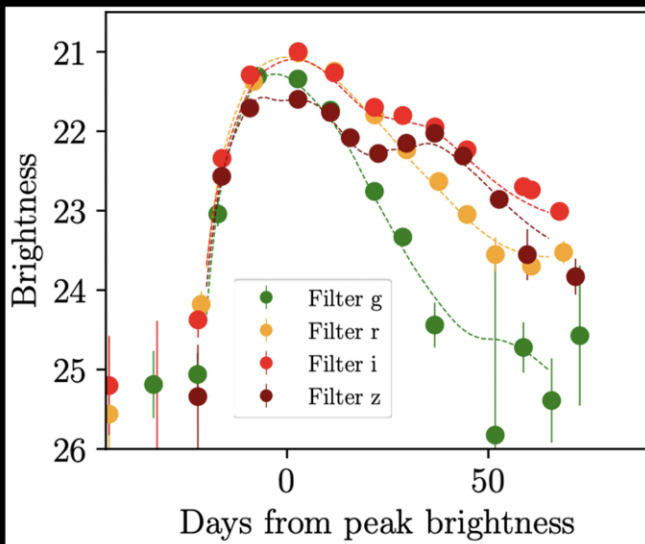
The Dark Energy Survey Supernova program: data

Data

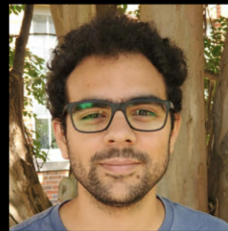
- Photometry and light curves
- Host galaxies

Accurate PSF photometry using *Scene Modelling* technique

Brout+19, Sanchez+in prep

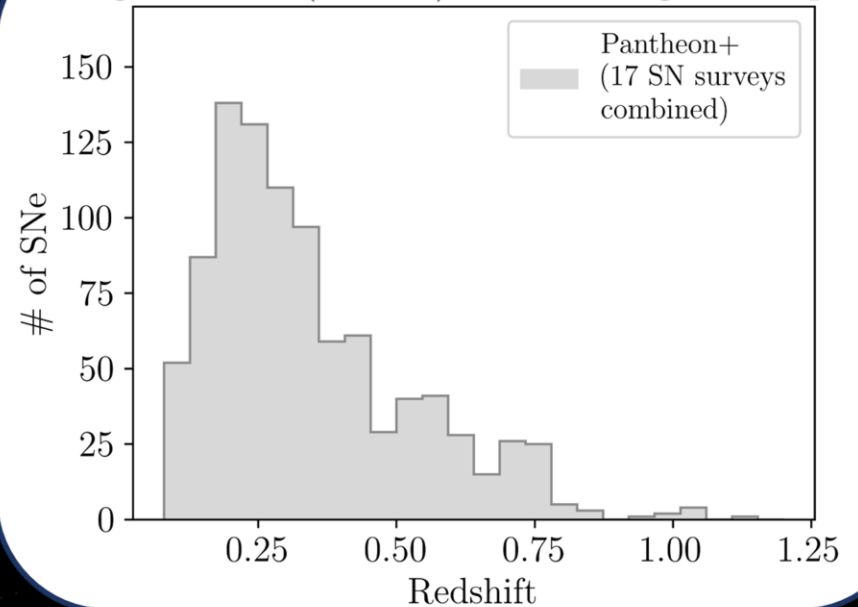


Dillon Brout



Bruno Sanchez

High redshift ($z > 0.1$) SN cosmological samples



The Dark Energy Survey Supernova program: data

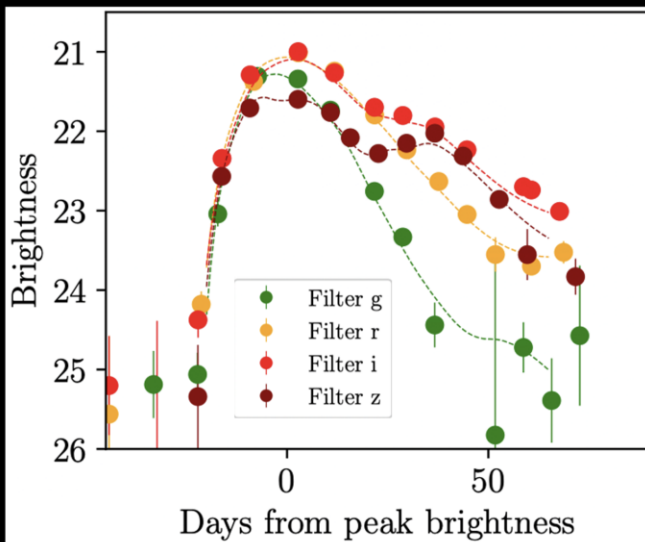
OzDES@AAT: Lidman+20

Data

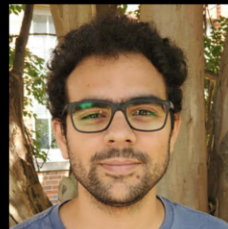
- Photometry and light curves
- Host galaxies

Accurate PSF photometry using Scene Modelling technique

Brout+19, Sanchez+in prep



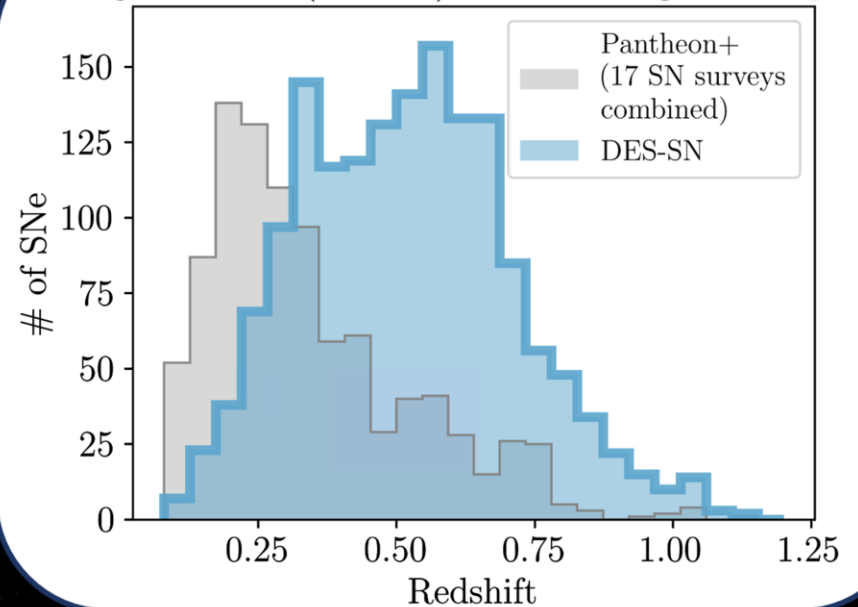
Dillon Brout



Bruno Sanchez

1499 likely SNe Ia with host-z

High redshift ($z > 0.1$) SN cosmological samples



Largest high-z sample from a single telescope

Large population of high redshift supernovae
Enabled by DECam and the near-infrared sensitive CCDs

2021-Present

Referenced Publications using data from the Dark Energy Camera (DECAM), Blanco Telescope, CTIO, FY23-present are available in the following ADS Public Library

2020

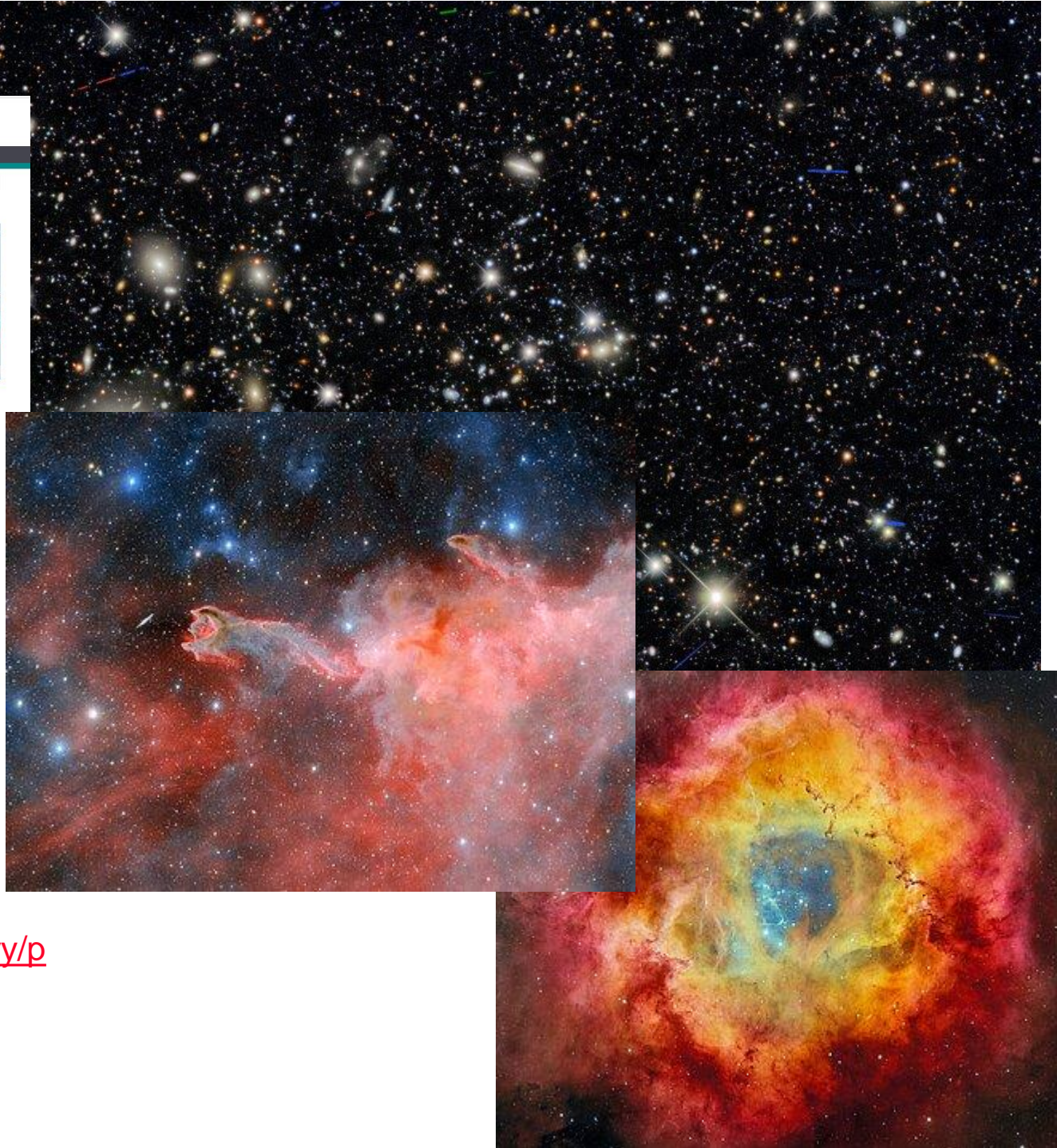
Community papers:

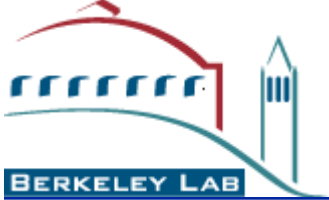
- Anderson et al. (2020), *MNRAS*, 491, 5852. Probing the average galaxy size transition by an infrared time-scales with DECAM
- Anderson et al. (2020), *AstJ*, 890, 118. CROWTH on S9030/Rev. Deep Synoptic Lines on the Optical/Near-Infrared Counterpart to a Neutron-Star-Black Hole Merger
- Baracca et al. (2020), *AstJ*, 899, 70. Variations in the Width, Density, and Direction of the Helium γ Triplet
- Calzetti et al. (2020), *AstJ*, 891, 302. The Near-Infrared Stellar Stream Drifts: Can a Evidence in Support of a Merging Scenario
- Chender et al. (2020), *AstJ*, 892, 138. Co-spatial Activity Discovered on a Distant Carinae: A Nonaqueous Sublimation Mechanism
- Chen et al. (2020), *AstJ*, 895, 16. The Most Recently Discovered Type I Supernova 2019qk/LC1007
- Cheng et al. (2020), *MNRAS*, 493, 4209. Optimizing automatic morphological classification of galaxies with machine learning and deep learning using Dark Energy Survey Imaging
- Coppoletta et al. (2020), *MNRAS*, 496, 123. A Milky Way-like Outflow from the Emergent, Post-Flaring Blue Optical Transient CSD4000 in a Dwarf Galaxy
- Courbin et al. (2020), *MNRAS*, 492, 263. Implications of the search for optical counterparts during the first six months of the Advanced LIGO and Advanced Virgo gravitational-wave observations: run possible limits on the compact mass and binary properties
- Ebinov et al. (2020), *ASA*, 634, 472. Small galaxy host of CWF0201: constraints on the recent galactic merger
- Fahnenstiel et al. (2020), *ASA*, 634, 453. Metal-poor nuclear star clusters in two dwarf galaxies near Centaurus A suggesting formation from the in-spiraling of globular clusters
- Galdo et al. (2020), *MNRAS*, 492, 1735. Search for the optical counterpart of the CWF0201 gravitational wave event with the VLT Survey Telescope
- Haveli et al. (2020), *MNRAS*, 493, 3954. Comparison of galaxy color-arm length measurements using manual and automated techniques
- Huang et al. (2020), *AstJ*, 894, 78. Finding Strong Gravitational Lenses in the DES/DECAM Legacy Survey
- Ji et al. (2020), *AstJ*, 895, 27. Unusual Absorptions in the Ultra-rare Magnetar SGR1806+09
- Johnson et al. (2020), *MNRAS*, 495, 2247. The Next Generation Fornax Survey (NGFS) VI. A MUSE View of the nuclear star clusters in Fornax dwarf galaxies
- Karapetrović et al. (2020), *MNRAS*, 493, 5496. An exceptionally massive thick disc of the anomalous edge-on irregular galaxy NGC 7572
- Kauramäkelä et al. (2020), *AstJ*, 893, 7. On the Bulk Off-Evaluation of the Stellar Mass Function of Massive Galaxies from $z = 1.5$ to 0.4
- Khosrowan et al. (2020), *MNRAS*, 493, 3966. A large, deep 3 deg² survey of H α , [OIII], and [OII] emitters from IACER: constraining luminosity functions
- Kim et al. (2020), *AstJ*, 894, 56. Gemini Multi-Object Spectrograph Integral Field Line Spectroscopy of the Double-peaked Broad Emission Line of a Red Active Galactic Nucleus
- Kormendy et al. (2020), *MNRAS*, 492, 2262. Imaging, spectroscopy, and clustering of DES main galaxies
- Luo et al. (2020), *MNRAS*, 494, 3686. Characterization of optical light curves of astrometric variability quasars over a ~ 16 -yr baseline
- Mészáros et al. (2020), *MNRAS*, 492, 4906. Search for LSST Targets with DECAM
- Morante-Palomera et al. (2020), *AstJ*, 893, 181. Introducing the Search for Intermediate-mass Black Holes in Nearby Galaxies (SHINE) Survey
- Muu et al. (2020), *AstJ*, 893, 136. Two Ultra-Faint Milky Way Stellar Systems Discovered in Early Data from the DECAM Local Volume Exploration Survey
- McNamara et al. (2020), *AstJ*, 893, 8. Dark Matter Distribution of Four Low- z Clusters of Galaxies
- Muñoz-Chávez et al. (2020), *MNRAS*, 491, 2020. Revisiting the merger scenario of the galaxy cluster Abell 1644: a new gas poor structure discovered by weak gravitational lensing
- Mészáros and Walter (2020), *MNRAS*, 492, 2262. Stellar Density Profiles of Dwarf Spheroidal Galaxies
- Palanca et al. (2020), *ASA*, 634, 448. MAXIMASH and MAXITRACK: Two new tools for identifying contaminants in astronomical images using convolutional neural networks
- Palumbo et al. (2020), *MNRAS*, 494, 4700. Linking compact dwarf star-forming galaxies in the DES/VI survey to downsized blue magpies
- Pálfi et al. (2020), *AstJ*, 894, 168. Assessment of Size Distribution and Colors from HETU
- Phibbs et al. (2020), *MNRAS*, 491, 164. Weak lensing analysis of CDFSD clusters using dark energy camera galaxy survey mass-richness relation
- Prati and Ferraro (2020), *ASA*, 634, 469. The $z = 0$ moderately over-dense low-density halo and its accretion history
- Priebe et al. (2020), *AstJ*, 895, 100. Variable H α Emission in the Nebular Spectra of the Low-luminosity Type Ia SN2018gwt/LA3010
- Rimkus et al. (2020), *AstJ*, 894, 36. A New Sample of (Wandering) Massive Black Holes in Dwarf Galaxies from High-resolution Spitzer Observations
- Roache et al. (2020), *MNRAS*, 495, 1021. Improving galaxy clustering measurements with deep learning: analysis of the DES/LSST data
- Sherman et al. (2020), *MNRAS*, 491, 1378. Exploring the high-mass end of the stellar mass function of star-forming galaxies at cosmic noon
- Soriccani et al. (2020), *AstJ*, 892, 52. A Classification Algorithm for Time-domain Newbies in Preparation for LSST Alerts: Application to Variable Stars and Transients Detected with DECAM in the Carinae Field
- Taniguchi et al. (2020), *MNRAS*, 491, 2636. Optimizing galaxy samples for clustering measurements in photometric surveys
- Tian, Wei and Prochaska (2020), *MNRAS*, 493, 3954. Constraining Magnetic Fields in the Chromospheric Medium
- Vokroucký et al. (2020), *Astronomy and Computing*, 30, 100396. Mega-Archive and the EUROEAR tools for data mining world astronomical images
- Vivas et al. (2020), *AstJ*, 895, 16. A Deep CFHT Optical Search for Counterparts to the Resolved Neutron-Star-Black Hole Merger CWF0201
- Vivas et al. (2020), *MNRAS*, 493, 1085. A DECAM View of the SFR100 dwarf galaxy Centaurus A: Variable stars
- Young et al. (2020), *MNRAS*, 495, 3693. Atomic Hydrogen clues to the formation of counterwinding stellar discs
- Zentgraf et al. (2020), *MNRAS*, 495, 1026. A new optical analysis of the dynamical states of 289 massive galaxy clusters
- Zucker et al. (2020), *ASA*, 634, 453. A compendium of distances to molecular clouds in the Star Formation Handbook

Papers from the Dark Energy Survey (DES) Collaboration:

- Bernardini et al. (2020), *ApJS*, 242, 32. Trans-Neptunian Objects Found in the First Four Years of the Dark Energy Survey
- Blum et al. (2020), *ApJS*, 242, 25. The SPH4D Extended Cluster Survey
- de Jaeger et al. (2020), *MNRAS*, 495, 4660. Studying Type II Supernovae as Cosmological Standard Candles Using the Dark Energy Survey
- Dines-Wagner et al. (2020), *AstJ*, 893, 67. Milky Way Satellite Carinae. I. The Observational Selection Function for Milky Way Satellites in DES-Y3 and Pan-STARRS DR1

<https://noirlab.edu/science/library/publications/dark-energy-camera/decam-science-papers>





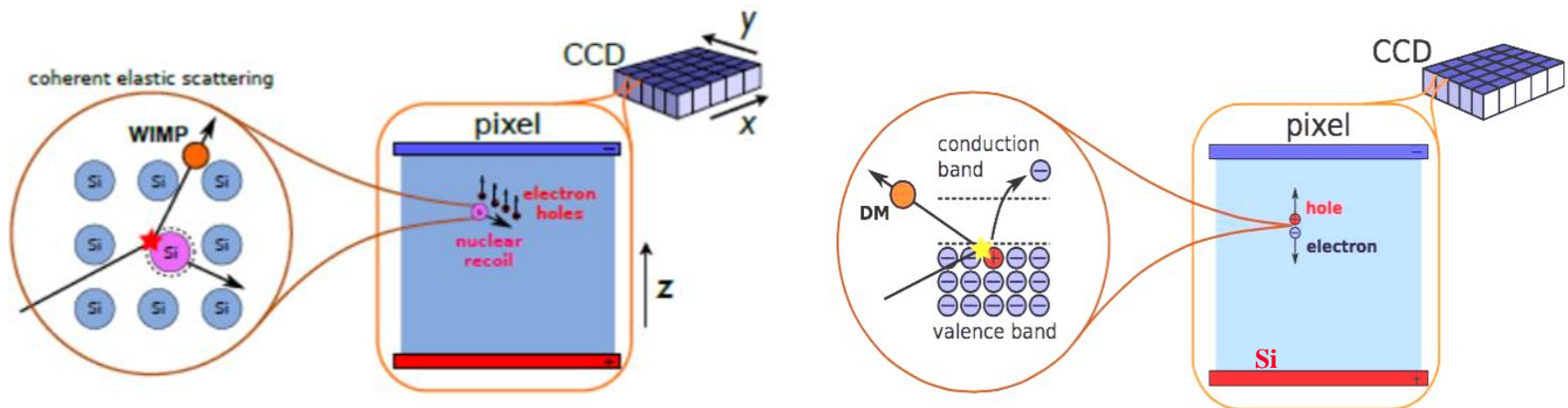
Remainder of the talk

- Invention of the CCD
- Brief history of scientific CCD development
- Fully depleted CCDs
 - Light absorption / charge generation
 - High red-shift Quasar & SuperNovae detection
- **CCDs for Dark Matter**

Dark Matter detection with CCDs

Proposed by Juan Estrada et al of FermiLab (2008)

- <https://doi.org/10.48550/arXiv.1105.5191>
- Thick CCDs for larger mass/CCD
- Low noise / improves low-energy detection threshold
 - Si bandgap ~ 1.1 eV
 - Electron counting with Skipper CCD readout amplifiers



- Nuclear recoil (left) or scattering off electrons (right)

Dark Matter detection with CCDs

1st underground engineering run / one 4 Mpixel DECam CCD

- <https://doi.org/10.1016/j.physletb.2012.04.006>

Physics Letters B 711 (2012) 264–269

Contents lists available at SciVerse ScienceDirect

Physics Letters B

www.elsevier.com/locate/physletb

Direct search for low mass dark matter particles with CCDs

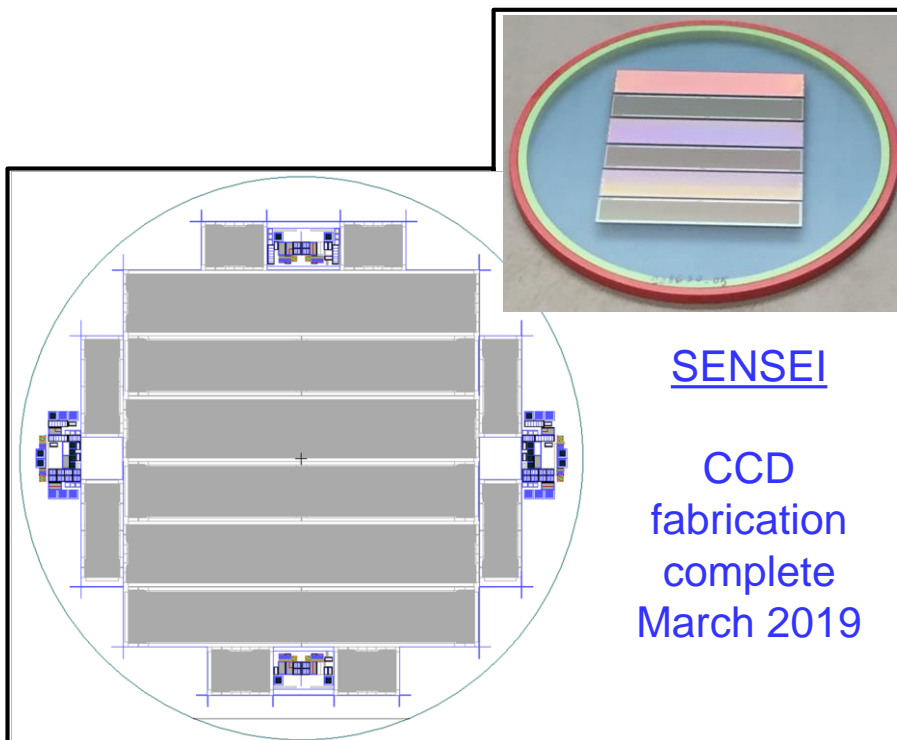
J. Barreto^a, H. Cease^b, H.T. Diehl^b, J. Estrada^{b,*}, B. Flaugher^b, N. Harrison^b, J. Jones^b, B. Kilminster^b, J. Molina^c, J. Smith^b, T. Schwarz^d, A. Sonnenschein^b

^a Universidade Federal do Rio de Janeiro (UFRJ), Rio de Janeiro, Brazil
^b Fermi National Accelerator Laboratory, Batavia, IL, USA
^c Facultad de Ingeniería, Universidad Nacional de Asunción (FIUNA), Asunción, Paraguay
^d University of California at Davis, CA, USA

<p>ARTICLE INFO</p> <p><i>Article history:</i> Received 6 July 2011 Received in revised form 31 March 2012 Accepted 2 April 2012 Available online 3 April 2012 Editor: S. Dodelson</p>	<p>ABSTRACT</p> <p>A direct dark matter search is performed using fully-depleted high-resistivity CCD detectors. Due to their low electronic readout noise (R.M.S. ~ 7 eV) these devices operate with a very low detection threshold of 40 eV, making the search for dark matter particles with low masses (~ 5 GeV) possible. The results of an engineering run performed in a shallow underground site are presented, demonstrating the potential of this technology in the low mass region.</p> <p>Published by Elsevier B.V. Open access under CC BY license.</p>
---	--

- 2 e- noise (2012) \Rightarrow now deep sub-electron (Skipper CCDs)
- 250 μm thick (2012) \Rightarrow now 650-725 μm (all fully depleted)
- Dark current orders of magnitude less than astronomy CCDs
- All processing at foundry
 - “Inexpensive”
- SENSEI / DAMIC-M / OSCURA are 0.1/1/10 kg scale

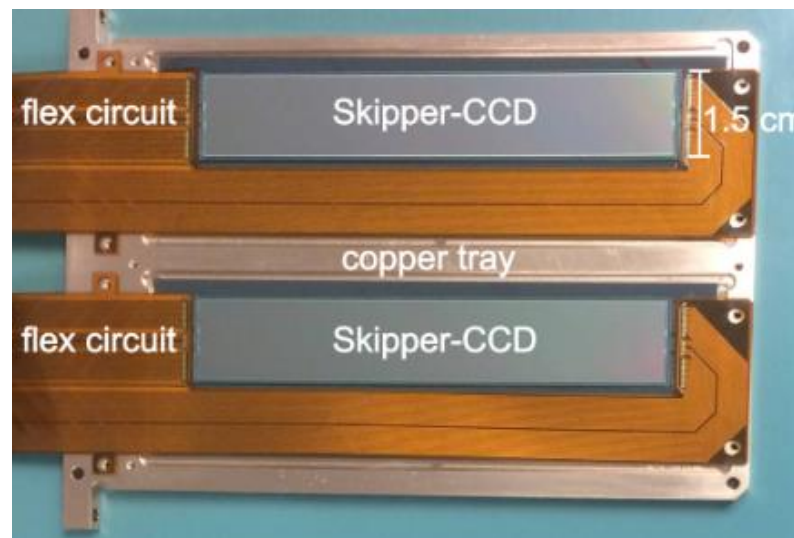
CCD development for Dark Matter



SENSEI

CCD
fabrication
complete
March 2019

SENSEI@SNOLAB



SENSEI@SNOLAB
2 km underground
100 g scale experiment
1 lot of 25 wafers
Full fabrication at DALSA
6k x 1k / $(15 \text{ } \mu\text{m})^2$ / 650 μm thick
100 g scale

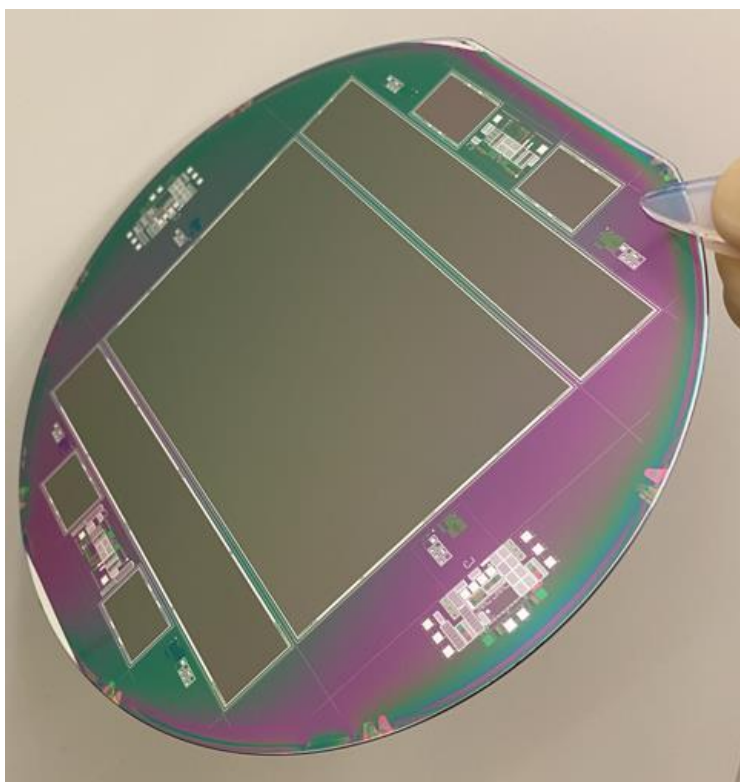


Copper cryostat

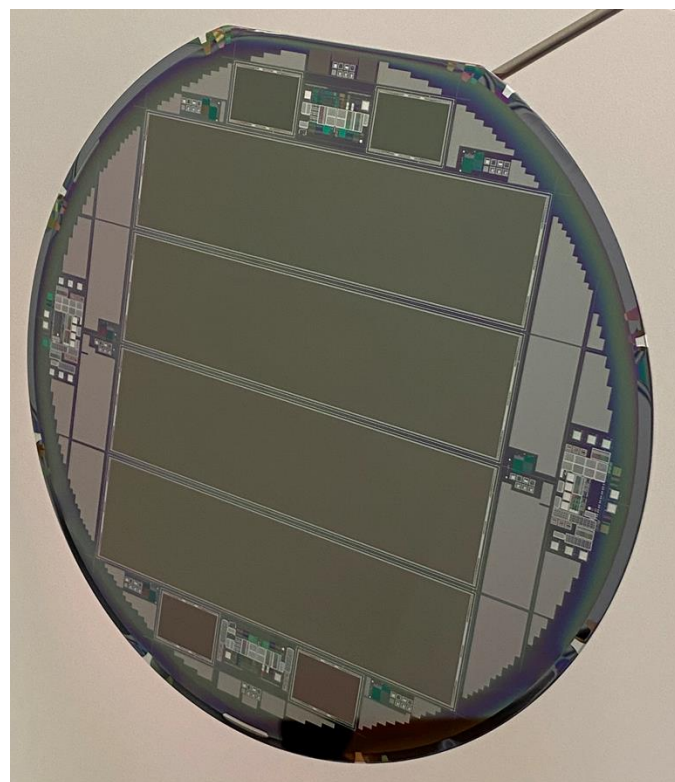


Lead shield

CCD development for Dark Matter

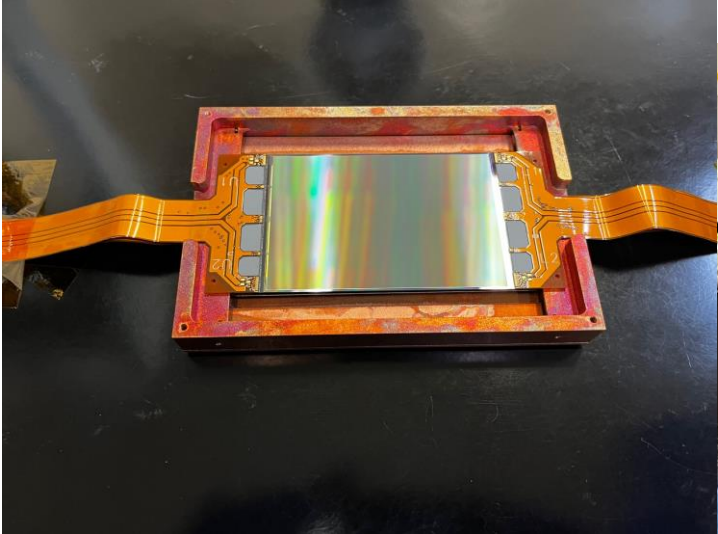


DAMIC-M R&D CCDs
650 um thick, fully depleted CCDs
150-mm wafers
6k x 4k's in use at SNOLAB



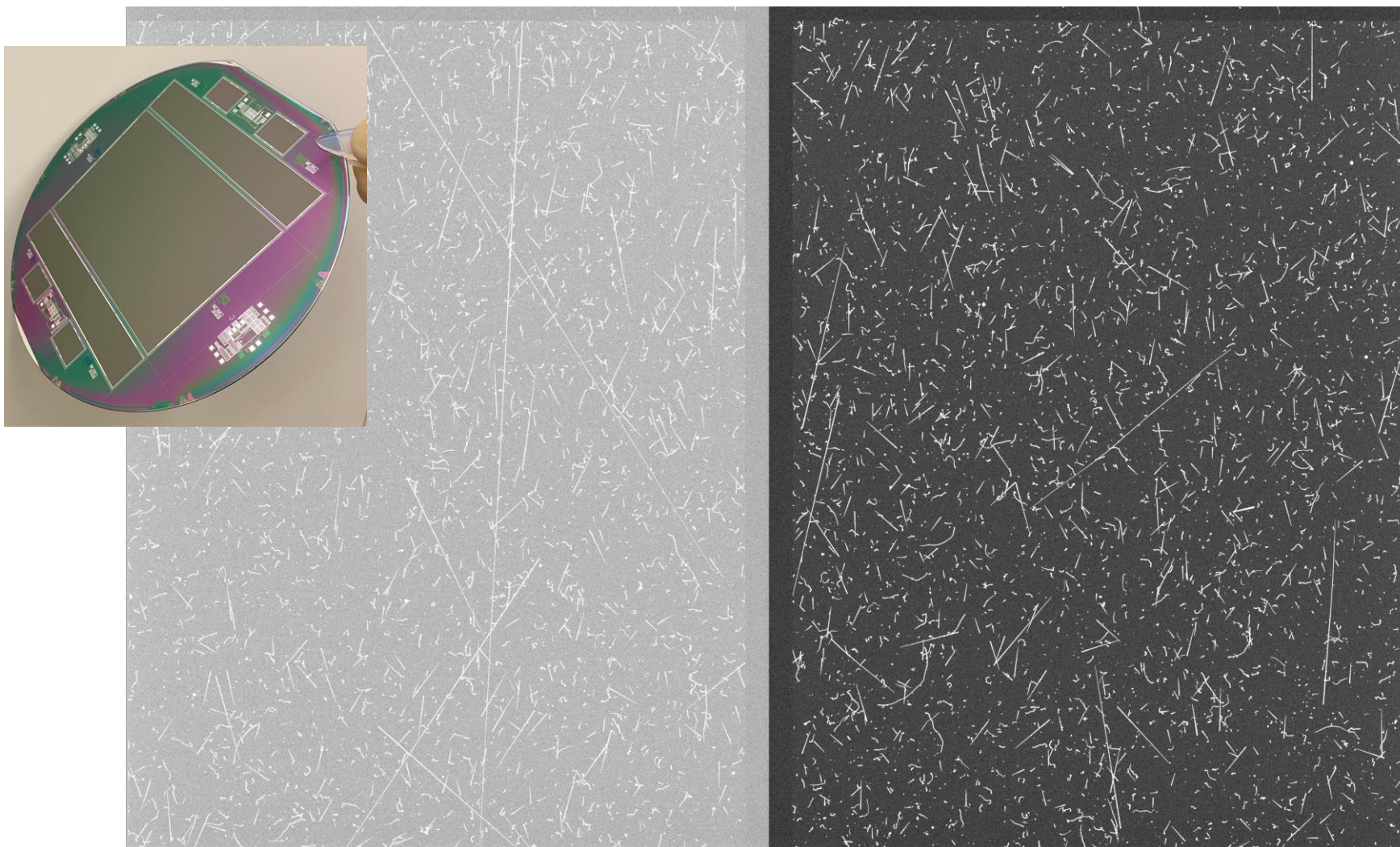
DAMIC-M production CCDs
1 kg scale dark matter
DALSA production complete

See DAMIC-M web site
<https://damic.uchicago.edu/>



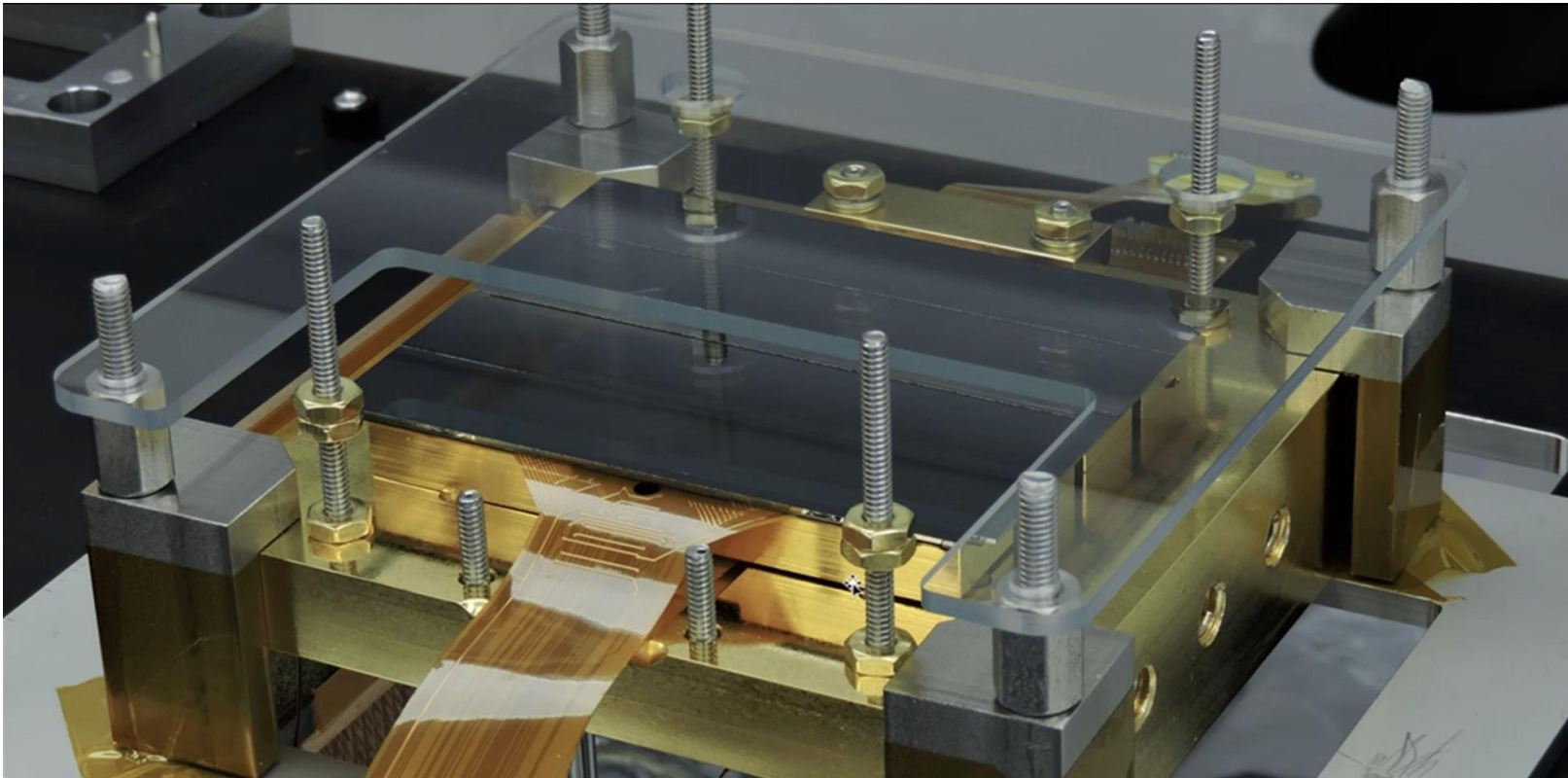
6k x 4k CCD for DAMIC@SNOLAB / Alvaro Chavarria (U Washington)

580 um thick, back-illuminated CCD



LBNL-processed 6k x 4k CCD: Thin n+ backside contact / no AR
1 hour dark / 60V / 120K
University of Chicago

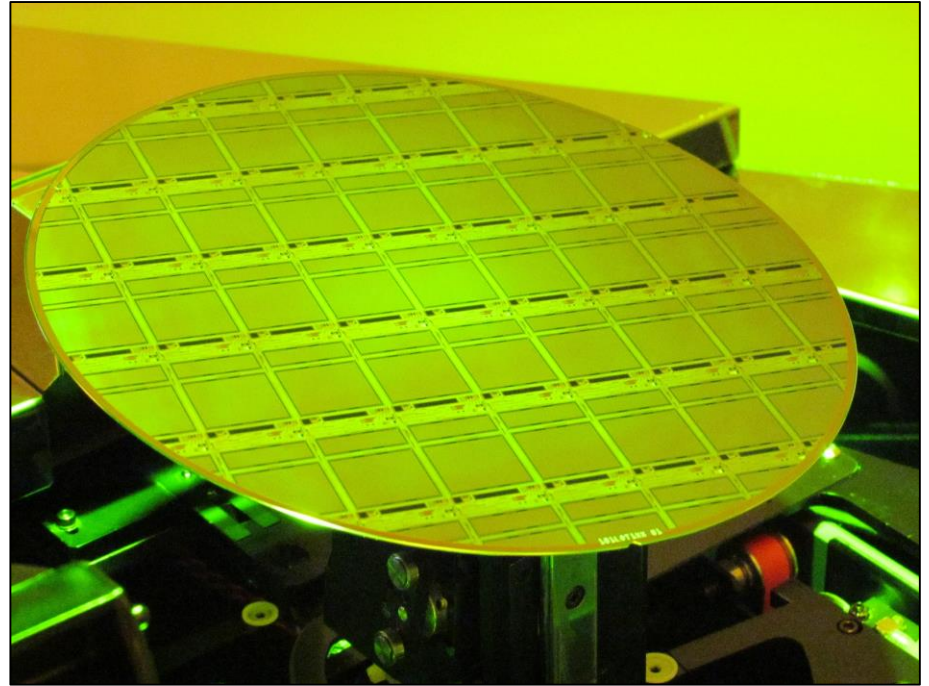
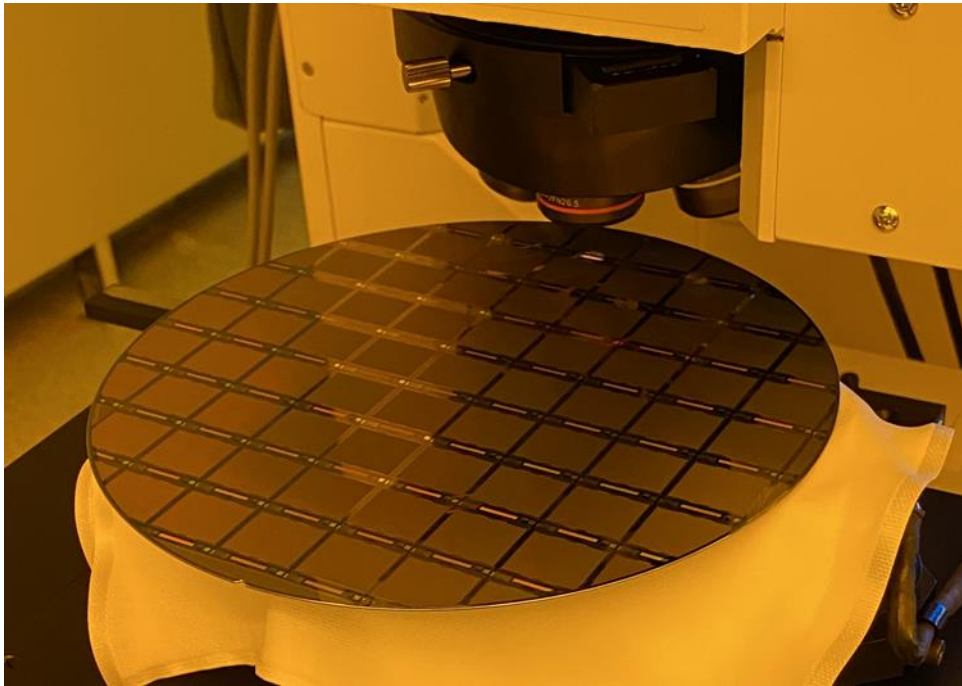
^3H detection with thick, BI, FD CCDs



- GRAIL focal plane for radiation detection (PNNL)
 - 4 1k x 6k, 580-um thick back-illuminated CCDs
 - Mix of finishing at LBNL and Lincoln Laboratory
 - Lincoln Labs molecular-beam epitaxy backside

OSCURA

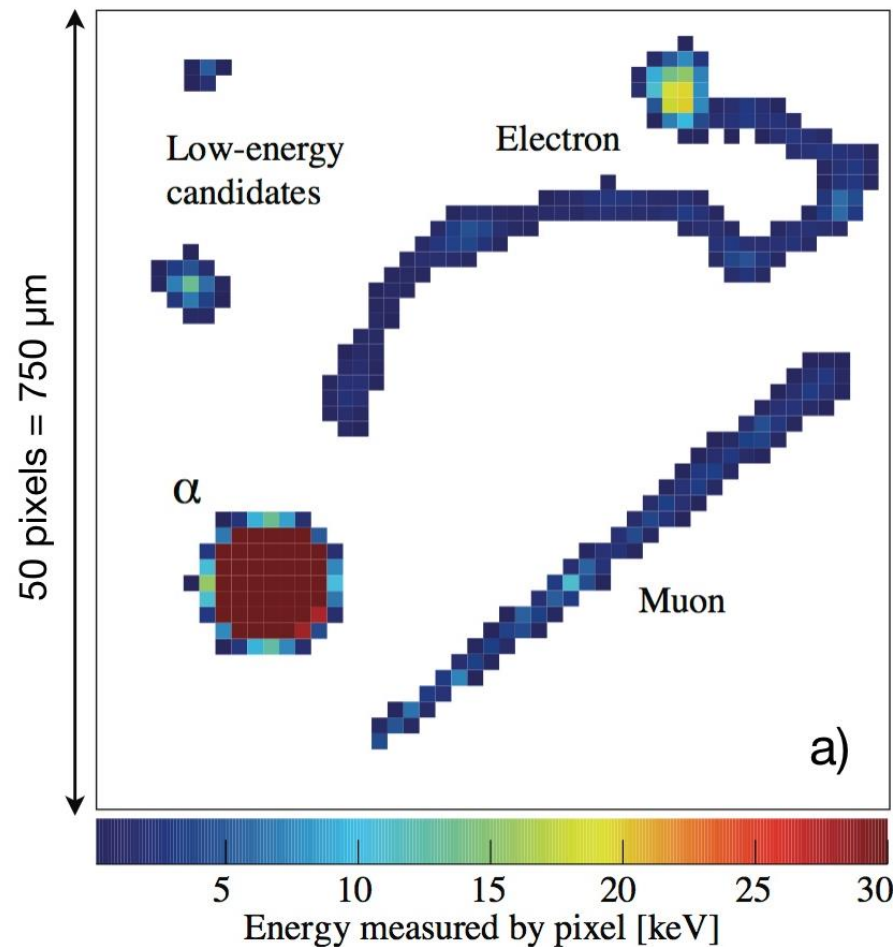
Observatory of Skipper CCDs Unveiling Recoiling Atoms



- Technology transfer of the LBNL p-channel fully depleted technology to Microchip Technology (above left) and Lincoln Laboratory (above right)
 - 200 mm wafers with step-and-repeat photolithography
 - 10 kg scale (~20k 1Mpix CCDs, 10x more pixels than Rubin/LSST)

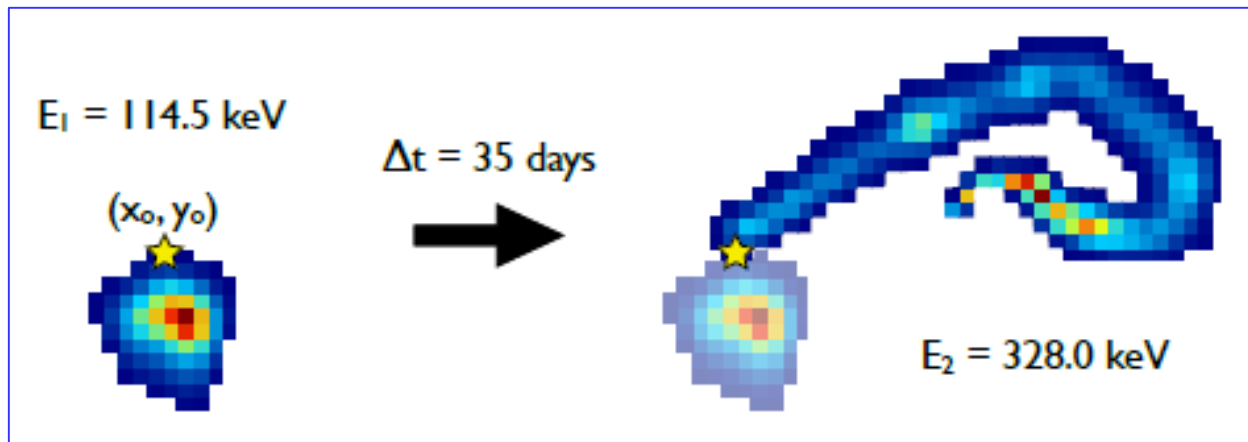
Dark Matter detection with CCDs

- Fully depleted CCDs for dark-matter detection cont'
 - Particle identification for background suppression
 - Spatial correlation and energy measurement



Dark Matter detection with CCDs

- Fully depleted CCDs for dark-matter detection cont'
 - Radioactive contamination in the silicon substrate
 - Decay chain products spatially correlated (double β event below)



Jinst

PUBLISHED BY IOP PUBLISHING FOR SISSA MEDIALAB

RECEIVED: June 9, 2015
ACCEPTED: July 11, 2015
PUBLISHED: August 25, 2015

Measurement of radioactive contamination in the high-resistivity silicon CCDs of the DAMIC experiment

The DAMIC collaboration

A. Aguilar-Arevalo,^a D. Amidei,^b X. Bertou,^c D. Bole,^b M. Butner,^{d,j} G. Canceled,^d A. Castañeda Vázquez,^a A.E. Chavarria,^{e,1} J.R.T. de Mello Neto,^f S. Dixon,^e J.C. D'Olivo,^a J. Estrada,^d G. Fernandez Moroni,^d K.P. Hernández Torres,^a F. Izraelevitch,^d A. Kavner,^b B. Kilminster,^e I. Lawson,^b J. Liao,^g M. López,ⁱ J. Molina,ⁱ G. Moreno-Granados,^g J. Pena,^e P. Privitera,^e Y. Sarkis,^e V. Scarpine,^d T. Schwarz,^b M. Sofo Haro,^c J. Tiffenberg,^d D. Torres Machado,^f F. Trillaud,^e X. You^f and J. Zhou^e

- Candidate $^{32}\text{Si} - ^{32}\text{P}$ event
- Cosmogenic activation of silicon
- Rejected by spatial / energy / decay time correlation

<https://iopscience.iop.org/article/10.1088/1748-0221/10/08/P08014>



Key developments for Dark Matter CCDs

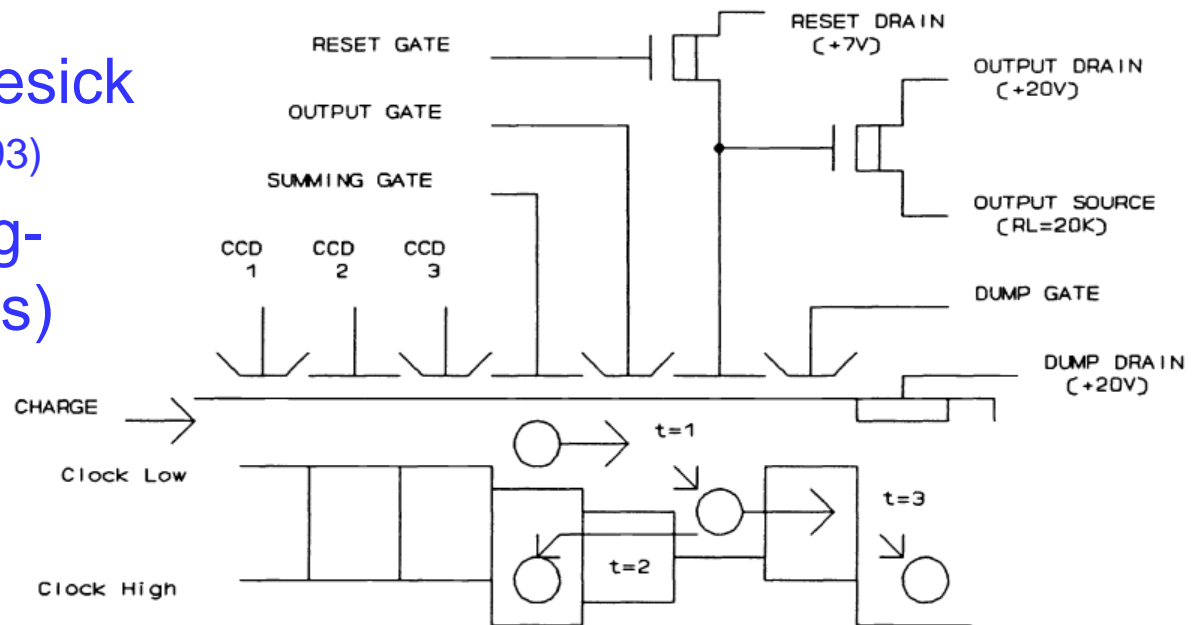
- Single-electron counting
 - Skipper CCD amplifiers
- High-voltage compatible CCD design / Very high-resistivity Float-zone silicon
- Gettering for low dark current
 - Single-electron event rate

Skipper CCDs for Dark Matter Detection

- Invented by Jim Janesick
 - U.S. patent 5250824 (1993)
- Based on the floating-gate amplifier (1970's)

<https://doi.org/10.1117/12.19452>

<https://doi.org/10.1117/12.19457>

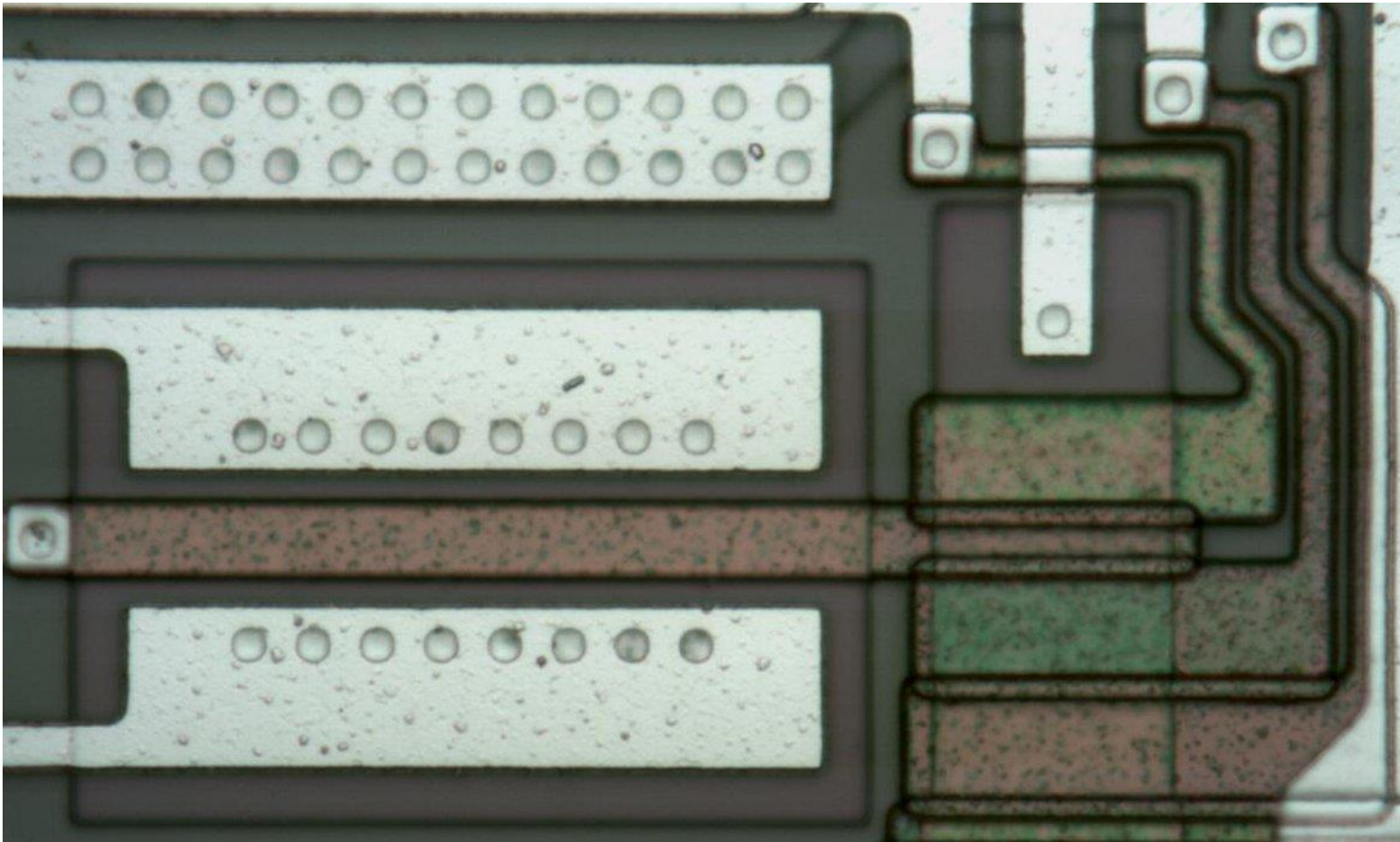


240 / SPIE Vol. 1242 Charge-Coupled Devices and Solid State Optical Sensors (1990)

- Multiple, nondestructive reads of the charge (floating-gate)
- Noise \propto Inverse square root of the number of samples
 - 1990 results
 - 0.5 e- noise

Floating-gate amplifier

- LBNL implementation (floating-gate amplifier)



- 2nd version (LDRD 2013)
 - 0.068 e⁻ after 4k samples (2017)

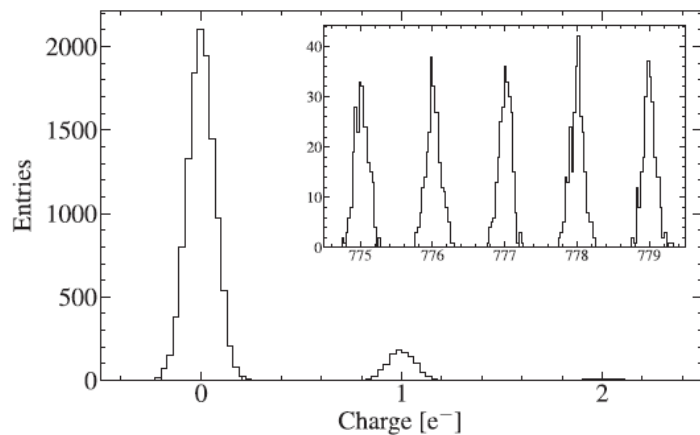


FIG. 1. Single-electron charge resolution using a Skipper CCD with 4000 samples per pixel (bin width of 0.03 e⁻). The measured charge per pixel is shown for low (main) and high (inset) illumination levels. Integer electron peaks can be distinctly resolved in both regimes contemporaneously. The 0 e⁻ peak has rms noise of 0.068 e⁻ rms/pixel while the 777 e⁻ peak has 0.086 e⁻ rms/pixel, demonstrating single-electron sensitivity over a large dynamical range. The Gaussian fits have $\chi^2 = 22.6/22$ and $\chi^2 = 19.5/21$, respectively.

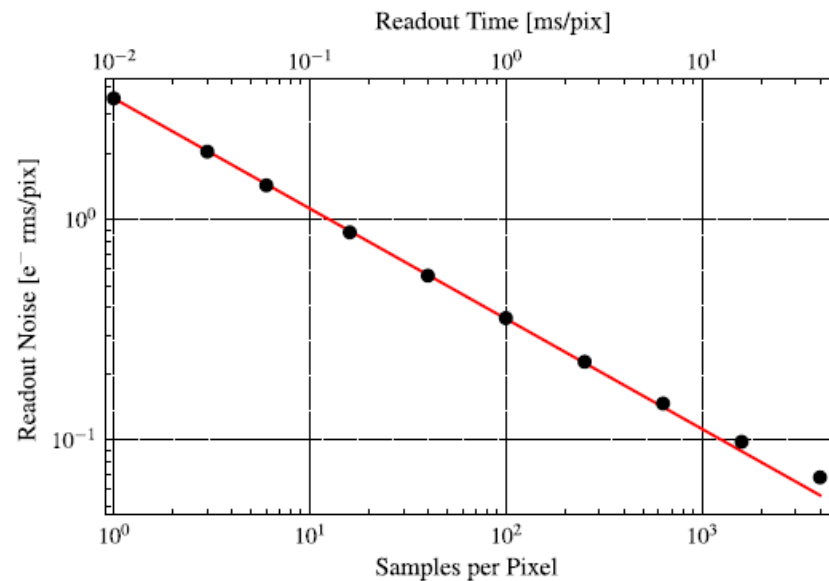


FIG. 3. Readout noise as a function of the number of nondestructive readout samples per pixel for the Skipper CCD. Black points show the rms of the empty-pixel distribution as a function of the number of averaged samples. The red line is the theoretical expectation assuming independent, uncorrelated samples [Eq. (1)].

Single-Electron and Single-Photon Sensitivity with a Silicon Skipper CCD

Javier Tiffenberg,^{1*} Miguel Sofo-Haro,^{2,1} Alex Drlica-Wagner,¹ Rouven Essig,³ Yann Guardincerri,^{1,†} Steve Holland,⁴ Tomer Volansky,⁵ and Tien-Tien Yu⁶

¹Fermi National Accelerator Laboratory, P.O. Box 500, Batavia, Illinois 60510, USA

²Centro Atómico Bariloche, CNEA/CONICET/IB, Bariloche R8402AGP, Argentina

³C.N. Yang Institute for Theoretical Physics, Stony Brook University, Stony Brook, New York 11794, USA

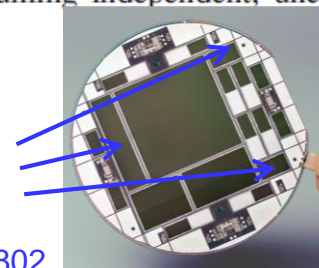
⁴Lawrence Berkeley National Laboratory, One Cyclotron Road, Berkeley, California 94720, USA

⁵Raymond and Beverly Sackler School of Physics and Astronomy, Tel-Aviv University, Tel-Aviv 69978, Israel

⁶Theoretical Physics Department, CERN, CH-1211 Geneva 23, Switzerland

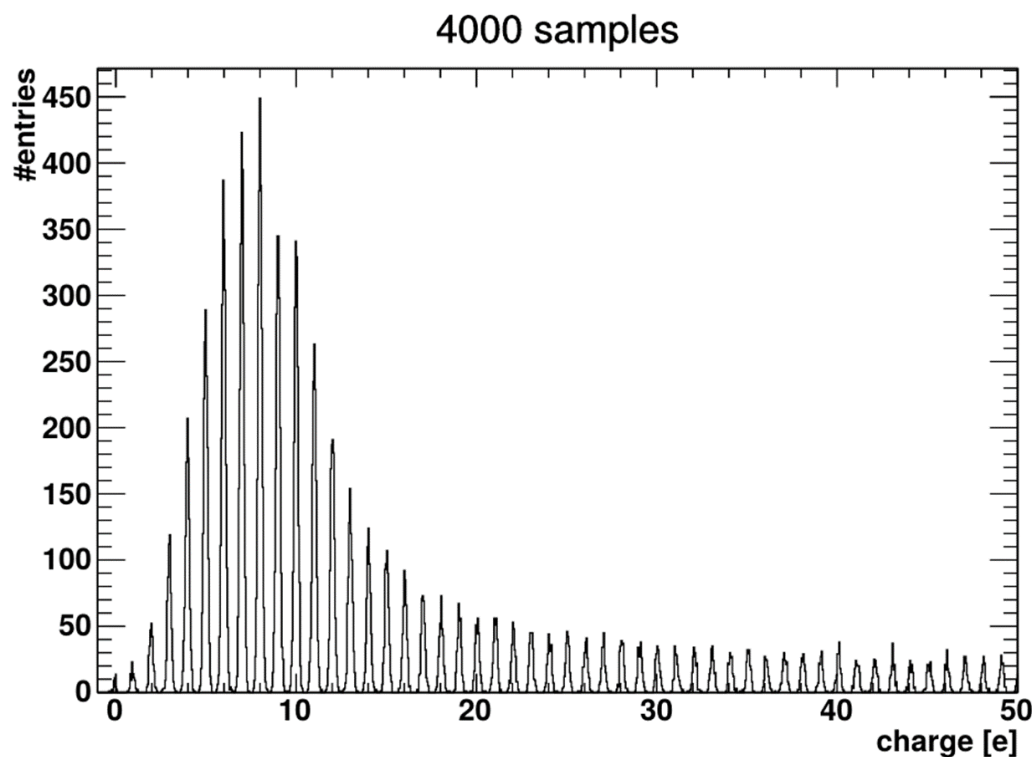
(Received 4 June 2017; published 26 September 2017)

FG amplifier CCDs

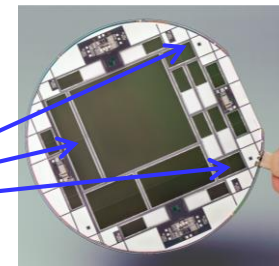


Version 2 Skipper CCD tested at FermiLab

- 2nd version (LDRD 2013)
 - Low-level light charge histogram (FermiLab)

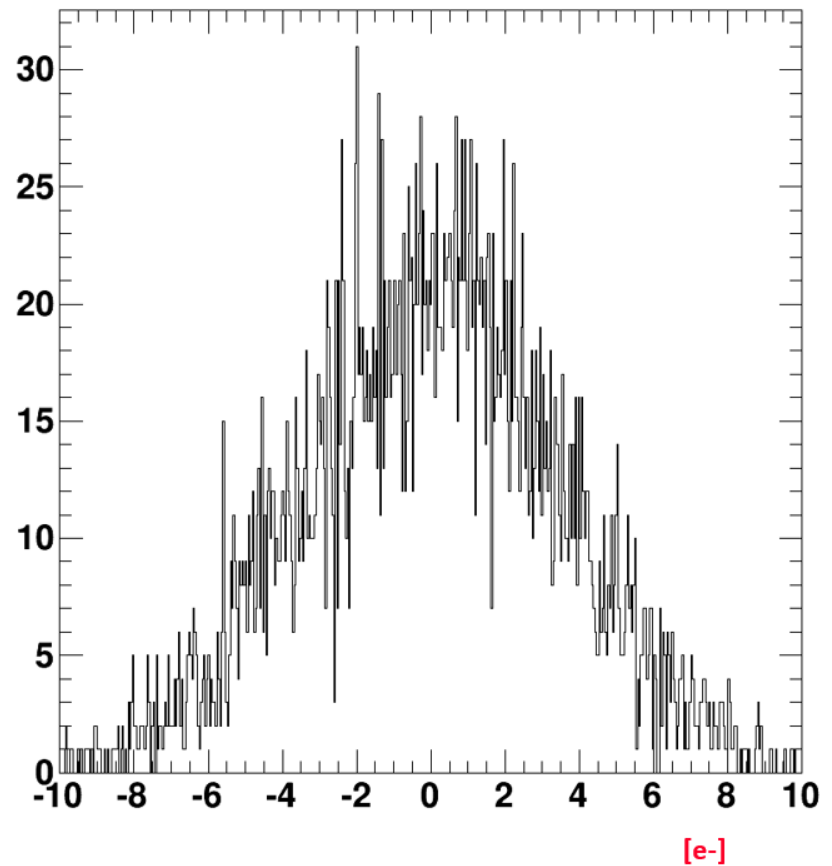
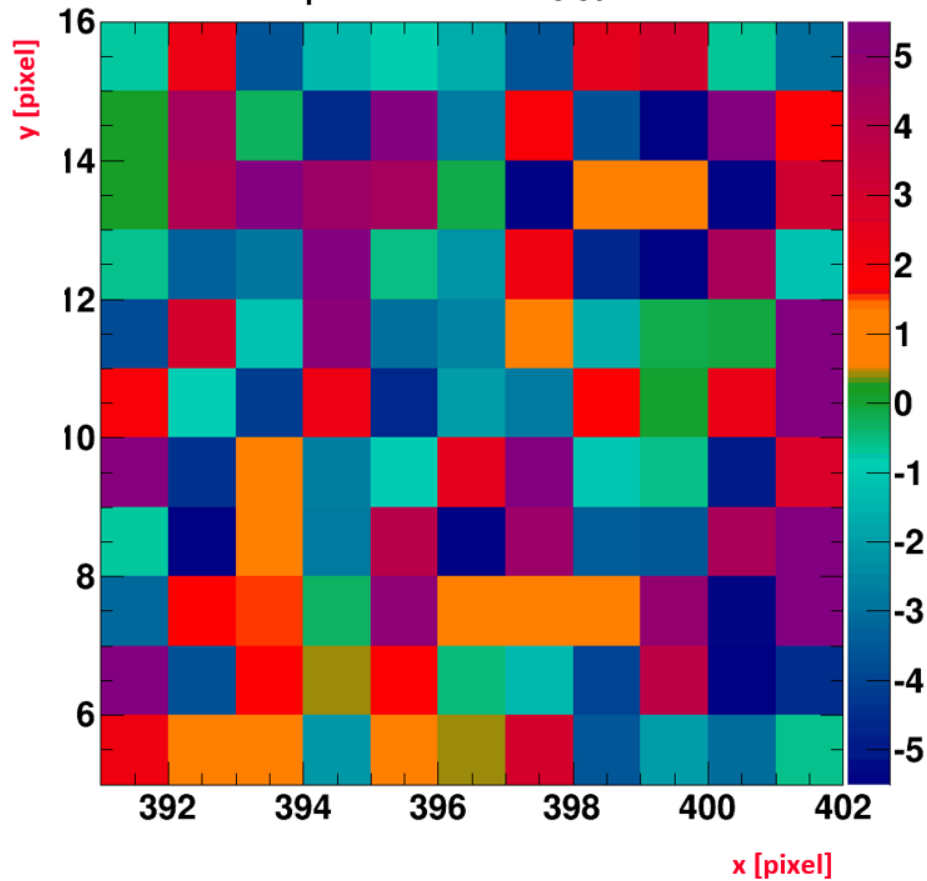


FG amplifier CCDs



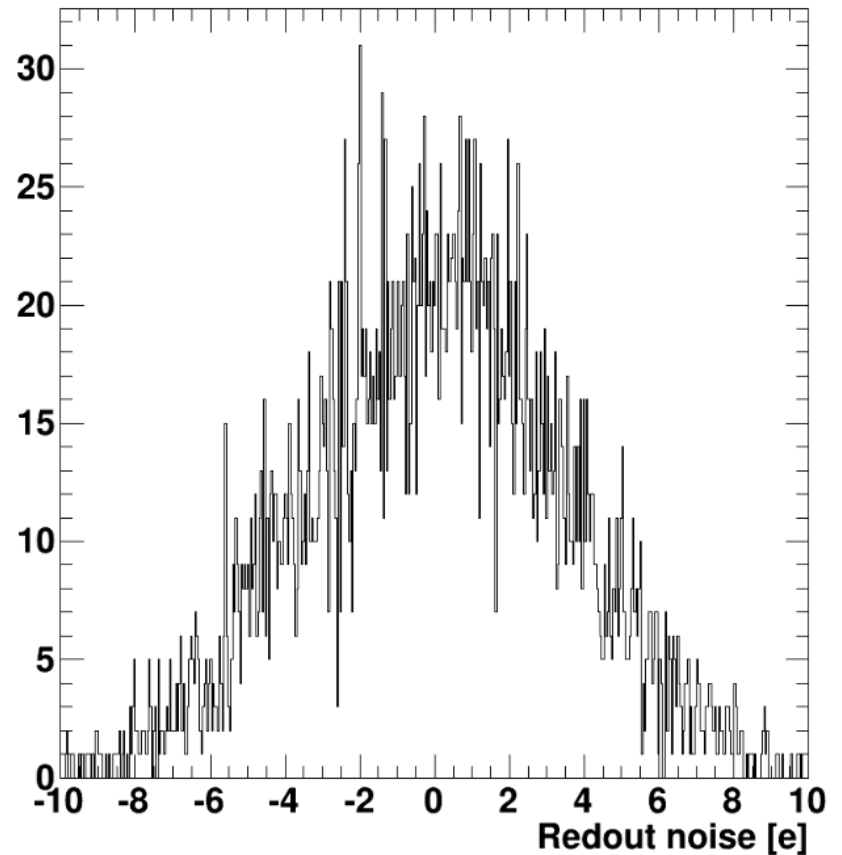
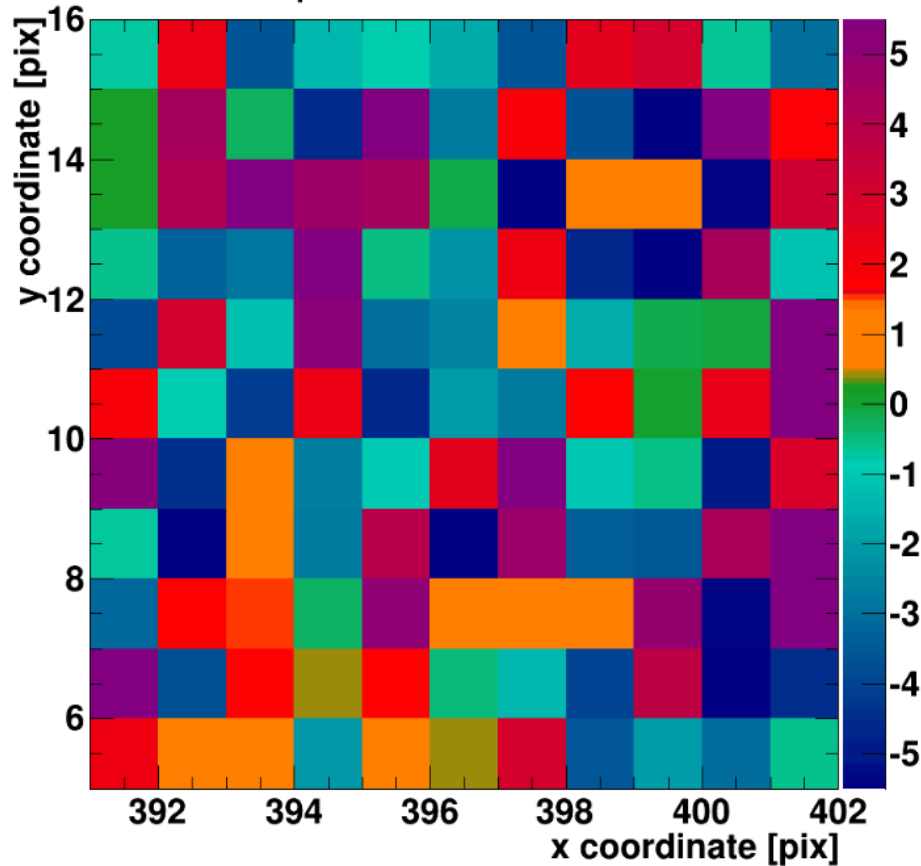
Skipper-CCD basics

$N_{\text{smp}} = 1$ $\sigma_{\text{noise}} = 3.5$



Skipper-CCD basics

$N_{\text{smpl}} = 1$ $\sigma_{\text{noise}} = 3.5$



Measurements and animation from FermiLab



Key developments for Dark Matter CCDs

- Single-electron counting
 - Skipper CCD amplifiers
- High-voltage compatible CCD design / Very high-resistivity Float-zone silicon
- Gettering for low dark current
 - Single-electron event rate

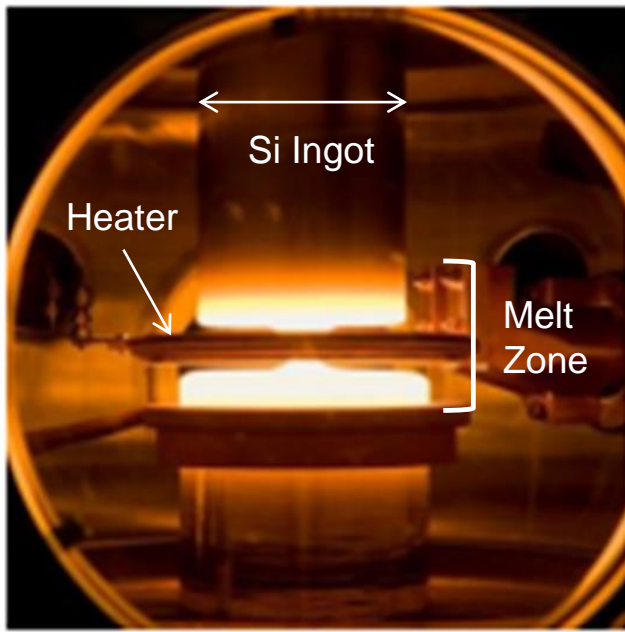


Dark Matter detection with CCDs

- CCD mass is limited by the standard wafer thickness
 - 675 μm for 150 mm, 725 μm for 200 mm wafer
 - Depletion voltage goes as (thickness)² and (resistivity)⁻¹
- Two advances for thick CCDs
 - LBNL high-voltage compatible CCD designs
 - DOI: [10.1109/TED.2009.2030631](https://doi.org/10.1109/TED.2009.2030631) and <https://doi.org/10.1117/12.672393>
 - Improvements in the production of float-zone silicon
 - Higher resistivity / lower depletion voltage

pn junction depletion voltage

$$V_{\text{depl}} = \frac{qN_D}{2\epsilon_{Si}} x_D^2 \quad \rho = \frac{1}{q\mu_n N_D}$$



Year Acquired	Topsil Crystal #	Resistivity ρ (k Ω -cm)	Lifetime τ (ms)
2009	2142946	5.5 – 7.0	4.4
2009	2143310	5.0 - 6.0	16.3
2009	2144322	14.0 - 20.0	3.4
2014	22-0572-10	20.0 - 28.0	7.3
2015	33-0203-20	22.0 - 26.0	21.4
2019	31-1062-10	> 10.0	22.4
2020	33-1751-30	> 10.0	18.9
2020	32-1345-20	18.0 – 20.0	23.5
2020	34-1802-10	17.7 – 22.4	18.4

[Link to Topsil Float-Zone silicon](#)

Blue table entries are 150-mm diameter

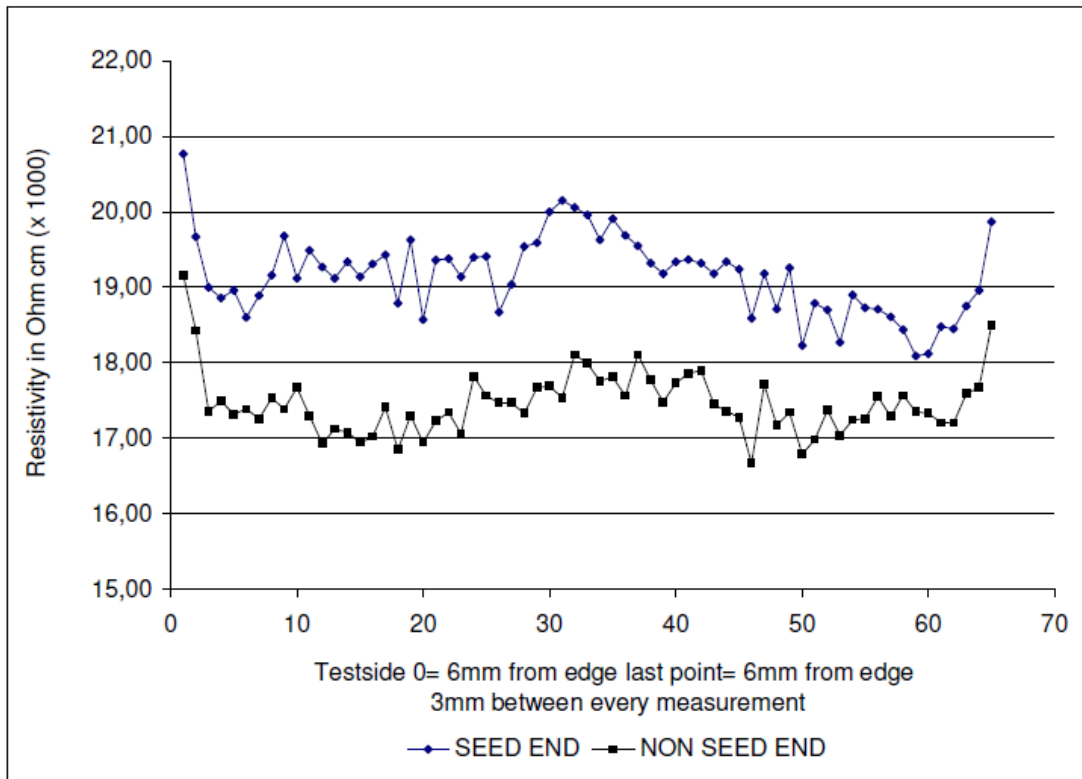
Red are 200-mm diameter wafers



High Purity, High Resistivity Silicon

HiRes™

Diascan resistivity measured by the 4-point method as defined by SEMI MF43

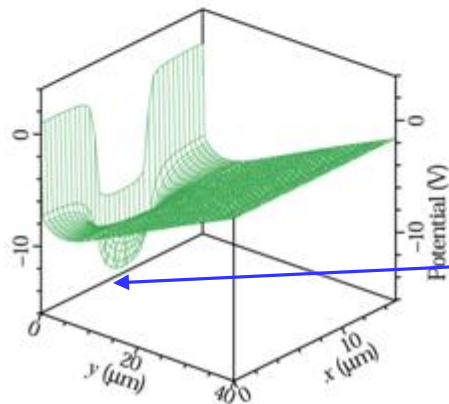
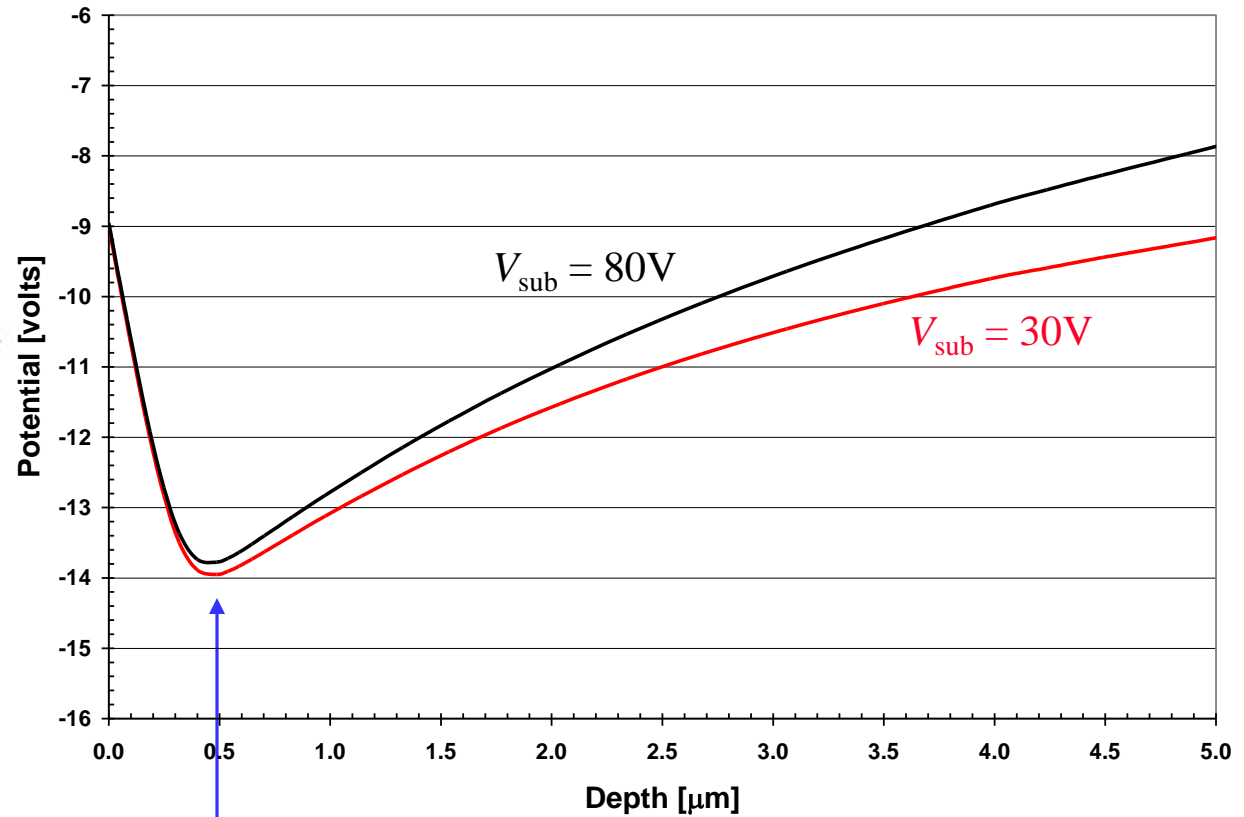
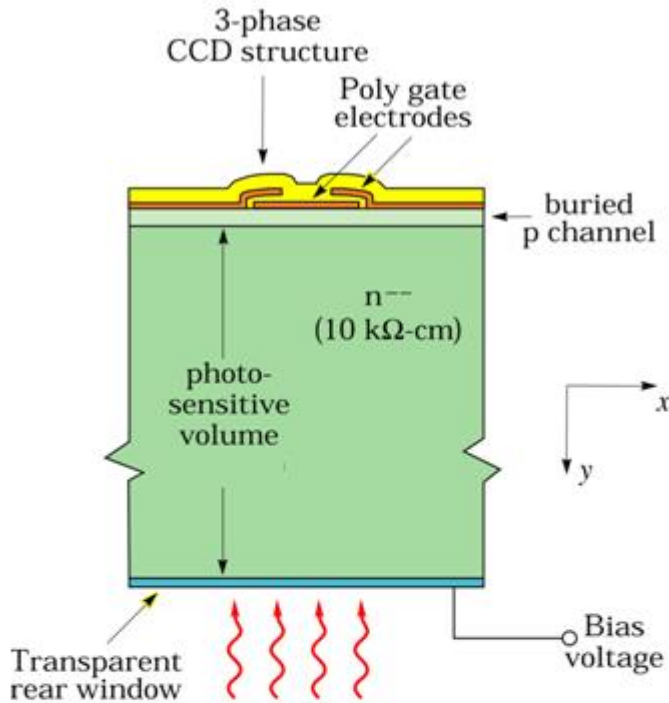


$V_{\text{depl}} \sim 90 - 120\text{V}$ for
15 – 20 kohm-cm and
725 um thick (200 mm)

Lifetime measured by the photo conductive decay method as defined by SEMI MF28

Lifetime: 23520 $\mu\text{sec.}$

Fully depleted CCDs / 2D simulations



MEDICI 2-D simulation

MEDICI simulations

Potential minimum (collecting phase)

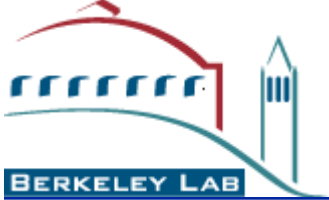
- Relatively insensitive to V_{sub}
- Capacitor voltage divider effect
- Wide range of V_{sub} possible



CCD development for Dark Matter

Key developments for DM CCDs

- Single-electron counting
 - Skipper CCD amplifiers
- High-voltage compatible CCD design / Very high-resistivity Float-zone silicon
- **Gettering for low dark current**
 - **Single-electron event rate**



DESI (astronomy) vs SENSEI (DM)

Parameter	DESI	SENSEI ¹
CCD format Thickness	4k x 4k (15 μm) ² 250 μm	6k x 1k (15 μm) ² 650 μm
Read noise	2.5 – 3.0 e- rms	0.13 e- rms See note 1
Dark current	~ 1 e-/pixel-hour (133K)	~ 1.4×10^{-5} e-/pix-day (~ 140K) See note 2
Exposure time	15 minutes	20 hours
Readout time	1 minute	7.7 hours

Note 1: Skipper CCD with 300 samples / pixel

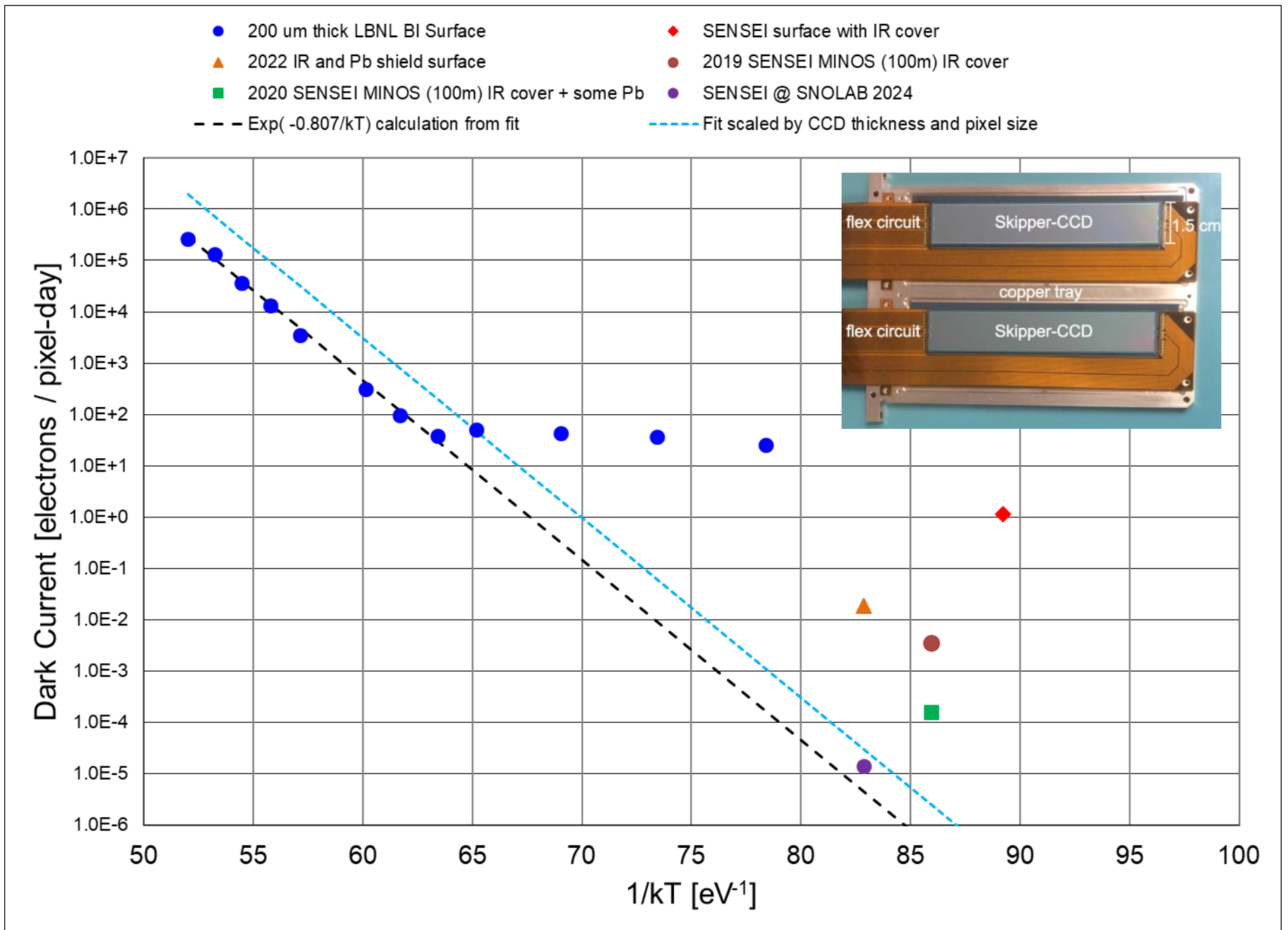
Note 2: Improved Cold Cu shielding / SNOLAB

Number quoted is the single-electron event rate

<https://arxiv.org/abs/2410.18716>

¹ Sub-GeV dark matter searches with SENSEI

Nate Saffold, for the SENSEI collaboration
APS April Meeting
4/15/2023



- Dark current from the substrate is determined by extremely low levels of metal impurities
- In the early semiconductor days metals in Si were referred to as “Deathnium” (William Shockley)

WILLIAM SHOCKLEY

Transistor technology evokes new physics

Nobel Lecture, December 11, 1956

It has also been found that copper and nickel chemical impurities in the germanium produce marked reductions in lifetime⁴.

The way in which deathnium catalyzes the recombination process is in-

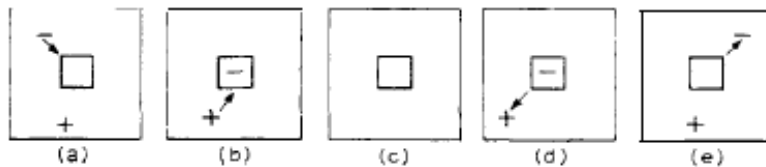


Fig. 1. A recombination center (deathnium) captures alternately an electron and a hole and thus catalyzes their recombination, as shown in parts (a), (b), and (c). The thermally activated generation process is shown in (d) and (e).

indicated in Fig. 1. In part (b) of this figure, an electron is captured by a deathnium center. The deathnium center thus becomes a baited trap which is ready to capture a hole. If a hole comes near to the deathnium center, the electron can drop into it, thus forming a normal covalent bond, and the deathnium center is then uncharged and ready to repeat the process.

- P in silicon can bond with metals, also disorder such as polycrystalline Si
- We use in-situ doped (P) polysilicon to trap metal impurities introduced during the fabrication process

Dark Current

- Diode dark current with / without gettering
 - Backside in-situ doped (P) polysilicon (ISDP)

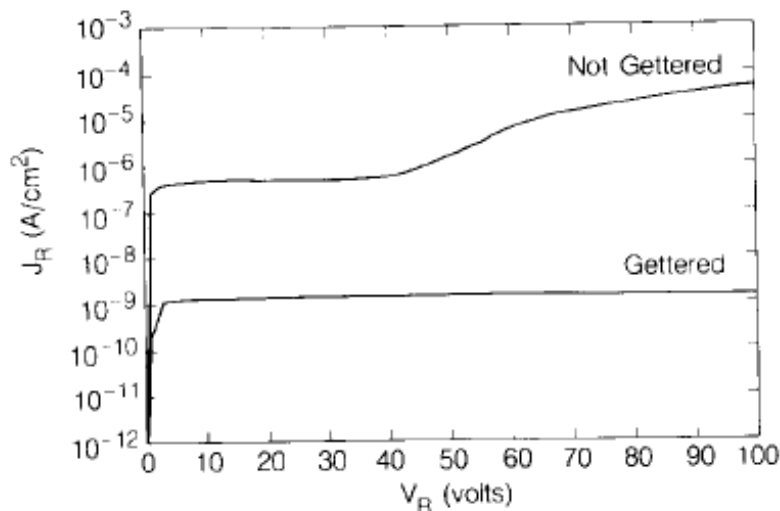
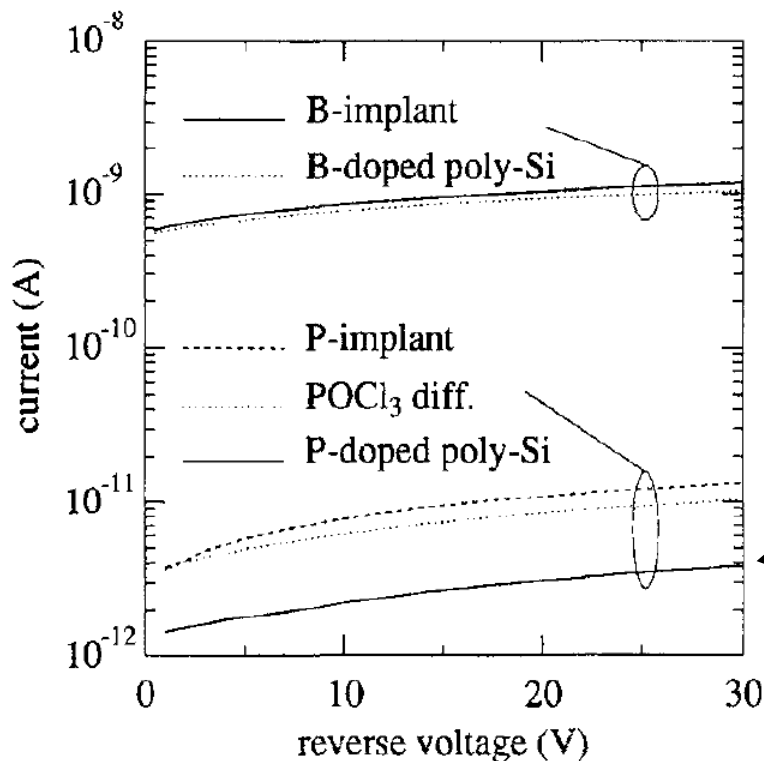


Fig. 2. The detector diode reverse-leakage current for a device with backside gettering compared to one without. The devices were fabricated on 10 k Ω cm $\langle 100 \rangle$ substrates, and both devices are from the same wafer.

Gettering Process for High- ρ silicon

- Dark current for high- ρ silicon pin diodes



- Comparison study of various gettering methods (1997)
- <https://www.sciencedirect.com/science/article/pii/S0168900297006128>

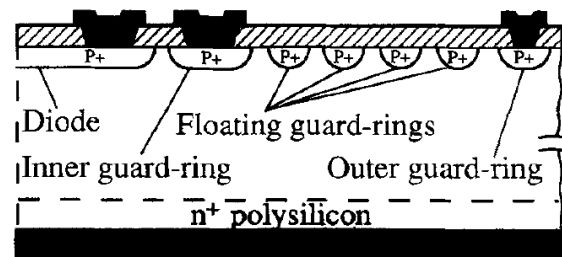


Fig. 2. Schematic cross-section (half device) of a PIN detector on n-type substrate.



Nuclear Instruments and Methods in Physics Research A 395 (1997) 344–348

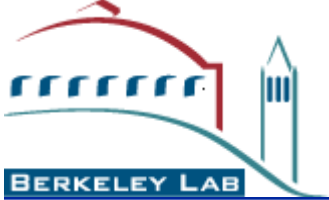
**NUCLEAR
INSTRUMENTS
& METHODS
IN PHYSICS
RESEARCH**
Section A

Si-PIN X-ray detector technology

G.F. Dalla Betta^a, G.U. Pignatelli^{a,*}, G. Verzellese^a, M. Boscardin^b

^aDipartimento di Ingegneria dei Materiali, Università di Trento, I-38050 Mesiano (TN), Italy

^bIRST-Microelectronics, 38050 Povo (TN), Italy



DESI (astronomy) vs SENSEI (DM)

Parameter	DESI	SENSEI ¹
CCD format Thickness	4k x 4k (15 μm) ² 250 μm	6k x 1k (15 μm) ² 650 μm
Read noise	2.5 – 3.0 e- rms	0.13 e- rms See note 1
Dark current	~ 1 e-/pixel-hour (133K)	~ 1.4 x 10 ⁻⁵ e-/pix-day (~ 140K) See note 2
Exposure time	15 minutes	20 hours
Readout time	1 minute	7.7 hours

Note 1: Skipper CCD with 300 samples / pixel

Note 2: Improved Cold Cu shielding / SNOLAB

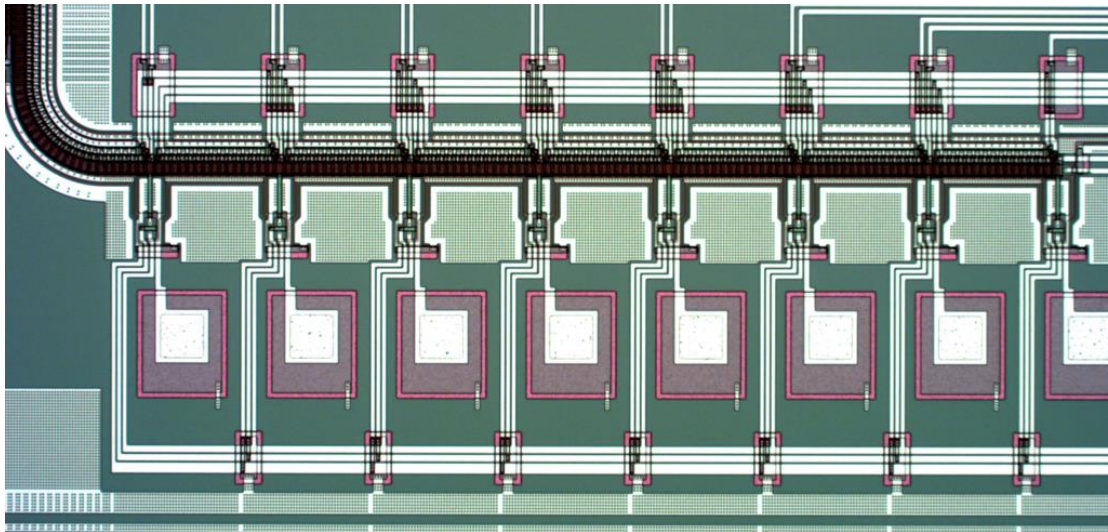
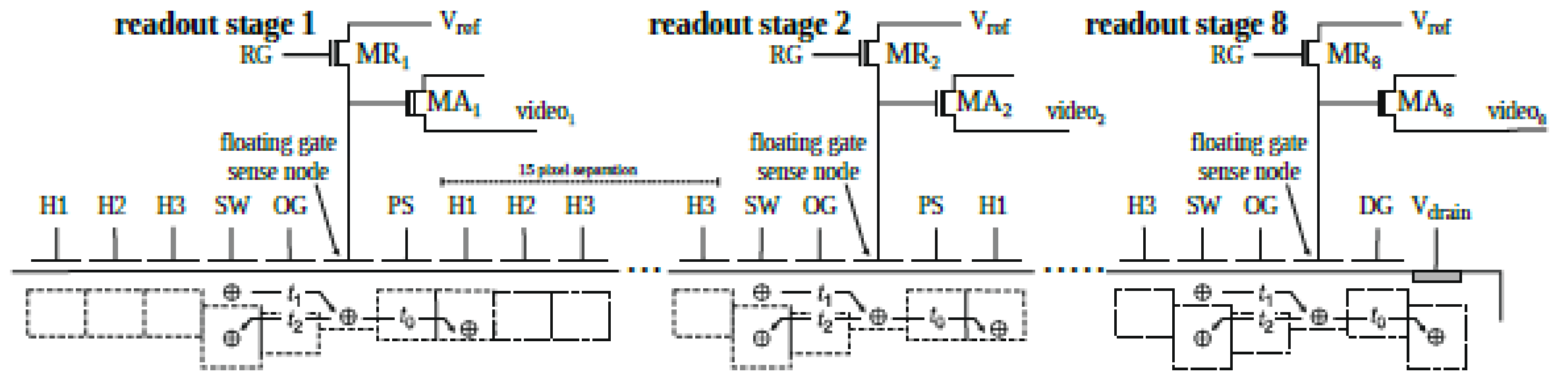
Number quoted is the single-electron event rate

<https://arxiv.org/abs/2410.18716>

¹ Sub-GeV dark matter searches with SENSEI

Nate Saffold, for the SENSEI collaboration
APS April Meeting
4/15/2023

Multiple-amplifier sensing CCD



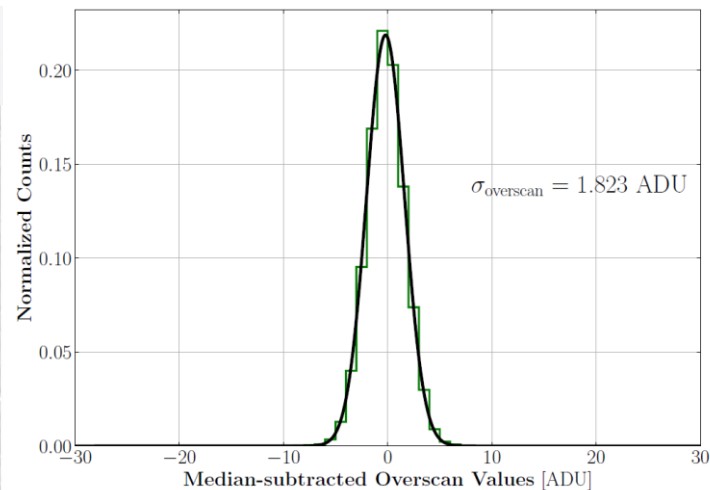
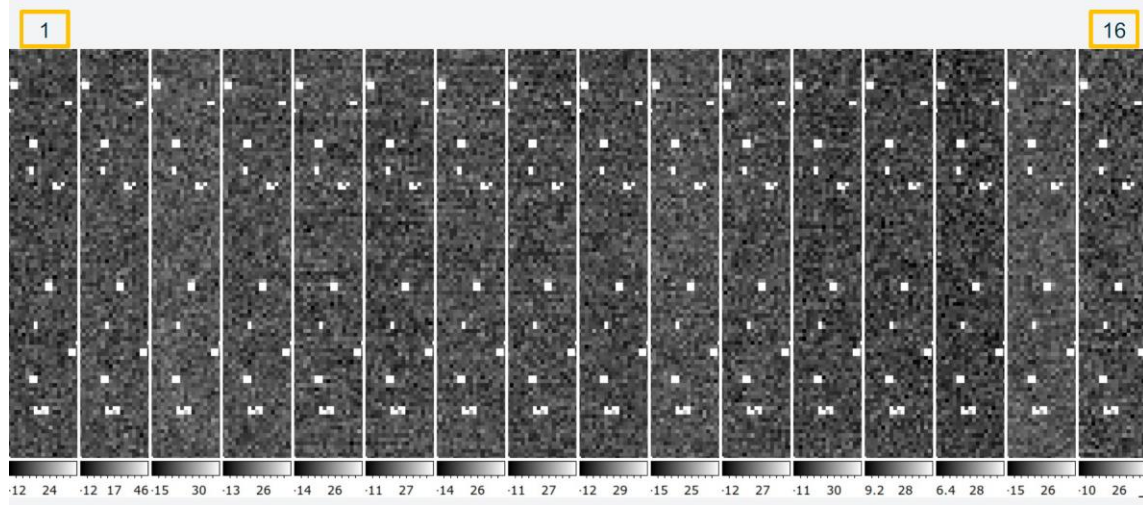
M amplifiers in series where $M = 8$ or 16 in the first LBNL prototype

- Single read per amp / Noise reduction of square root of M
 - $\sim 1e-$ noise for 16 amplifiers achieved (single read)
 - Overhead in time to read the first pixel per row, after that the pixels are read out as in a conventional CCD


Experimental results

Encouraging results with the MAS prototype 16-ch CCDs


Lowest demonstrated noise performance



16-ch combined noise ~ 1.06 e- rms/pixel



BERKELEY LAB
Bringing Science Solutions to the World




U.S. DEPARTMENT OF ENERGY
Office of Science

Sub-electron noise CCDs with the MAS Architecture for astronomy

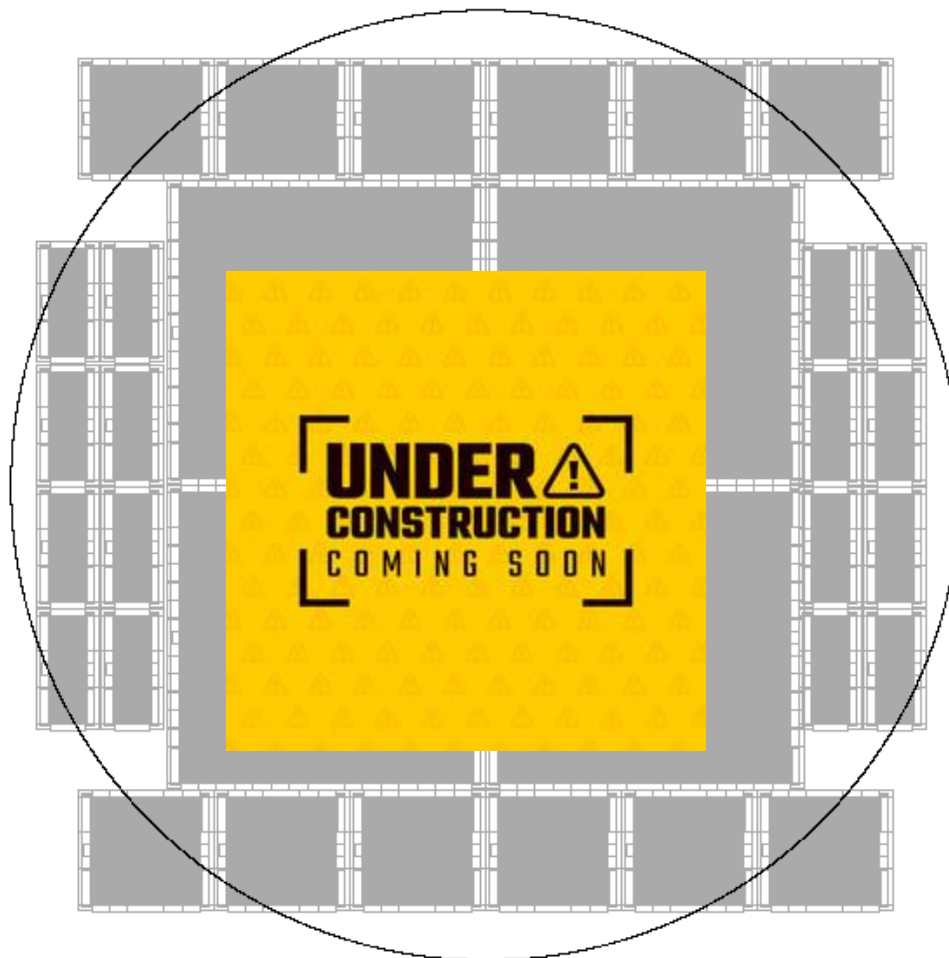
Kenneth Lin
University of California, Berkeley

03/12/2024
New Detector Technologies Track ISPA 2024 @ SLAC



Berkeley
UNIVERSITY OF CALIFORNIA

4 x 16 MAS CCD design in progress



Thank you for your attention

Showing 1–50 of 53 results for all: skipper ccd

Search v0.5.6 released 2020-02-24

skipper ccd All fields

Show abstracts Hide abstracts

Advanced Search

50 results per page. Sort results by Announcement date (newest first)

1 2

Next

1. arXiv:2410.06417 [pdf, other] [astro-ph.IM](#) [physics.ins-det](#)

A multi-channel silicon package for large-scale skipper-CCD experiments

Authors: A. M. Botti, C. Chavez, M. Sofo-Haro, C. S. Miller, F. Chierchie, M. Jonas, M. Lisovenko, H. Gutti, D. Czaplewski, A. Lathrop, J. Tiffenberg, G. Fernandez-Moroni, J. Estrada

Abstract: The next generation of experiments for rare-event searches based on skipper Charge Coupled Devices (... [More](#))

Submitted 8 October, 2024; originally announced October 2024.

Comments: 14 pages, 13 figures, 2 tables

Report number: FERMILAB-PUB-24-0716-PPD
2. arXiv:2410.06261 [pdf, other] [astro-ph.IM](#) [astro-ph.CO](#) [astro-ph.EP](#) [hep-ex](#) [doi: 10.1117/12.3019241](#)

Cherenkov Photon Background for Low-Noise Silicon Detectors in Space

Authors: Manuel E. Gaido, Javier Tiffenberg, Alex Drlica-Wagner, Guillermo Fernandez-Moroni, Bernard J. Rauscher, Fernando Chierche, Darío Rodrigues, Lucas Giardino, Juan Estrada

Abstract: ...Imaging and spectroscopy of extra-solar planets will require ultra-low-noise detectors that are sensitive over a broad range of wavelengths. Silicon charge-coupled devices (CCDs), such as EMCCDs,... [More](#)

Submitted 8 October, 2024; originally announced October 2024.

Comments: SPIE Proceeding; 9 pages, 6 figures

Report number: FERMILAB-CONF-24-0282-LDRD-PPD

Journal ref: Proc. SPIE 13103, X-Ray, Optical, and Infrared Detectors for Astronomy XI, 131031P (2024)
3. arXiv:2409.20290 [pdf, other] [hep-ex](#)

The search for light dark matter with DAMIC-M

Authors: R. Smida

Abstract: The DAMIC-M (DARk Matter In CCDs at Modane) experiment will use... [More](#)

Submitted 30 September, 2024; originally announced September 2024.
4. arXiv:2407.17872 [pdf, other] [physics.ins-det](#) [astro-ph.CO](#)

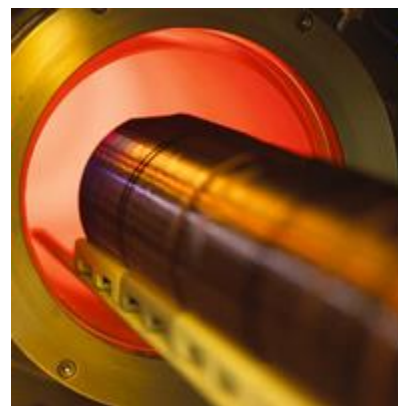
The DAMIC-M Low Background Chamber

Authors: I. Arnquist, N. Avalos, P. Bailly, D. Baxter, X. Bertou, M. Bogdan, C. Bourgeois, J. Brandt, A. Cadiou, N. Castello-Mor, A. E. Chavarria, M. Conde, J. Cuevas-Zepeda, A. Dastgheibi-Fard, C. De Dominicis, O. Deligny, R. Desani, M. Dhellot, J. Duarte-Campderros, E. Estrada, D. Florin, N. Gadola, R. Gaior, E.-L. Gkougkousis, J. Gonzalez Sanchez, et al. (44 additional authors not shown)

Abstract: The DARk Matter In CCDs at Modane (DAMIC-M) experiment is designed to search for light dark matter ($m_\chi < 10 \text{ GeV}/c^2$) at the Laboratoire Souterrain de Modane (LSM) in France. DAMIC-M will use... [More](#)

Submitted 27 September, 2024; v1 submitted 25 July, 2024; originally announced July 2024.

- Industrial fabrication at Teledyne DALSA
 - Commercial CCD foundry located in Bromont, Quebec, Canada / 150 mm silicon wafers



- Dark Matter detection: Full fabrication at DALSA
- For back illuminated CCDs, the wafers are partially processed at DALSA with the steps needed for back illumination done at the LBNL MicroSystems Lab

High-voltage compatible CCDs

- Spatial resolution in fully depleted CCDs goes as $\sim 1/(V_{\text{sub}})^{-1/2}$
 - Carrier transit time (holes)

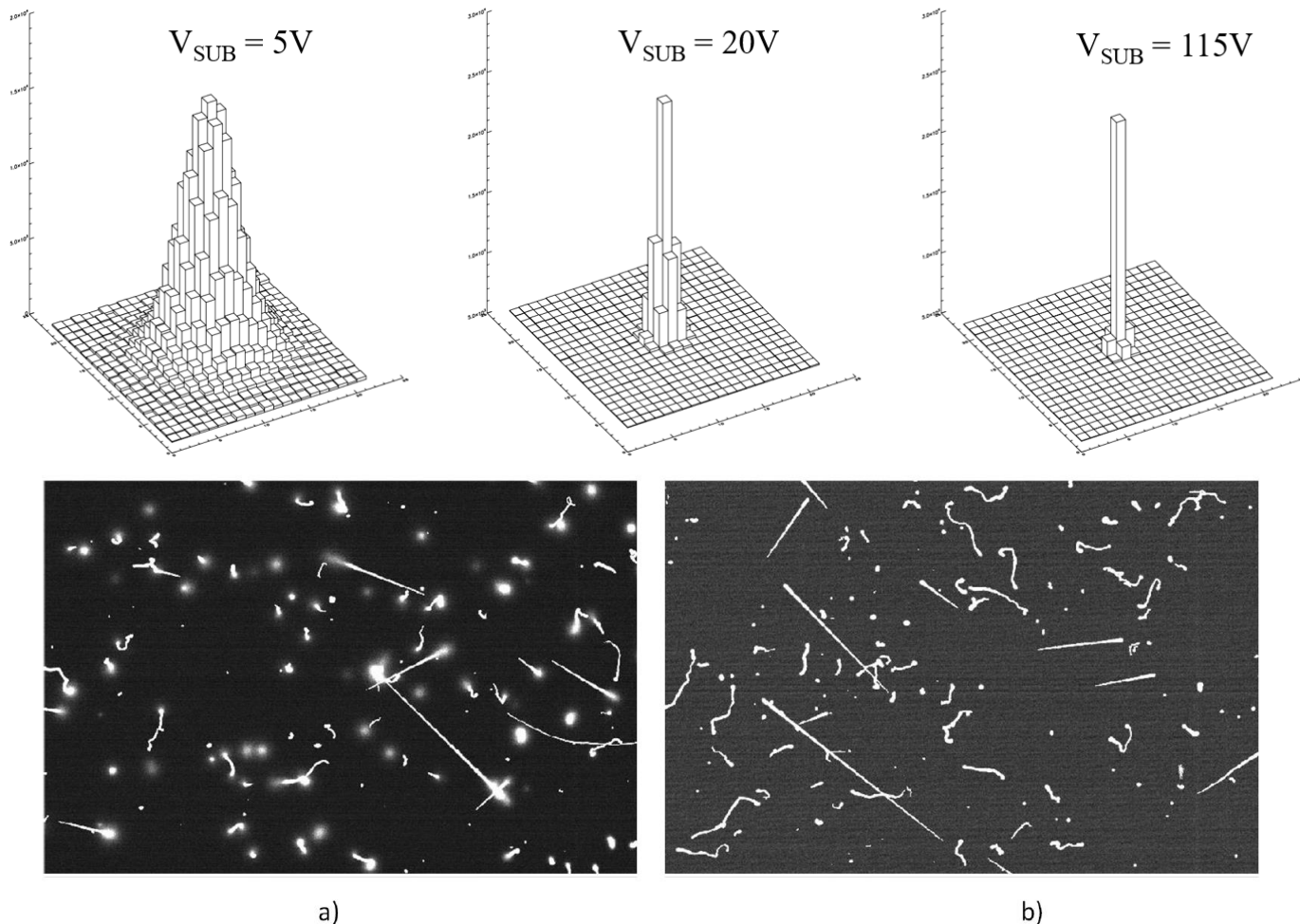


Figure 4. Sub-images of 30 minute dark exposures taken at -140°C on a $500\ \mu\text{m}$ -thick, $4\text{k} \times 2\text{k}$, $(15\ \mu\text{m})^2$ -pixel CCD fabricated on $\sim 20,000\ \Omega\text{-cm}$ silicon. The size of the sub-image is approximately 650 rows by 770 columns. a) $V_{\text{sub}}=30\text{V}$ b) $V_{\text{sub}}=60\text{V}$.

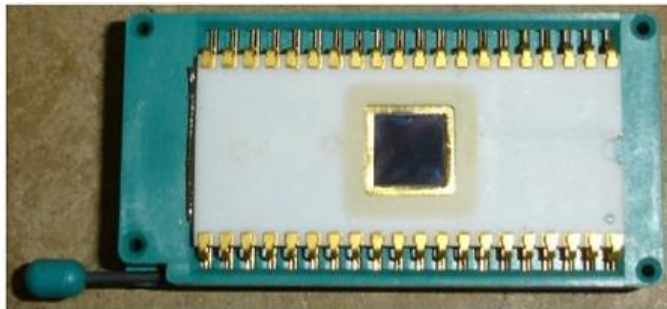
Development of Scientific CCDs at NASA/JPL

- CCDs were introduced in 1972 by Bell Labs to NASA as a potential detector for the proposed Large Space Telescope (later the Hubble Space Telescope)
 - NASA was considering film and vidicons
- 10 year R&D effort with the NASA Jet Propulsion Laboratory and Texas Instruments to develop buried-channel, back-illuminated CCDs
- In 1976 JPL introduced the CCD to astronomers with the “traveling camera”
 - Texas Instruments 400 x 400 CCD with 15 um pixels

J. R. Janesick, *Scientific Charge-Coupled Devices*, SPIE Press, 2001

Development of Scientific CCDs at NASA/JPL

- CCDs were introduced in 1972 by Bell Labs to NASA as a potential detector for the proposed Large Space Telescope (later the Hubble Space Telescope)
 - NASA was considering film and vidicons
- 10 year R&D effort with the NASA Jet Propulsion Laboratory and Texas Instruments to develop buried-channel, back-illuminated CCDs
- In 1976 JPL introduced the CCD to astronomers with the “traveling camera”
 - Texas Instruments 400 x 400 CCD with 15 um pixels



THE 400 x 400 PIXEL BACKSIDE ILLUMINATED CCD USED IN THE JPL TRAVELING CAMERA SYSTEM.

Credit: Jim Janesick and
<http://www.digicamhistory.com/>



JANESICK AS YOUNG MAN AND CCD CAMERA SYSTEM USED AT MT. LEMMON TO TAKE THE FIRST PROFESSIONAL CCD ASTRONOMICAL IMAGES.

2019 IISS Exceptional Lifetime Achievement Award goes to James R. Janesick

Jim Janesick is a Distinguished Engineer at Sarnoff Inc., developing high-performance CMOS imagers for various scientific and government projects. In the beginning of his career Jim was with the Jet Propulsion Lab for 22 years, where he was group leader of the Advanced CCD Sensors Development Group with a focus on scientific CCD test and characterization. He pioneered scientific CCD and support electronic designs for several NASA space-borne imaging systems. Jim authored the text books *Scientific Charge-Coupled Devices* and *Photon Transfer*.

He received the NASA Exceptional Engineering Achievement Medal in 1982 and 1992. Over his career, he has had a great impact on characterization methodology of image sensors, particularly for scientific devices but applicable to nearly every CCD and CMOS imager.

For example, while at JPL, Jim developed the Photon Transfer Curve (PTC), world famous among image sensor technologists. This characterization method for image sensors makes it possible to characterize an imager without knowing particular details of the device. The technique is used in academia as well as in industry, and many devices are tested daily around the world making use of the PTC method.

The International Image Sensor Society is pleased to recognize Jim's contribution to the imaging technology field by presenting him with the 2019 IISS Lifetime Achievement Award at the 2019 IISW at Snowbird in June.

Congratulations and thank you Jim!

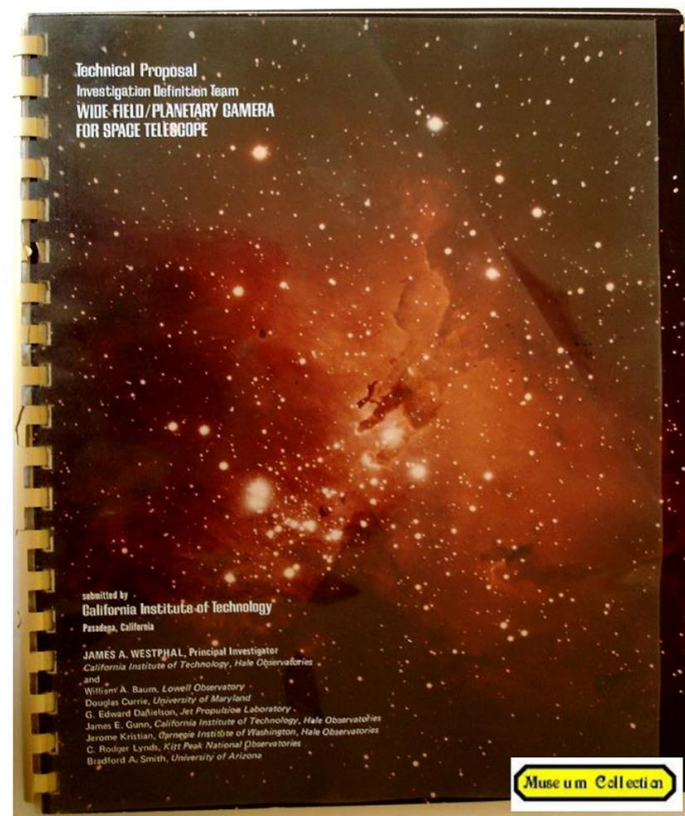


J. R. Janesick, *Scientific Charge-Coupled Devices*, SPIE Press, 2001

HST Camera proposal

- The contract for the first Hubble Space Telescope CCD camera was awarded in 1977 to a team led by James Westphal[†]
 - California Institute of Technology
- Subcontractor was NASA Jet Propulsion Laboratory
- The CCD proposed for the camera was the TI 800 x 800 (4 x 800 x 800)

WIDE FIELD PLANETARY CAMERA (WF/PC I) TECHNICAL PROPOSAL



Credit: Jim Janesick and
<http://www.digicamhistory.com/>

The Palomar Observatory Four-shooter camera

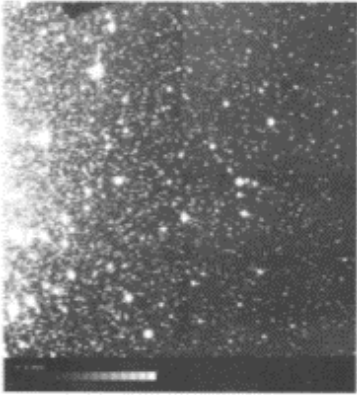
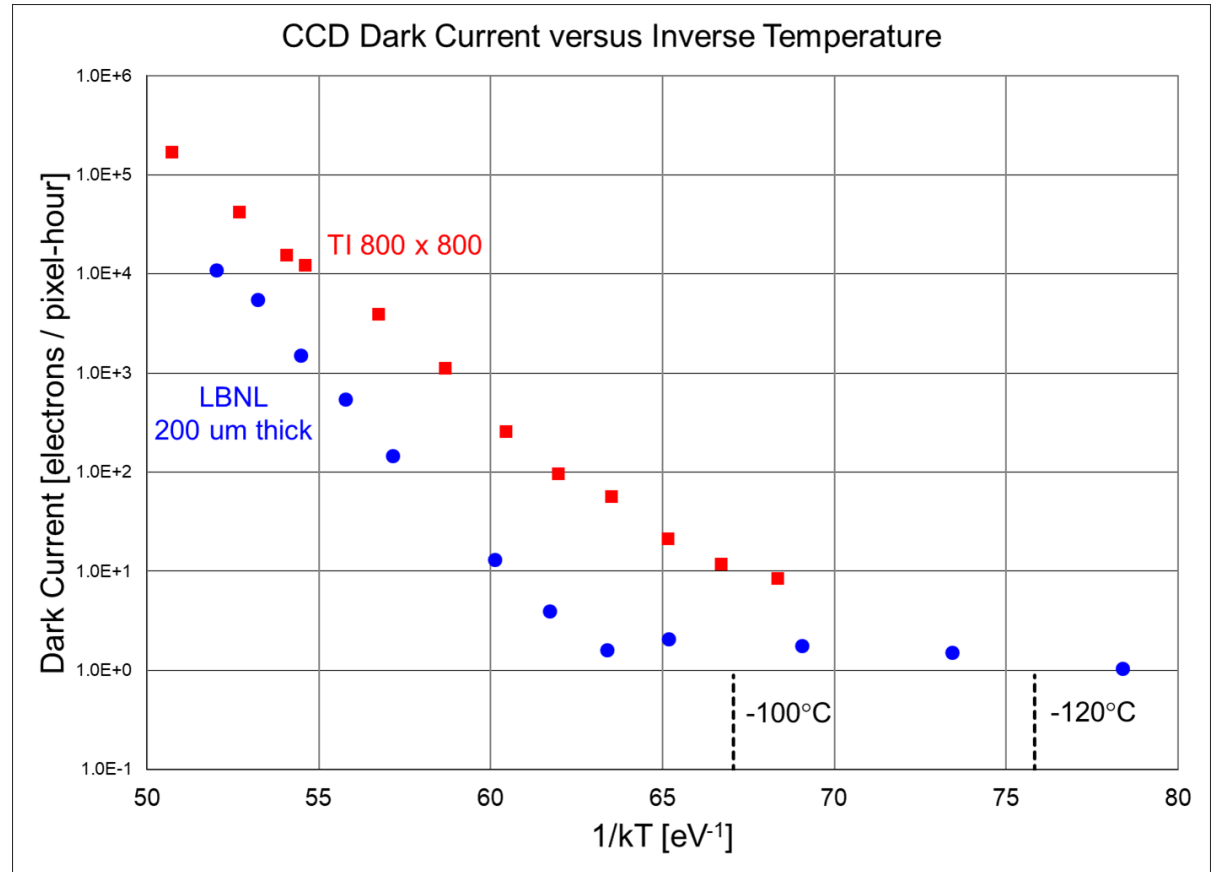


Fig. 9. The outskirts of the globular star cluster Messier 3. This 30-min exposure in the red, obtained in excellent seeing, reaches to a red magnitude of about 26.0. The guider arm and mirror can be seen in shadow in the upper left.



- A 30 minute exposure on the Four-Shooter camera is shown above
- CCDs are cooled to reduce the “dark current” (silicon surface and bulk)

CCD Linearity

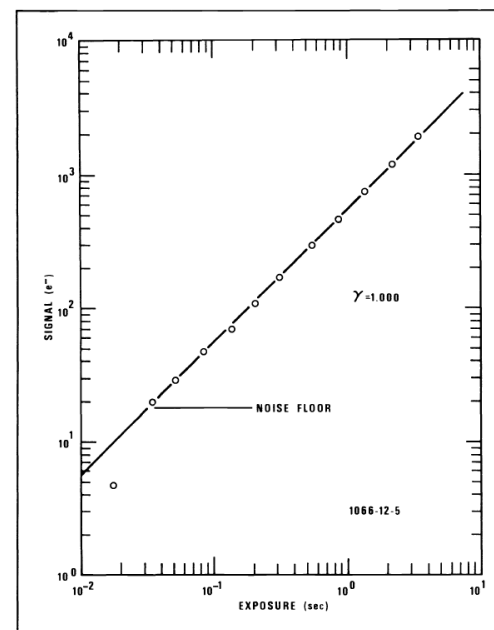
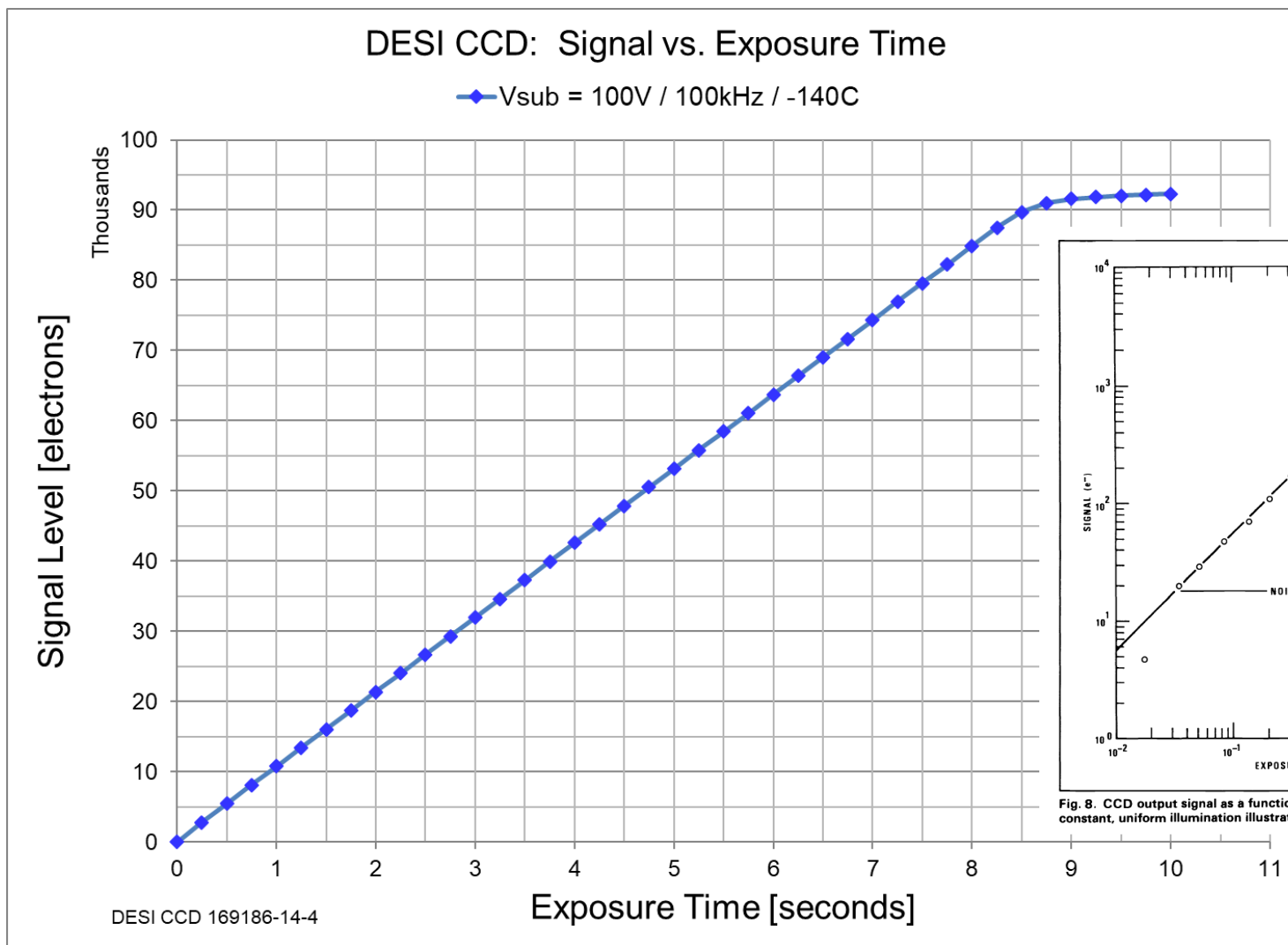


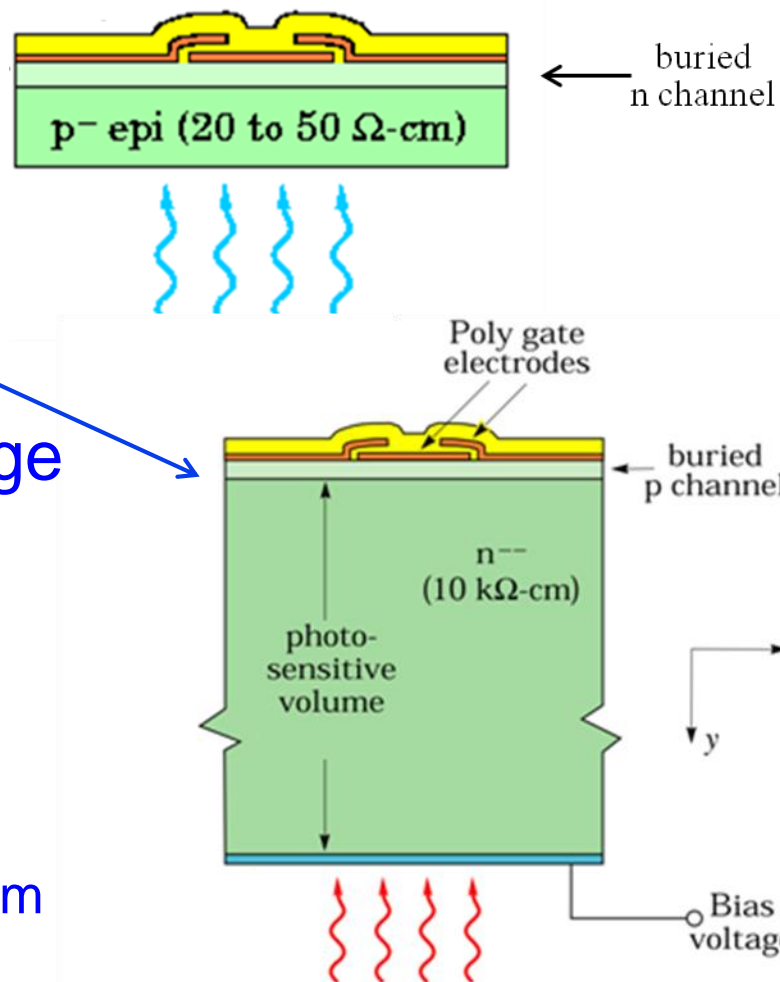
Fig. 8. CCD output signal as a function of exposure time to a source of constant, uniform illumination illustrating the linearity of the device.

TI 800 x 800

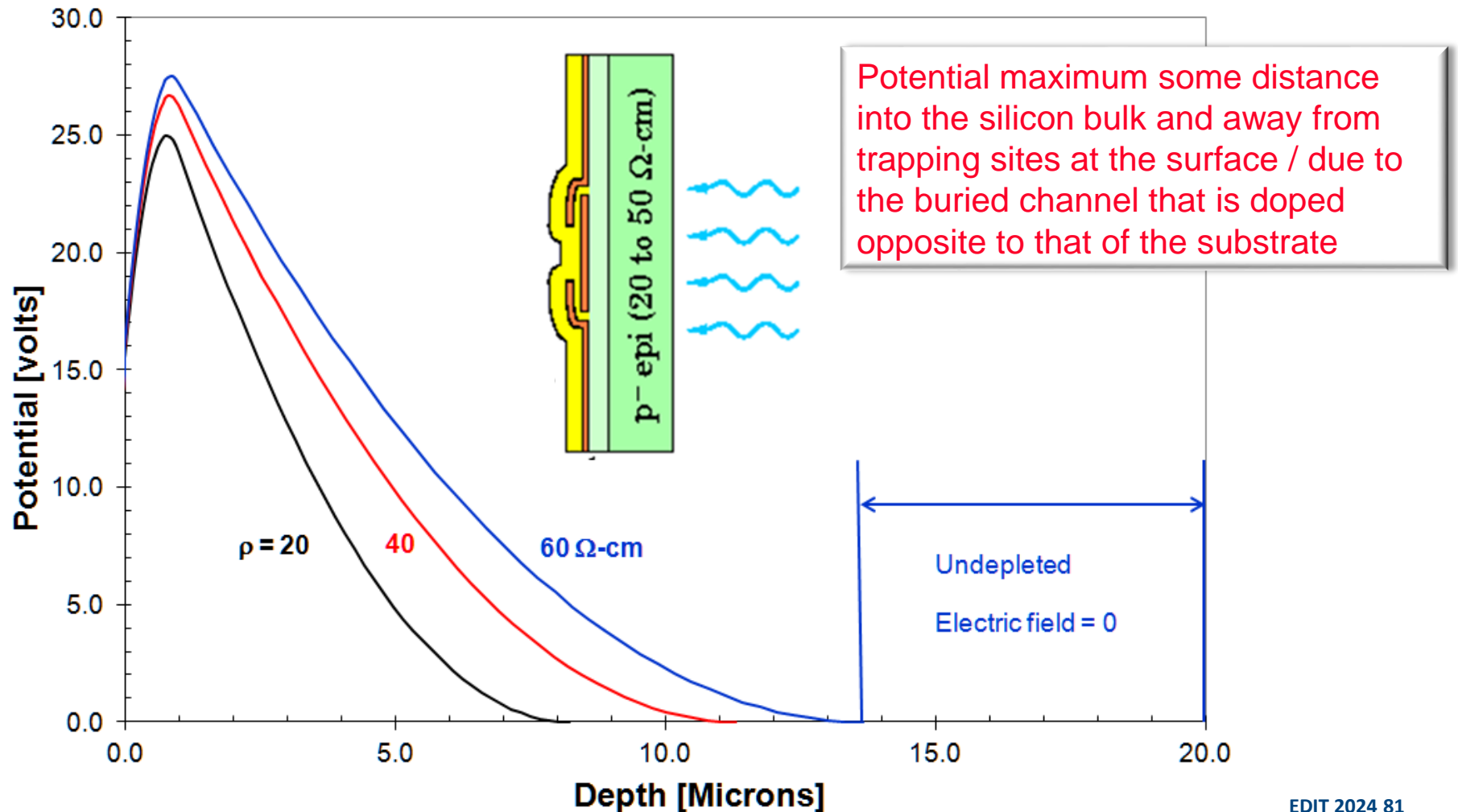
- CCDs have a linear response to the input light level and high dynamic range
- “Photometry”: Quantitative measure of the amount of light collected
 - Unit is electrons (one electron per photon in the visible-near IR)
- Charge converted to voltage on-chip with a few electrons read noise

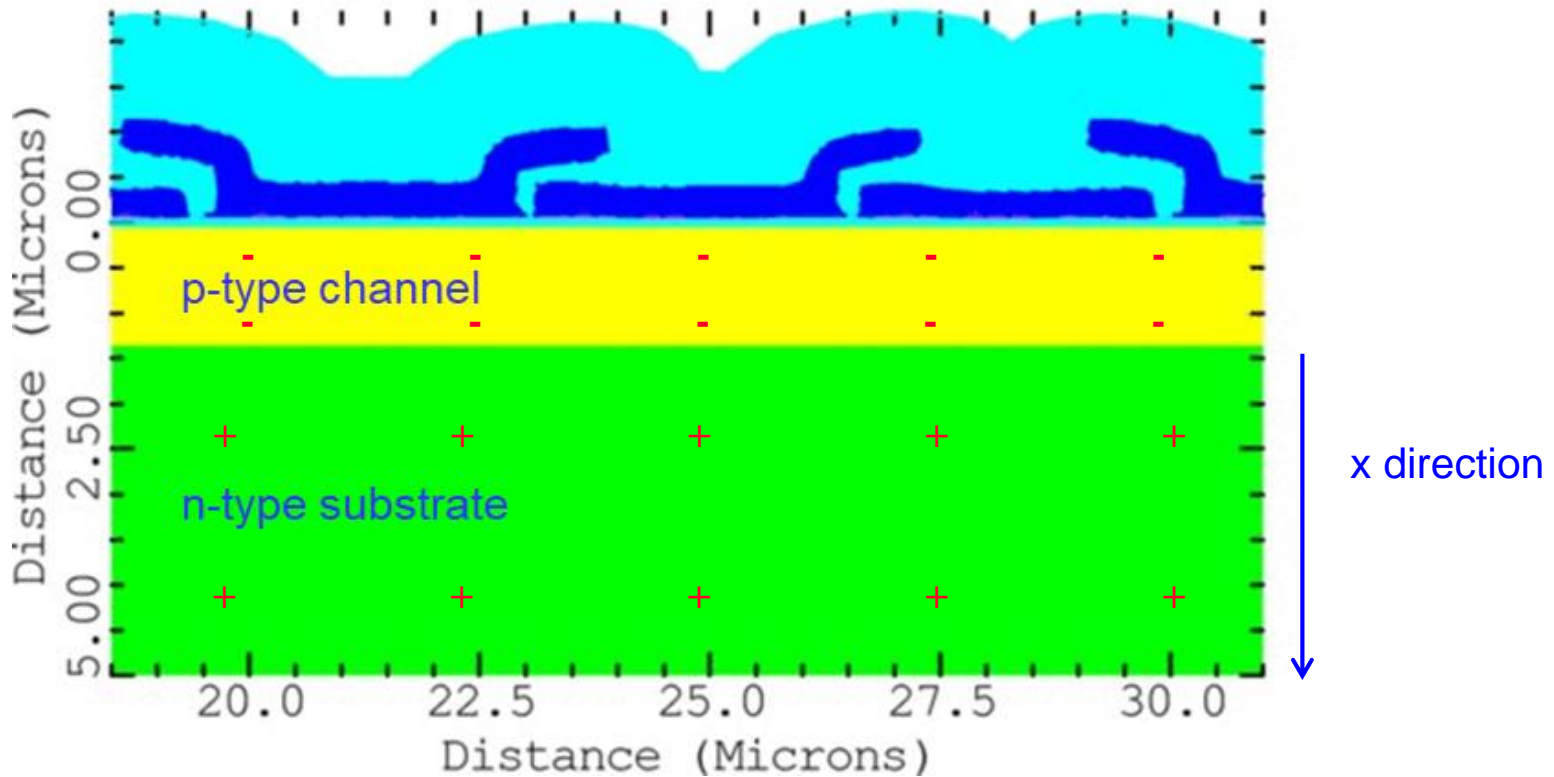
CCDs for Astronomy

- Thinned and back-illuminated
 - 10 – 20 microns thick
- Thick and fully depleted
 - 250 – 650 microns thick
 - Fully depleted with bias voltage
- Note the difference in resistivity
 - Conventional silicon $\sim 50 \Omega\text{-cm}$
 - p-type doping $\sim 3 \times 10^{14} \text{ cm}^{-3}$
 - Float-zone refined silicon 10 - 20 $\text{k}\Omega\text{-cm}$
 - n-type doping $\sim 2 - 4 \times 10^{11} \text{ cm}^{-3}$



- Thinned CCDs: Electrostatic potential at surface
 - 1-D solution of the Poisson Eq (depletion approx)





- + : Ionized donor atoms with single + charge (Density N_D in cm^{-3})
- : Ionized acceptor atoms with single - charge (Density N_A in cm^{-3})

Electric field in the n-type substrate $\sim N_D x$ (space charge)

Potential drop across the depleted region $V_D \sim N_D x_D^2$ (Poisson Eq)

Large depleted thickness x_D requires low doping N_D

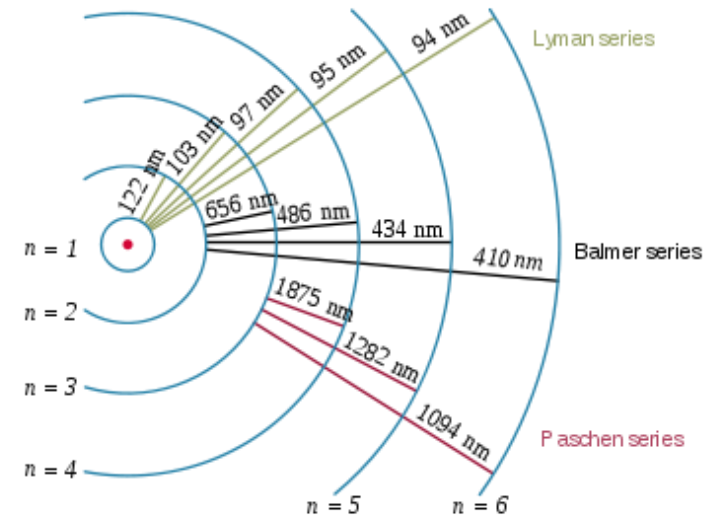
Redshift

H Ly α emission $\lambda_{\text{rest}} = 1216\text{\AA}$:
Quasars (Active Galactic Nuclei) & Ly α Galaxies

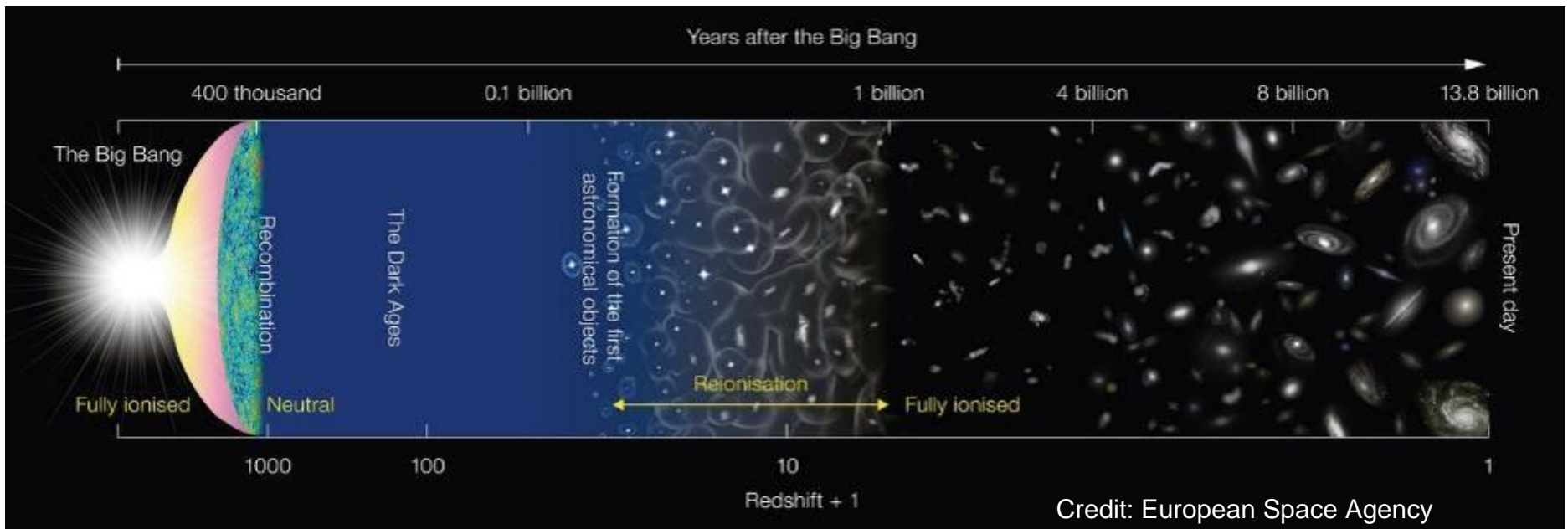
Thick CCDs can detect Ly α emission to $z \sim 7$

Probe the Reionization Era

Hydrogen Spectral Series



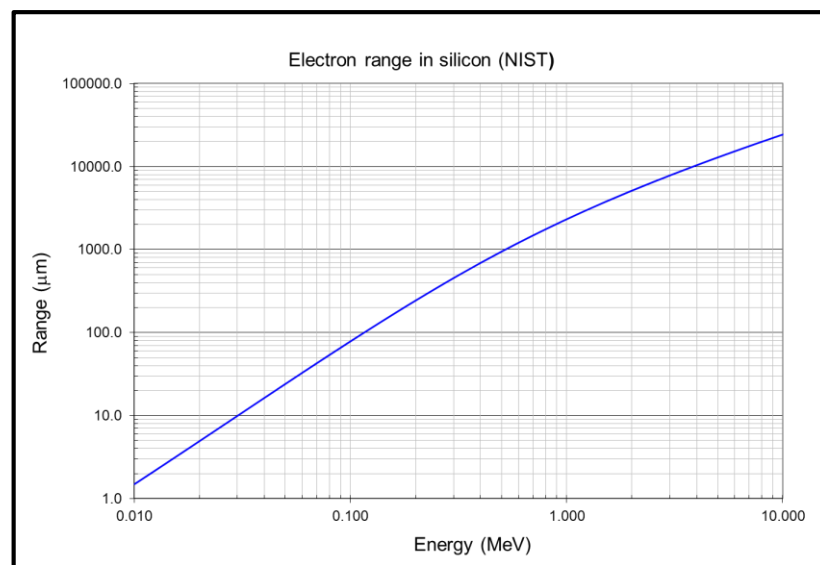
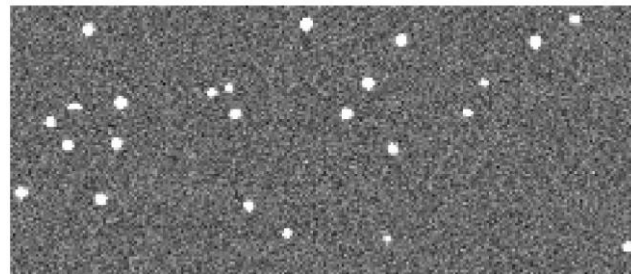
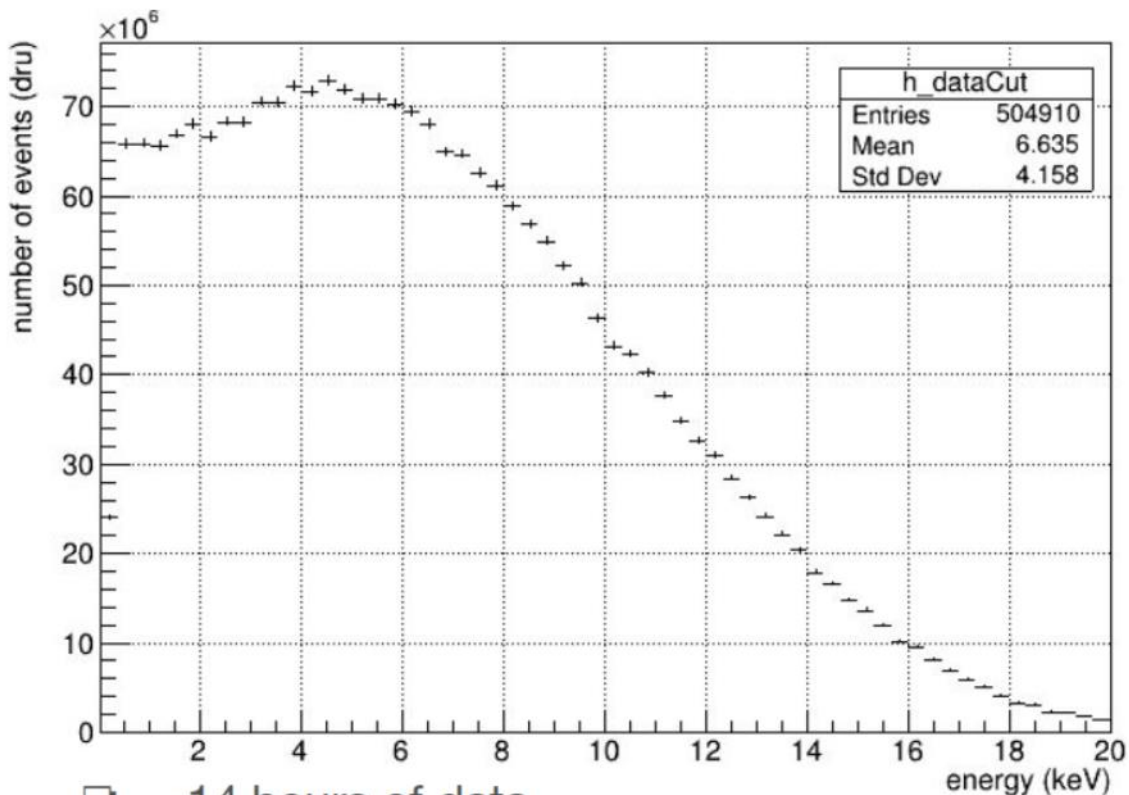
Credit: Wikipedia



Credit: European Space Agency

^3H detection with thick, BI, FD CCDs

Measured tritium spectrum using G2-CCD

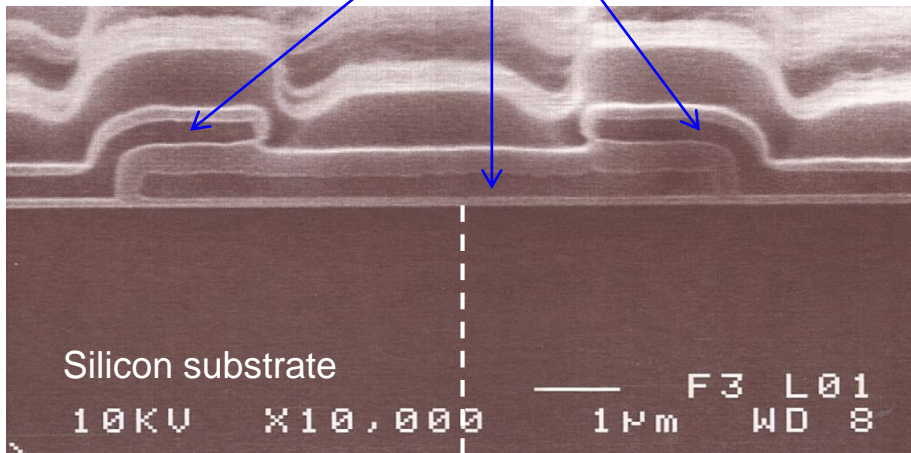


☐ ~14 hours of data

- GRAIL project with PNNL, LBNL, FermiLab, Lincoln Laboratory
 - ~ 2 keV β -electron detection

Charge-collection simulation

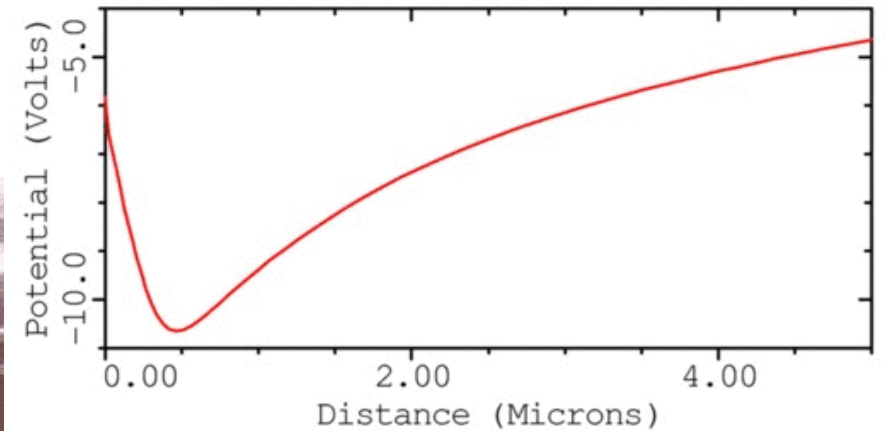
Polycrystalline silicon electrodes (leads)



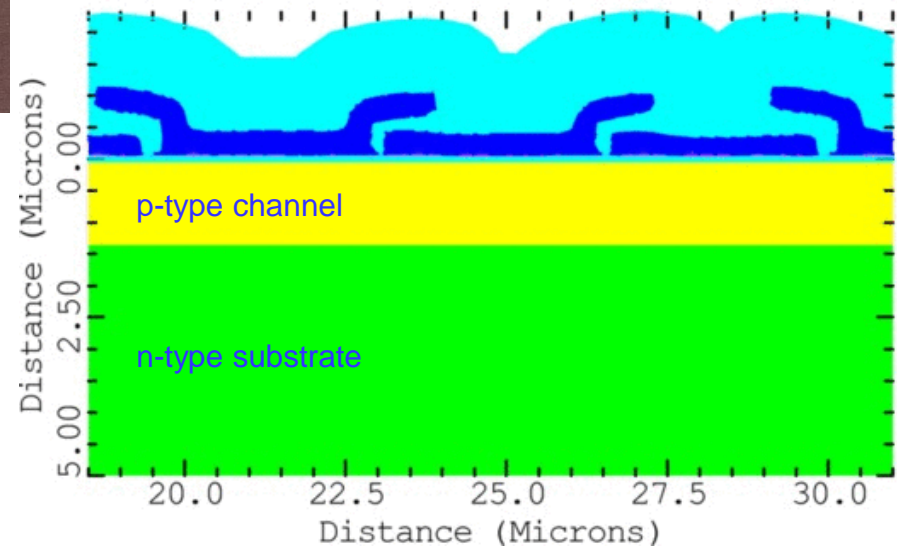
Electrostatic potential vs depth
Simulated potential along dashed line above

p-n junction at the surface creates
a potential minimum away from
the surface and the interface traps
Buried-channel CCD

Potential versus depth, $V_{sub}=50V$, 140K

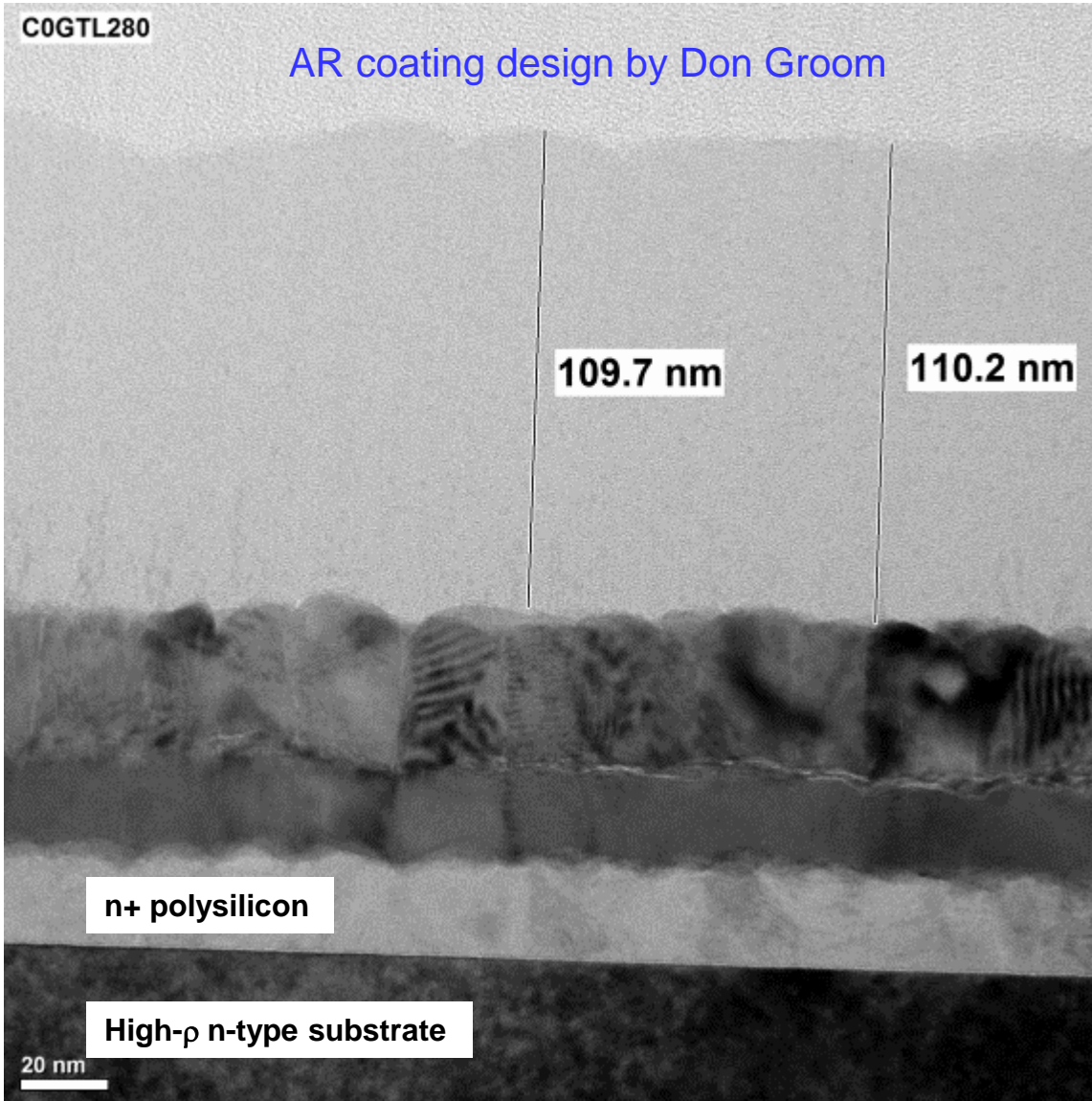


Holes/ μm width = 0 holes/ μm



Backside layers: LBNL CCDs

TEM cross-sectional image



SiO ₂ / 106 nm
ZrO ₂ / 38 nm
Indium tin oxide / 20 nm
In-situ doped polysilicon / 20 nm / $\sim 1 \times 10^{20} \text{ cm}^{-3} \text{ P}$
<p>Silicon substrate > 10,000 ohm-cm n-type</p>

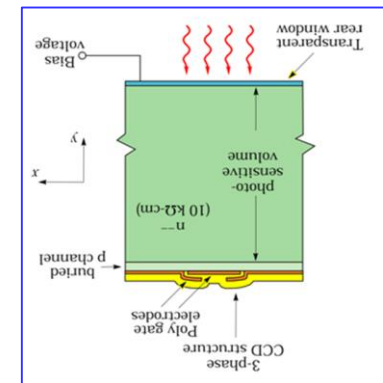
SiO₂

ZrO₂

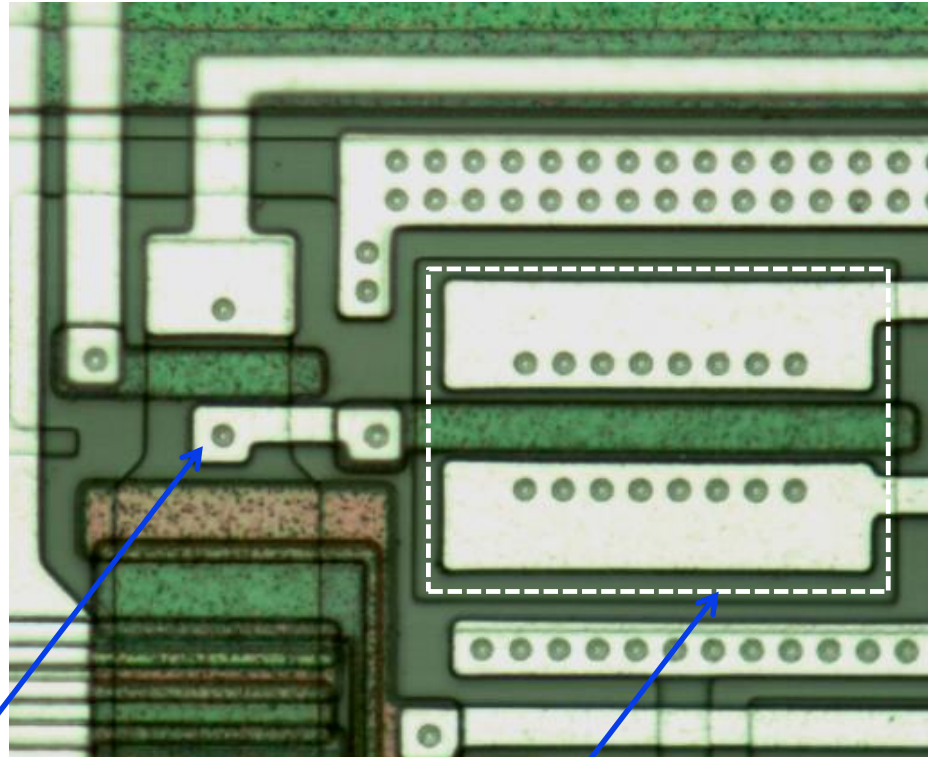
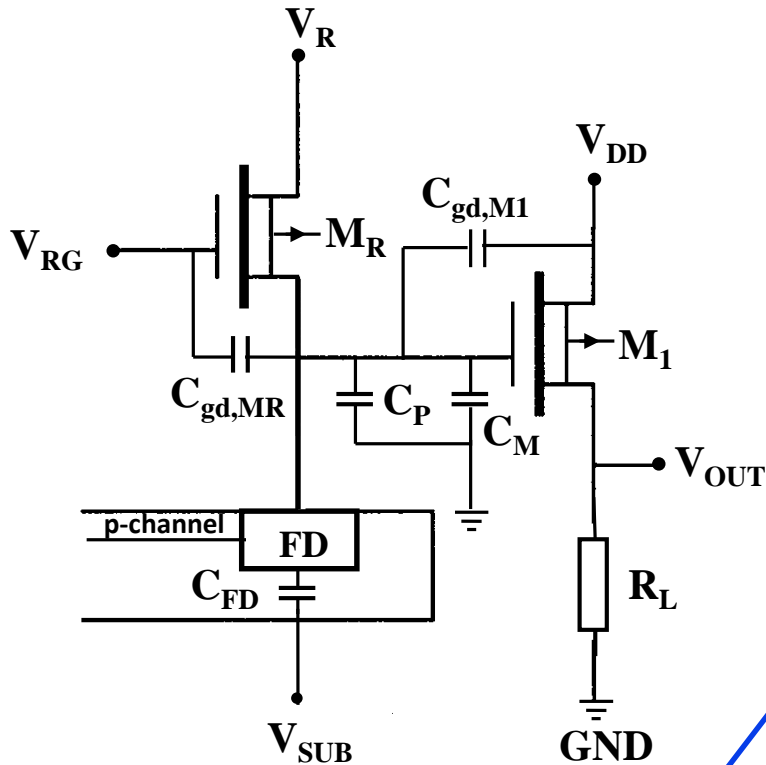
ITO

In-situ doped polysilicon

Silicon substrate



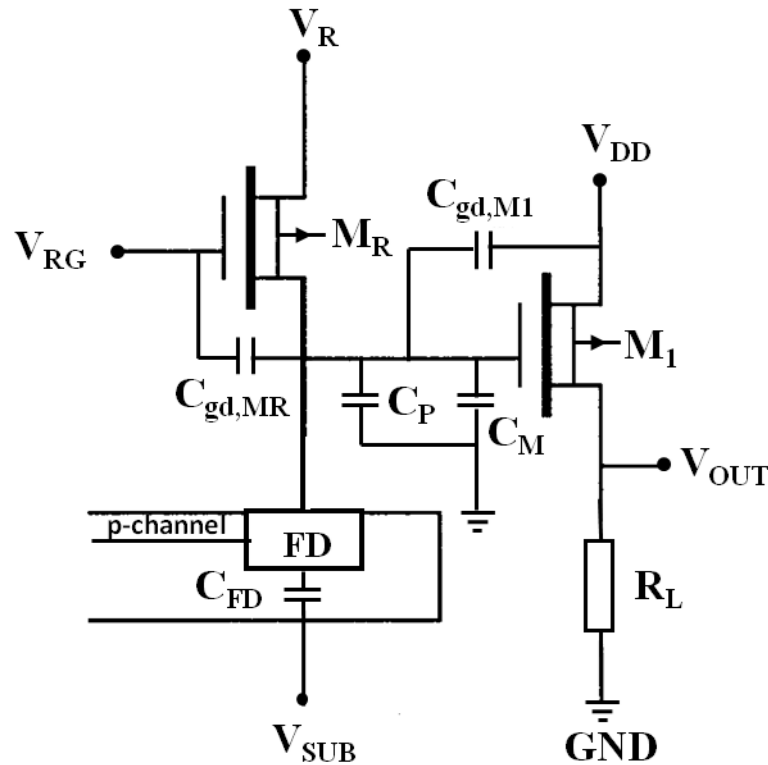
CCD amplifier noise



Floating diffusion
Diode sense node

Output transistor M_1

CCD amplifier noise



$$Q_n = \frac{V_{W,M1} C_T}{q}$$

Noise in electrons Q_n depends on

- 1) SF transistor M1 noise
- 2) Total capacitance at the floating diffusion

White noise in M1 is given by

$$V_{W,M1}^2 = 4kT \frac{2}{3} \frac{1}{g_m} \Delta f$$

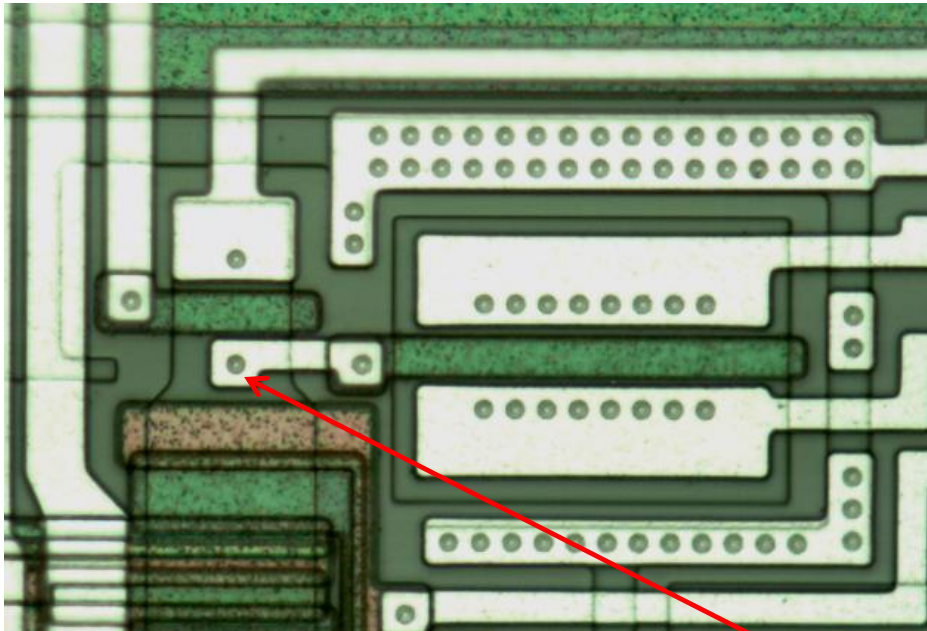
$$C_M = (1 - A_v) C_{gs,M1}$$

Reduce C_T and/or improve the transistor (g_m) to reduce noise

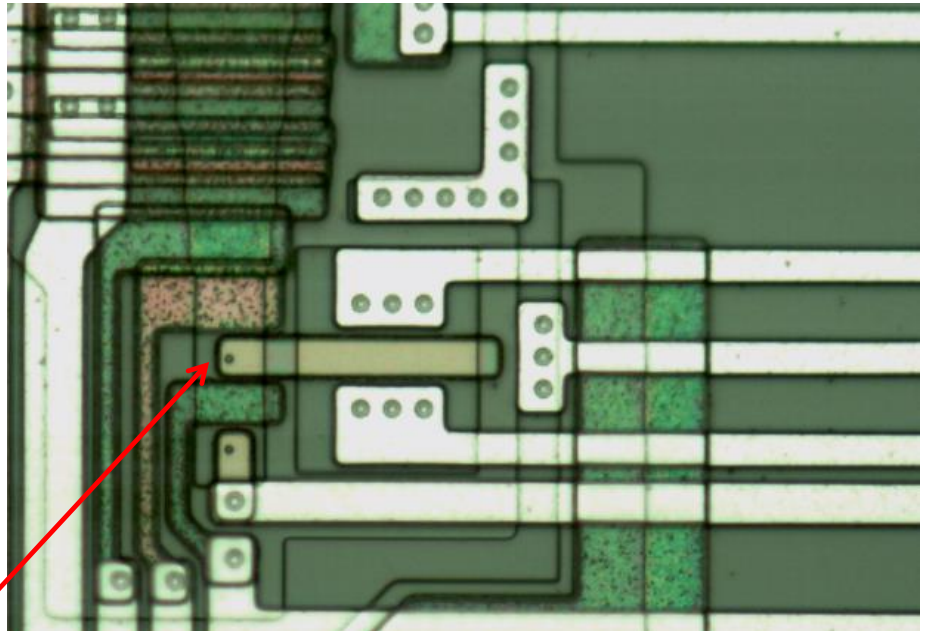
CCD Noise

Read noise reduction

- Technology development with Teledyne DALSA Semiconductor



Conventional amplifier with aluminum connection to source follower transistor

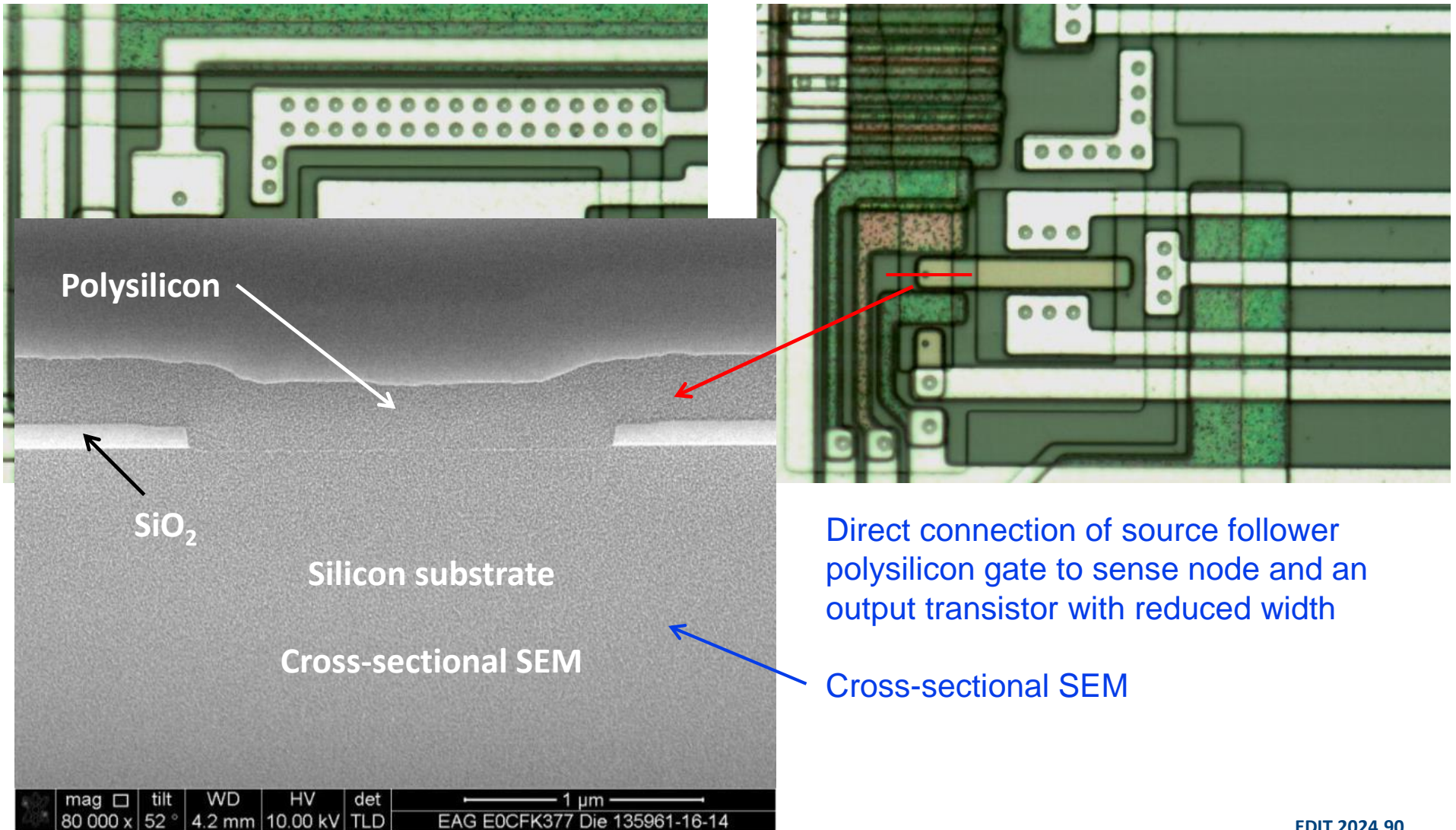


Direct connection of source follower polysilicon gate to sense node and an output transistor with reduced width

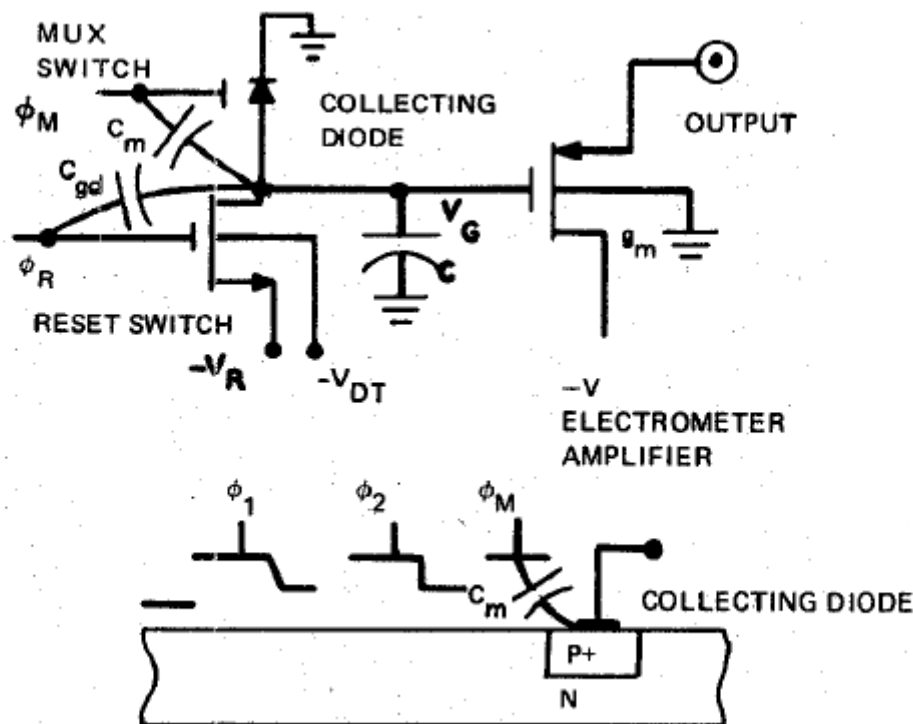
CCD Noise

Read noise reduction

- Technology development with Teledyne DALSA Semiconductor



Correlated double sampling



IEEE JOURNAL OF SOLID-STATE CIRCUITS, VOL. SC-9, NO. 1, FEBRUARY 1974

Characterization of Surface Channel CCD Image Arrays at Low Light Levels

[Presently](#) ←
[Ohio State](#)
[ECE Prof.](#)

MARVIN H. WHITE, SENIOR MEMBER, IEEE, DONALD R. LAMPE, MEMBER, IEEE,
 FRANKLYN C. BLAHA, MEMBER, IEEE, AND INGHAM A. MACK, MEMBER, IEEE



Correlated double sampling

Another key invention from the 1970's:

Correlated Double Sampling:

Eliminate kTC noise from the reset switch

10 $\mu\text{V}/e^-$ conversion factor implies 15 fF

kTC noise would be about 49 electrons!

Scientific CCDs achieve a few e^- noise

Method:

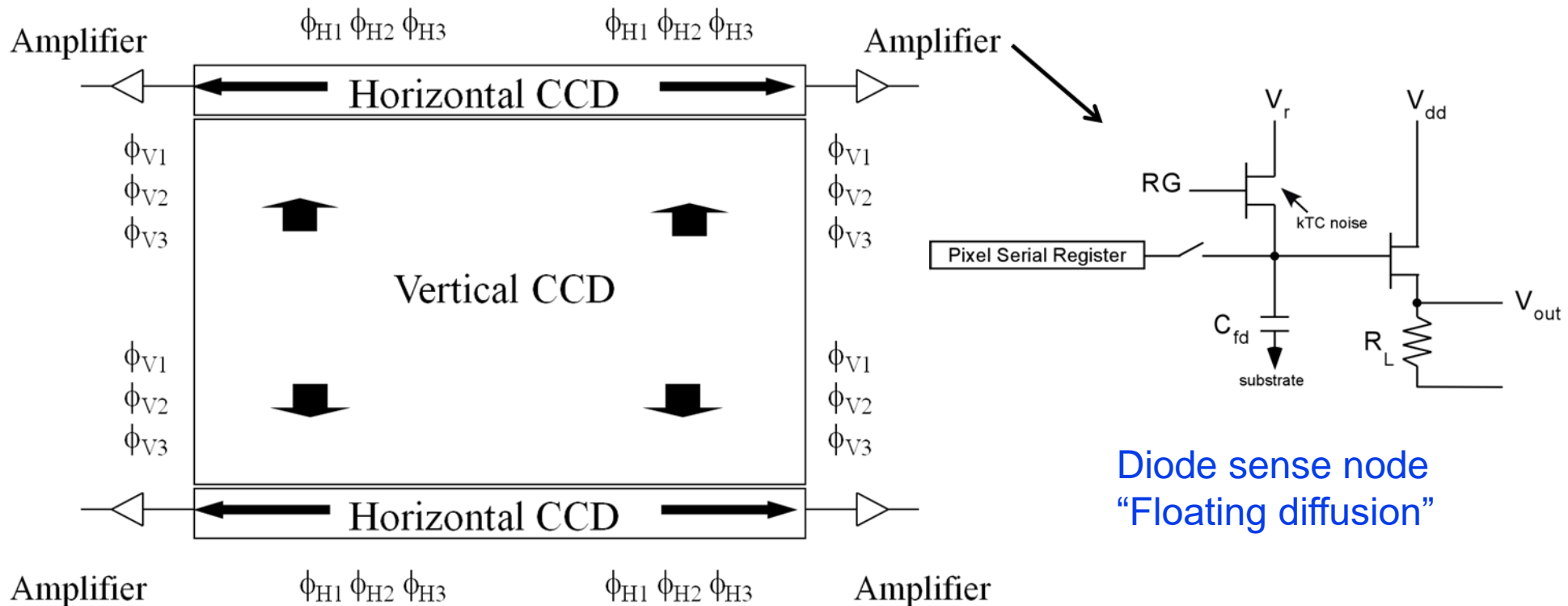
- 1) Measure reset level
- 2) Transfer charge to the sense node
- 3) Measure signal
- 4) Subtract reset from signal

¹M.H. White, D.H. McCann, I.A.G. Mack, F.C. Blaha, U.S. Patent 3,781,574, Dec. 1973

Link to [patent](#) and [paper](#)

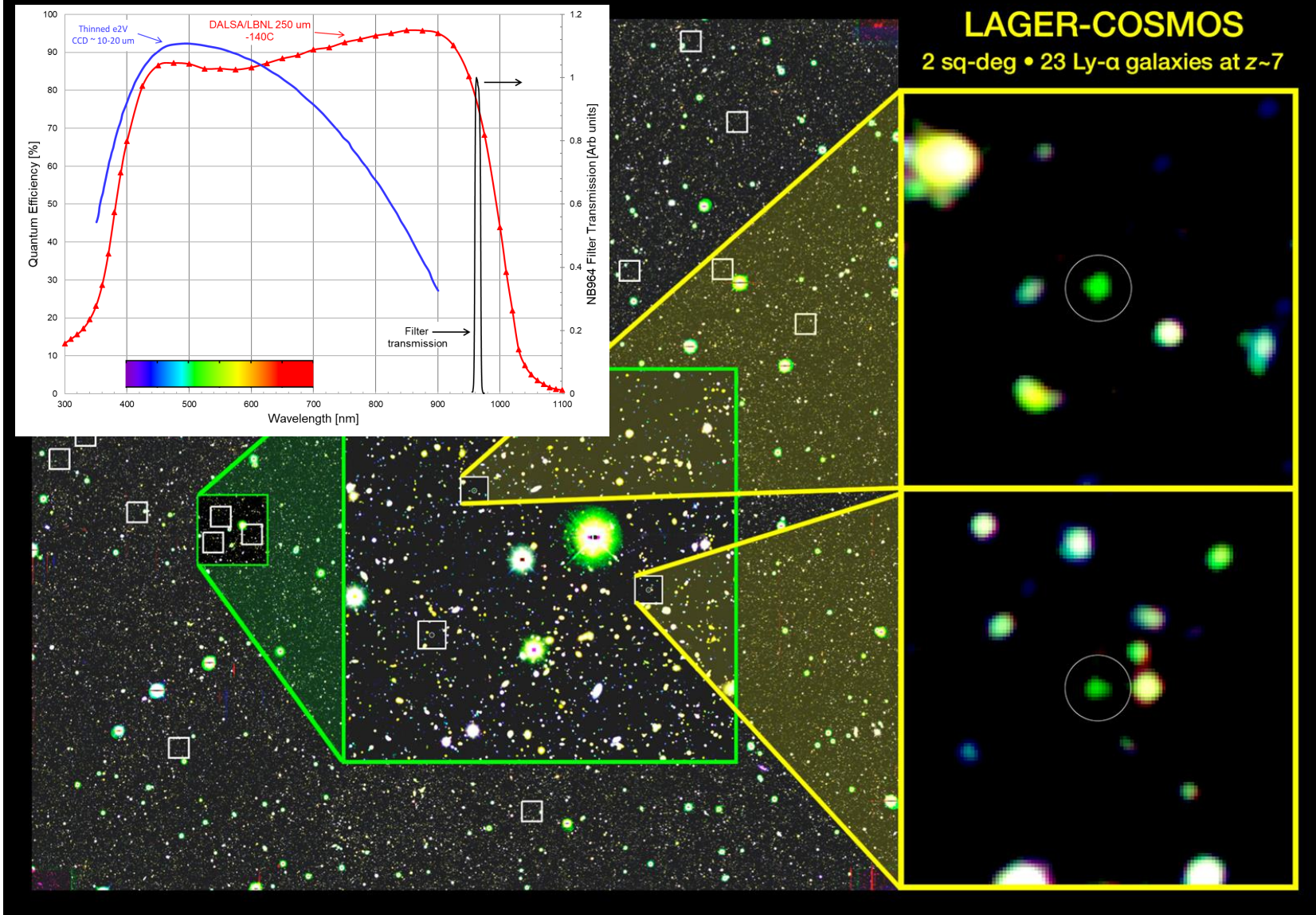
Scientific CCD typical operation

Charge is transferred from the imaging area a row at a time into serial registers where the charge is shifted to source follower amplifiers that convert the charge to voltage (noise determined at this step)



LAGER-COSMOS

2 sq-deg • 23 Ly- α galaxies at $z \sim 7$



False color image of a 2 square degree region of the LAGER survey field, created from images taken in the optical at 500 nm (blue), in the near-infrared at 920 nm (red), and in a narrow-band filter centered at 964 nm (green). The last is sensitive to hydrogen Lyman alpha emission at $z \sim 7$. The small white boxes indicate the positions of the 23 LAEs discovered in the survey. The detailed insets (yellow) show two of the brightest LAEs; they are 0.5 arcminutes on a side, and the white circles are 5 arcseconds in diameter.

Credit: Zhen-Ya Zheng (SHAO) & Junxian Wang (USTC). NOIRLAB